Dissertation

Oxygen modulates the response of first-trimester trophoblasts to hyperglycemia

submitted by

Mag. rer. nat.

Julia D. Fröhlich

for the Academic Degree of

Doctor of Philosophy

(Ph.D.)

at the

Medical University of Graz

Institute of Cell Biology, Histology & Embryology and

Clinic of Obstetrics and Gynecology

under Supervision of

Univ. Prof. Dr. Berthold Huppertz

and

a.o. Univ. Prof. Dr. Gernot Desoye

2011

Declaration

I hereby declare that this thesis is my own original work and that I have fully acknowledged by name all of those individuals and organisations that have contributed to the research for this thesis. Due acknowledgment has been made in the text to all other material used. Throughout this thesis and in all related publications I followed the guidelines of "Good Scientific Practice".

Please note that parts of this thesis are already published in Fröhlich JD, Huppertz B, Abuja PM, König J, Desoye G. *Oxygen modulates the response of first-trimester trophoblasts to hyperglycemia;* Hiden U, Froehlich J, Desoye G. *Diabetes and the Placenta*. In: Helen H, Kay D, Nelson M and Wang Y, editors. The Placenta: From Development to Disease. Blackwell Publishing Ltd.; 2011. p. 228-236 and Lappas M, Hiden U, Froehlich J, Desoye G, Haugel-de Mouzon S, Jawerbaum A. *The Role of Oxidative stress in the Pathophysiology of Gestational Diabetes Mellitus*. Antioxidant Redox Signal, 2011.

Graz, September 2011

Acknowledgements

First of all I would like to thank my supervisors Berthold and Gernot, who guided me through the last three years. Both supported me in every aspect during my thesis. I am thankful that I learned a lot, that they challenged me every day and for the opportunity to travel in- and outside Europe.

Special thanks go to Peter who tried to help me with his entire requests and for the constructive discussions.

I am appreciating that Prof. Gottfried Dohr gave me the opportunity to carry out the work at the Institute of Cell Biology, Histology and Embryology. Some more thanks go Beate Scheiber and Sandra for their administrative help and to Daniel for helping me with technical problems.
It was a great time to be part of the Histo-Team, therefore I would like to thank all my colleagues, Julia, Gerit, Amin, Veronika, Kiki, Kerstin and Nina. Particularly, I would like to thank two persons at the Histo, Martin and Monika; both tried to help me whenever they could and for their sympathetic ear if anything worked out.
But I was not just a part of the Histo-Team; I had also the luck to be a part of the Frauenklinik-Team. Thus, I am grateful for the support from Heidi, Uris, Luciana, Susi and Christian. I will really miss the nice trips and skiing weekends.

Last but not least I would like to thank my family and all my friends for their support during the last three years. Special thanks go to Andi who always was there for me and encouraged me.

Summary

Pregestational diabetes retards embryonic growth in early pregnancy. Placental and fetal growth are tightly associated suggesting that also placental growth is impaired. At the end of the first trimester of gestation, oxygen tension rises steeply leading to excessive production of reactive oxygen species (ROS), which is exacerbated in diabetes and may affect placental development. Additionally, during the first half of pregnancy HLA-G negative proliferative trophoblasts form cell columns from which HLA-G positive extravillous trophoblasts invade maternal tissues.

The hypotheses of the present study are that oxygen modifies hyperglycemic effects on ROS formation resulting in decreased first-trimester trophoblast growth and that cell survival of both trophoblast subpopulations can be differential influenced by the first trimester gradient ranges from placental low oxygen to decidual high oxygen under hyperglycemic conditions.

To test this hypothesis the first trimester trophoblast-derived cell line ACH-3P was cultured up to 3 days under normoglycemia (5.5mmol/l D-glucose) and hyperglycemia (25mmol/l D-glucose) at different (2.5%, 8% and 21%) oxygen tensions. Intracellular and mitochondrial ROS levels were measured by fluorescence assays (H_2DCFDA; MitoSOX Red). Proliferation and cell cycle were determined. Cell numbers of ACH-3P cells were measured with and without cytosolic and mitochondrial ROS formation inducers and inhibitors.

Under normoglycemia oxygen did not alter trophoblast proliferation. Hyperglycemia reduced cell number by 65% and resulted in cell cycle (G_1- and S-phase) changes but only at 21% oxygen. Proliferation reduction could be partially restored by an ERK1/2 but not Akt/PkB inhibitor. At 2.5% and 8% oxygen proliferation and cell cycle were unchanged. Intracellular ROS elevation under hyperglycemia was oxygen-independent, whereas mitochondrial superoxide levels were enhanced under hyperglycemia only at 21% oxygen. Intervention to modulate cytosolic and mitochondrial ROS did not alter cell growth under hyperglycemia at 21% oxygen.

Furthermore, after separation, HLA-G positive and negative first trimester trophoblast-derived ACH-3P cells exhibit fewer viable cells under hyperglycemia at 2.5% and 8% oxygen, while at 21% oxygen no viable cells were detectable.

A combination of hyperglycemia and high oxygen-levels (21%) reduce proliferation of human first-trimester trophoblasts in a ROS-independent manner

involving MAPK. This may account for reduced placental growth and, therefore, also for embryonic growth during the first trimester of pregestational diabetic pregnancies when the oxygen tension increases. Furthermore, in conclusion separated cell types are sensitive to both oxygen and glucose independent from each other.

Zusammenfassung

Zu Beginn einer Schwangerschaft hat mütterlicher Diabetes große Auswirkungen auf das Wachstum des Embryos, welches gegenüber normalen Schwangerschaften vermindert ist. Bei allen Schwangerschaften besteht eine Korrelation zwischen dem Geburtsgewicht und dem Plazentagewicht, was bei diabetischen Schwangerschaften zu einer Beeinträchtigung des Wachstums und der Entwicklung der humanen Plazenta führen kann. Gegen Ende des ersten Trimenons steigt der Sauerstoffpartialdruck innerhalb der Plazenta und es kommt zu einer übermäßigen Produktion von reaktiven Sauerstoff Spezies (ROS), die in diabetischen Schwangerschaften vermehrt beobachtet werden. Dies kann möglicherweise das Plazentawachstum beeinflussen. Während der ersten Hälfte einer Schwangerschaft proliferieren HLA-G negative Zellen und bilden sogenannte Zellsäulen aus, von denen extravillöse HLA-G positive Zellen in das angrenzende maternale Gewebe invadieren.

Basierend auf diese Fakten ist das Ziel dieser Arbeit die Hypothesen zu bestätigen, dass Sauerstoff hyperglykämische Effekte modifiziert, indem die Produktion von ROS beeinflusst wird und dass im ersten Trimenon die Überlebensrate von beiden Subpopulationen durch den Anstieg des Sauerstoffpartialdrucks unterschiedlich reguliert wird.

Um die Hypothese zu testen, wurde eine trophoblastäre Zelllinie (ACH-3P) bis zu drei Tage unter Normoglykämie (5,5mmol/l D-Glukose) und Hyperglykämie (25mmol/l D-Glukose) bei verschiedenen (2,5%, 8% und 21%) Sauerstoffkonzentrationen kultiviert.

Intrazelluläre und mitochondriale ROS Level wurden mittels Fluoreszenz Assays gemessen (H_2DCFDA; MitoSOX Red). Proliferation und Zellzyklus Phasen wurden bestimmt. Die Zellzahl von ACH-3P Zellen wurde mit und ohne zytosolische und mitochondriale ROS-Produktion-Stimulanzien und -Inhibitoren gemessen.

Unter normoglykämischen Bedingungen hatte Sauerstoff keinen Einfluss auf die Proliferation von Trophoblastzellen. Hyperglykämie reduzierte die Zellzahl um bis zu 65% und führte zu Veränderungen im Zellzyklus (G_1- und S-Phase), allerdings nur bei 21% Sauerstoff. Vermindertes Zellwachstum konnte partiell durch einen ERK1/2 Inhibitor aufgehoben werden, Zugabe eines Akt/PkB Inhibitor hatte keinen Effekt. Bei 2,5% und 8% Sauerstoff konnten keine Änderungen im Zellwachstum und Zellzyklus

beobachtet werden. Ein Anstieg der intrazelluläre ROS Bildungen unter Hyperglykämie war Sauerstoff unabhängig, allerdings wurden unter denselben Bedingungen und nur bei 21% Sauerstoff erhöhte mitochondriale Superoxid Level detektiert. Erhöhung und Verminderung der zytosolischen und mitochondrialen ROS Produktion hatte keinen Einfluss auf die Proliferationsrate unter hyperglykämischen Bedingungen bei 21% Sauerstoff.

Nach der Trennung von HLA-G positiven und negativen Trophoblastzellen zeigten beide Subpopulationen ein vermindertes Zellwachstum unter Hyperglykämie bei 2,5% und 8% Sauerstoff, während bei 21% Sauerstoff keine lebenden Zellen detektierbar waren.

Eine Kombination von Hyperglykämie und hoher Sauerstoffkonzentration (21%) reduzierte das Zellwachstum von humanen Trophoblastzellen des ersten Trimenons. Diese Verminderung der Lebendzellzahl ist ROS unabhängig, wird aber unter anderem durch MAPK vermittelt.

Vermutlich führt dies zu vermindertem Wachstum der Plazenta und damit auch zur Wachstumsretardierung des Embryos bei diabetischen Schwangerschaften innerhalb des ersten Trimenons, wenn der Sauerstoffpartialdruck ansteigt. Darüber hinaus sind beide Subpopulationen, HLA-G positive und negative Zellen, sehr empfindlich gegenüber Glukose als auch gegenüber Sauerstoff.

Abbreviations

Akt/PkB	Protein kinase B
AM	Acetoxymethyl
6-AN	6-aminonicotinamide
BCNU	1,3-bis-(2-chloroethyl)-1-nitrosourea
B2M	Beta-2-microglobulin
BSA	Bovine serum albumin
CAT	Catalase
Cdk	Cyclin-dependent kinase
CT	cytotrophoblast
cDNA	Complementary deoxyribonucleic acid
CO_2	Carbon dioxide
CREB	cAMP response element-binding protein
CSDE	Cold shock domain containing E1
CuZn-SOD	Cytosolic copper-zinc superoxide dismutase
CYBG	Cytoglobin
DAPI	4,6 diamidino -2-phenylindoledihydrochloride
DNA	Deoxyribonucleic acid
DMEM	Dulbecco`s Modified Eagle Medium
DMSO	Dimethyl sulfoxide
DUOX	Dual oxidase
ECT	Electron transport chain
Em	Emission
ERK	Extracellular signal-regulated kinases
EtOH	Ethanol
Ex	Excitation
FCCP	4- (trifluoromethoxy)phenylhydrazone
FCS	Fetal calf serum
G_1-phase	Gap1-phase
G_2/M-phase	Gap2/mitosis-phase
GSTZ	Glutathione transferase zeta
GPX	Glutathione peroxidase

GR	Glutathione reductase
H_2DCFDA	2,7-dichlorodihydrofluorescein diacetate
HBSS	Hank's Balanced Salt Solution
HG	Hyperglycemia
HKG	House keeping gene
HLA-G	Human leukocyte antigen-G
HMXO-1	Heme oxygenase
HRP	Horseradish peroxidise
H_2O_2	Hydrogen peroxide
HPRT1	Hypoxanthine phosphoribosyltransferase 1
HRP	Horseradish peroxidase
JNK	c-Jun N-terminal kinases
MAPK	Mitogen-activated protein kinase
Mn-SOD	Mitochondrial manganese superoxide dismutase
mRNA	Messenger ribonucleic acid
NAC	*N*-acetylcysteine
NADH	Nicotinamide adenine dinucleotide
NADPH	Nicotinamide adenine dinucleotide phosphate
NFE2L2	Nuclear factor (erythroid-derived 2)-like 2
NG	Normoglycemia
n.s.	Not significant
O_2	Oxygen
O_2.-	Superoxide anion
$^{\cdot}$OH	Hydroxyl radical
PBS	Phosphate buffered saline
PCR	Polymerase chain reaction
PI3K	Phosphatidylinositol 3-kinases
pm	Post menstruationem
PRDX	Peroxiredoxin
ROS	Reactive oxygen species
RPL30	Ribosomal protein L30
RT	Room temperature
RT-PCR	Reverse transcription polymerase chain reaction

SAPK	Stress activated protein kinase
S-phase	Synthesis-phase
SD	Standard deviation
SOD	Superoxide dismutase
TBS	Tris buffered saline
XO	Xanthine oxidase
XOR	Xanthine oxidoreductase

Index

1 Introduction

1.1 The human placenta

The human placenta is a unique, transient organ for sustaining development and survival of the embryo in the uterine environment of the mother. In the first weeks of gestation distinct trophoblast cell types are generated within the organ, which is required to fulfil the complex biological processes of implantation, immunological adaption and vascular connection to the maternal circulation. This provides transfer of nutrients, gas and hormones from the mother to the fetus. The implantation process begins with the development of the blastocyst (Fig. 1), which triggers attachment to and implantatio into the maternal endometrium, the uterine deciuda (Loregger et al., 2003).

The placental structure consists of floating and anchoring villi and its specialised cell types, the syncytium and the invasive extravillous trophoblasts. During the first trimester of pregnancy extravillous trophoblasts develop from anchoring villi and invade the maternal decidua basalis and in further consequence uterine spiral arteries, leading to endovascular remodelling by replacing maternal endothelium. Invasion and remodelling of spiral arteries by endovascular trophoblasts provides increased maternal blood flow into the intervillous space. Thus, the endovascular invasion allows the reorganisation of the uterine spiral arteries leading to the onset of the uteroplacental circulation. Hence, all these processes are crucial for the successful progression of normal pregnancies (Staun-Ram and Shalev, 2005, Benirschke K et al., 2006).

1.1.1 Oxygen tension during first trimester of pregnancy

Early in pregnancy the placenta and embryo develop in a state of low oxygen tension and nutrients are supplied by maternal plasma and by secretion of maternal endometrial glands. The placental oxygen tension steeply rises between 8 to 12 weeks of gestation, reflecting the onset of maternal blood flow. Concomitantly, establishment of placental blood flow is associated with a burst of oxidative stress in this organ. Increasing oxygen concentrations lead to generation of reactive oxygen species (ROS),

thus, exposing the placenta to oxidative stress even in normal pregnancies (Huppertz et al., 2009, Jauniaux et al., 2000, Burton, 2009).

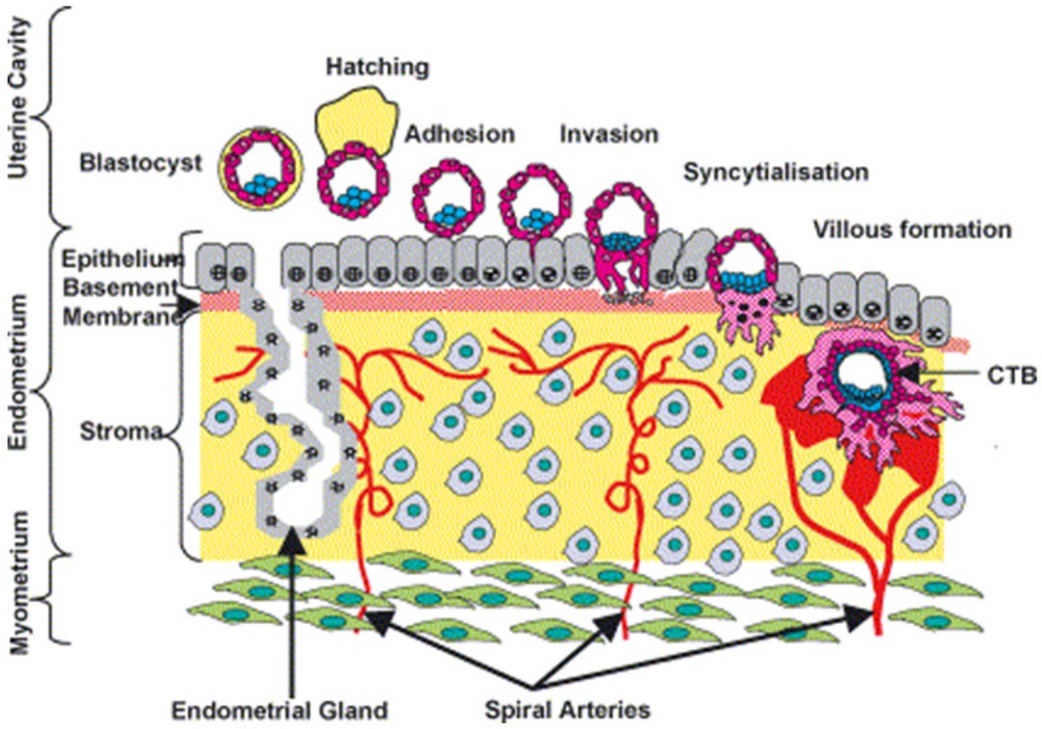

Figure 1 **Implantation process. The** blastocyst attaches to the maternal endometrium by adhesion. During the invasion process the trophoblast differentiates into the multinuclear syncytiotrophoblast and mononuclear cytotrophoblast cells. Villous formation is initiated followed by invasion of extravillous cytotrophoblasts into the decidua basalis and maternal spiral arteries, known as endovascular remodeling (Bischof and Irminger-Finger, 2005).

1.2 The human placenta in diabetic pregnancies

Pathologic pregnancies in particular those complicated by early pregnancy failure (Jauniaux and Burton, 2005), preeclampsia (Huppertz, 2008) and intrauterine growth restriction (Burton et al., 2010) are associated with inadequate placental development.

In pregnancies of diabetic women the incidence of these pathologies is increased (Sibai, 2000, Mammon et al., 2005, Biggers and Summers, 2008). Maternal diabetes is often associated with high plasma glucose levels which in turn lead to fetal hyperglycemia (Freinkel, 1980). During the first trimester of a diabetic pregnancy, embryonic growth may be transiently reduced, known as early embryonic growth delay (Pedersen et al., 1984, Brown et al., 1992). The tight association between fetal and

placental weight (Thame et al., 2004, Weiss et al., 2001) makes it tempting to speculate that early embryonic growth delay in diabetes is associated with impaired placental development. Lower maternal serum levels of the human trophoblast-specific hormones placental lactogen and pregnancy-associated plasma protein A support this notion (Pedersen et al., 1998). Trophoblast proliferation is the key driver of placental growth in early pregnancy. However, little is known about potential changes of placental development in first trimester of diabetic pregnancies and the underlying molecular mechanisms.

1.3 Oxidative stress and glucose metabolism in diabetic pregnancy

1.3.1 Cytosolic ROS formation

Oxidative stress is defined as an imbalance between ROS formation and antioxidant defense mechanisms in a cell or tissue (Forbes et al., 2008). Pregnancy pathologies, such as early pregnancy failure, preeclampsia and diabetes mellitus, are often associated with an imbalance between ROS production and the antioxidant defense systems (Hiden et al., 2011). The biologically most important ROS are superoxide anion (O_2.-), peroxyl radical and hydrogen peroxide (H_2O_2). Excessive production of ROS can lead to massive cellular damage of proteins, lipids and DNA (Myatt and Cui, 2004). This damage is prevented usually by protective systems consisting of low-molecular mass antioxidants and enzymatic defense systems. In the human placenta they comprise among others mitochondrial manganese and cytosolic copper-zinc superoxide dismutase (Mn-SOD; CuZn-SOD), catalase (CAT), glutathione peroxidase/reductase (GPX/GR), glutathione, ascorbate and tocopherols. Under normal conditions these defense systems have the capacity to induce conversion of ROS into water and molecular oxygen and prevent ROS overproduction as a consequence of increased metabolic activity of placental mitochondria throughout gestation (Roberts and Sindhu, 2009).

At the same time physiologic ROS levels can promote and control cellular fate, playing a crucial role in placental development through cellular signaling. Under normal conditions the placental antioxidant defence systems, which have the capacity to induce conversion of ROS to water and molecular oxygen, prevent ROS overproduction as a consequence of increased metabolic activity of placental mitochondria throughout gestation (Roberts and Sindhu, 2009).

In several tissues hyperglycemia appears to be directly linked to ROS production (Choi et al., 2008). Thus, high-glucose concentrations as found in maternal diabetes can increase oxidative stress and may lead to biochemical disturbances in the complex processes of fetal development and growth (Dennery, 2007). Several studies have reported that oxidative stress appears to be a key event in diabetic complications (Wentzel et al., 2003, Wentzel and Eriksson, 1998, Qi et al., 2007). This notion is supported by the findings of decreased vitamin C and vitamin E levels and reduced antioxidant capacity of SOD in diabetic women (Peuchant et al., 2004).

In most mammalian cells, ROS can be generated in the cytosol by xanthine and nicotinamide adenine dinucleotide phosphate (NADPH) oxidase, cytochromes P450 and other NADPH-dependent oxidoreductases, and in mitochondria by the electron transport chain. These mechanisms are also operative in the human placenta (Myatt, 2010). Cytosolic NADPH oxidase, xanthine oxidase or cytochrome P450 in the endoplasmic reticulum produce superoxide anion and hydrogen peroxide by transferring electrons from NADPH or NADH, respectively, to molecular oxygen (Myatt and Cui, 2004, Gao and Mann, 2009). Mitochondrial ROS is produced due to electron transport in the mitochondrial respiratory chain incorrectly coupled to oxidative phosphorylation. Incomplete reduction of oxygen yields O_2.-, which is eventually converted to H_2O_2 and hydroxyl radical ($^{\cdot}$OH) (Zhang and Gutterman, 2007, Murphy, 2009). Recent work reported enhanced mitochondrial O_2.- production under hyperglycemic conditions compared to cells cultured at low glucose levels (Makino et al., 2010).

1.3.1.1 NADPH oxidase

NADPH oxidase is a cytosolic enzyme complex responsible for ROS generation by electron transport and especially important in redox signaling. It was first discovered in neutrophils, where it plays a crucial role in nonspecific host-pathogen defense (Forbes et al., 2008, Gill and Wilcox, 2006). It is composed of membrane-bound subunits gp91 phox (Nox2)/Nox1/Nox4, p22 phox, the catalytic site of the oxidase, and the cytoplasmic regulatory components p47 phox and p67 phox.. Five isoforms exist named Nox1-5, Nox2 and Nox4 are constitutively active and do not need any regulatory subunits (Gill and Wilcox, 2006, Gnudi et al., 2007, Dworakowski et al., 2008). Under diabetic conditions it can be stimulated by advanced glycation end-products, insulin and angiotensin II. Under diabetic conditions possibly all these stimuli are induced, which can activate NADPH oxidase (Fig. 2). Once activated in response to high glucose NADPH oxidase catalyzes the transfer of electrons from NADPH to molecular oxygen to produce O_2.- - and H_2O_2 (Gupte et al., Gao and Mann, 2009). High glucose levels lead to generation of ROS by stimulation of NADPH oxidase (Xia et al., 2008).
Under physiological conditions ROS is eliminated by cellular defense mechanisms, including diverse enzymes and vitamins. However, imbalance of ROS production and antioxidant systems of a cell can lead to an up-regulation of antioxidant gene expression through activation of nuclear antioxidant response elements (ARE) by the redox sensitive transcription factor Nrf2 (Gao and Mann, 2009). Hyperglycemia causes excessive ROS formation, thus activating the Nrf2/ARE pathway (Xue et al., 2008). It appears that basal activity of NADPH oxidase provides ROS production to trigger Nrf2/ARE-mediated antioxidant gene expression to sustain redox homeostasis (Mann et al., 2007). Expression of Nox1 was observed in the syncytiotrophoblasts, in villous endothelium and in some stromal cells of human placenta (Cui et al., 2006). This is paralleled by superoxide production via NADPH oxidase in the human placenta. Therefore, it is suggested that NADPH oxidase is the major enzymatic source of superoxide within the placenta (Poston and Raijmakers, 2004).

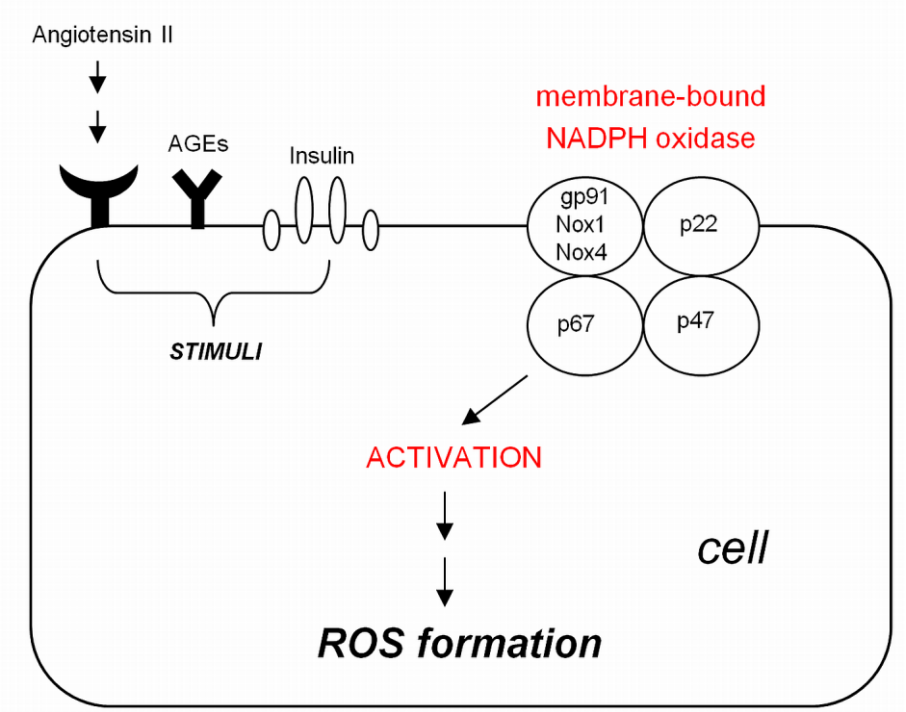

Figure 2 **Activation of membrane-bound NADPH oxidase by stimuli such as angiotension II, insulin and AGE under diabetic conditions;** adaped from (Kaneto et al., 2010).

1.3.1.2 Xanthine oxidase

Xanthine oxidoreductase (XOR) belongs to a group of enzymes known as molybdenum iron-sulfur flavin hydroxylases and occurs as two inter-convertible forms including xanthine oxidase (XO) and xanthine dehydrogenase (XDH). XOR is present *in vivo* as XDH but it can easily be oxidized to XO. Normally, XDH does not lead to raised ROS production because of its greater affinity for NAD^+ compared to oxygen molecules. Nevertheless, the two enzymes XO and XDH are capable to oxidize NADH resulting in ROS generation. XOR is the rate limiting enzyme in the conversion of hypoxanthine to xanthine and of xanthine to urate. During XO re-oxidation the enzyme transfers its six free electrons onto molecular oxygen causing the production of hydrogen peroxide and superoxide (Myatt and Cui, 2004, George and Struthers, 2009). Immunohistochemistry demonstrated XO expression in the human placenta (Poston and Raijmakers, 2004). Observation in diabetic mice showed increased activity of XO in tissue and serum. Treatment with the XO inhibitor allopurinol reduced the activity of XO again (Rajesh et al., 2009).

1.3.2 ROS production via mitochondria

In most mammalian cells mitochondria are the major source of reactive oxygen species. ROS are produced as a result of incorrectly coupled electron transport in the mitochondrial respiratory chain by oxidative phosphorylation. Once generated, ROS can either mediate mitochondrial damage or it can play a crucial role in redox signaling from the mitochondrion to the rest of the cell. Glycolysis converts glucose to pyruvate which can be transported directly into mitochondria. Subsequently, it is oxidized by the tricarboxylic acid cycle (TCA) to generate four molecules of NADH, one molecule of $FADH_2$, CO_2 and H_2O (Rolo and Palmeira, 2006, Murphy, 2009, Forbes et al., 2008, Lappas et al.).

Four major protein complexes are responsible for the electron flow through the mitochondrial electron transport chain. First, complex I (NADH-ubiquitin oxidoreductase) accepts electrons from NADH, which are carried to complex II (succinate dehydrogenase), where they are used to oxidize succinate to fumarate. Electrons move along the electrochemical gradient to complex III (ubiquina-cytrochrome *c* oxidoreductase) and complex IV (cytochrome *c* oxidase).

Finally, the electrons are used to convert molecular oxygen molecules to water (Zhang and Gutterman, 2007). At complexes I, III and IV electron transfer is associated with proton pumping into the intermembrane space generating a H^+-based electric and chemical gradient, which is used to generate ATP from ADP by complex V (ATP synthase). Uncompleted reduction of oxygen can trigger the formation of superoxide by complexes I and III (Fig. 3) (Ramalho-Santos et al., 2009).

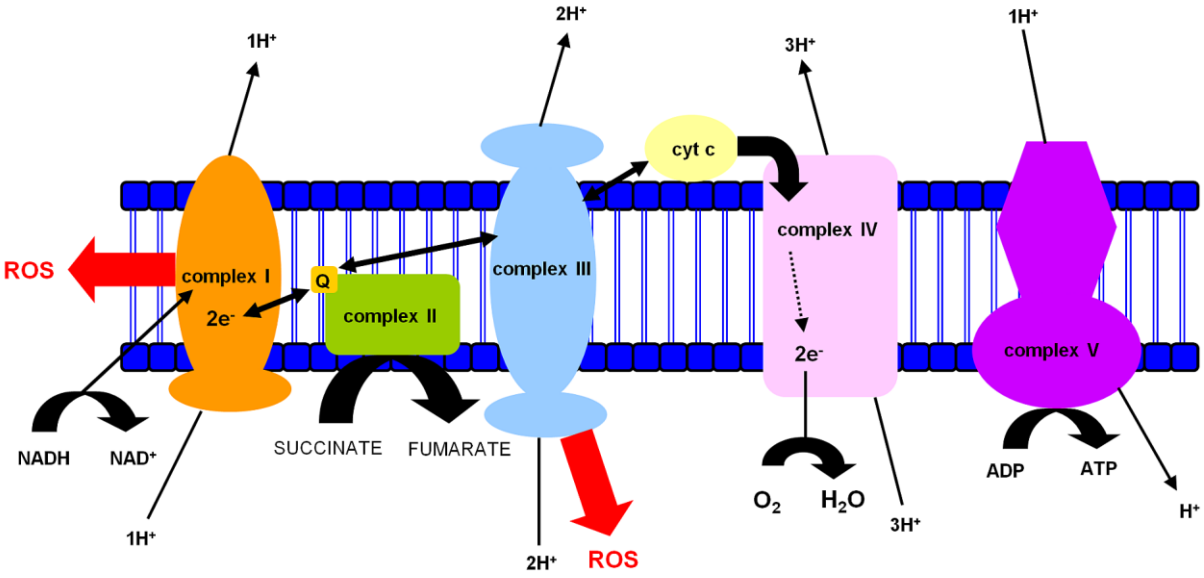

Figure 3 **Mitochondrial ROS generation at complexes I and III through electron transfer in the respiratory chain.** Electron transfer trough the respiratory chain triggers proton pumping resulting in ATP production. Uncompleted reduction of molecular oxygen molecules result in ROS production via complexes I and III; adapted from (Stowe and Camara, 2009).

Superoxide can not move across the mitochondrial membrane. Therefore it is converted to hydrogen peroxide and hydrogen radicals by superoxide dismutase to diffuse across the mitochondrial membrane. Hydrogen peroxide itself can further be degraded to water via catalase and glutathione peroxidase, which represents the primary elimination process of ROS in mitochondria (Zhang and Gutterman, 2007).

In vitro hyperglycemia-induced ROS production was reduced by an inhibitor of electron transport chain complex II, by an uncoupler of oxidative phosphorylation, by uncoupling protein-1 and by manganese superoxide dismutase, suggesting that the TCA cycle is the major source of high glucose-induced ROS production (Nishikawa et al., 2000). Furthermore it was shown that elevated ROS levels caused by hyperglycemia are involved in morphological changes of mitochondria (Yu et al., 2006), which also supported their involvement in ROS generation.

1.4 HLA-G expression in first-trimester trophoblasts

During first trimester of pregnancy cytotrophoblast cells invade the uterus and develop multilayered structures, the trophoblastic cell columns at the tip of the anchoring villus. Those cells losing contact with the villus also lose their generative potential and become extravillous cytotrophoblasts, which invade maternal tissue and uterine spiral arteries (Huppertz et al., 2009, Korgun et al., 2006). Subsequently, vascular endothelial cells and smooth muscle cells are replaced by fetal trophoblast cells. Endovascular remodelling of the spiral arteries results in increased maternal blood flow into the intervillous space (Harris, 2010, Whitley and Cartwright, 2010). As a consequence of invasion extravillous cytotrophoblasts change their phenotype, thus they express the human leukocyte antigen-G (HLA-G), amongst others, compared to trophoblast cells located at the tip of the anchoring villus (Benirschke K et al., 2006, Moser et al., 2010).

Early in pregnancy the placenta and embryo develop in a state of low oxygen, indeed onset of free maternal blood flow is accompanied with elevated oxygen tensions within the placenta (Jauniaux et al., 2000).

Diabetic pregnancies are characterised by shallow trophoblast invasion and inadequate or incomplete remodelling of spiral arteries and therefore predisposes to early pregnancy loss, preeclampsia and intrauterine growth restriction (Harris, 2010, Hiden et al., 2011).

2 Hypothesis and Objectives

The present study tested the hypothesis that diabetes-associated hyperglycemia leads to a ROS-induced reduction of placental growth during the first trimester of pregnancy in an oxygen-tension dependent manner.

Since placental growth is mainly driven by trophoblast growth in early pregnancy, the current study focused on first-trimester trophoblasts. However, primary trophoblasts do not proliferate in culture. Therefore, to proof the hypothesise, a recently generated first trimester trophoblast-derived cell line, ACH-3P, which closely resembles primary trophoblasts (Hiden et al., 2007) was used. Since ACH-3P cells proliferate *in vitro* they represent a particularly suitable model for the purpose of the present study.

Additionally, the influence of HLA-G expression, after separation of HLA-G positive and negative ACH-3P cells, on cell proliferation under hyperglycemic conditions was investigated.
The current study tested the hypothesis that HLA-G positive and negative trophoblasts differ in their proliferative response under diabetic and varying oxygen conditions.
Therefore, ACH-3P cells which represent a heterogeneous cell line, comprising both subpopulations villous cytotrophoblasts (HLA-G negative cells) and invasive extravillous trophoblasts (HLA-G positive cells) was used again.

Finally, proliferation of first-trimester villous placental explants (7, 8 and 10 weeks of gestation) under diabetic conditions and varying oxygen concentrations was studied as a more complex tissue model.

3 Materials and Methods

3.1 Tissue collection and cell culture

3.1.1 Explant collection and culture

Villous explants were obtained from first-trimester placentas derived from elective terminations of pregnancies (gestational age 7, 8 and 10 weeks). Each patient gave informed consent for collection and investigational use of tissue. **Approval of the Ethical Committee of the Medical University of Graz was granted (No. 23-203 ex 10/11)**.

Placental explants were rinsed in Hank`s buffered salt solution (HBSS; Gibco, Invitrogen Ltd, Paisley, UK), supplemented with 1% penicillin/streptomycin and 1% amphotericin B (PAA Laboratories, Pasching, Austria) and placed in culture medium Dulbecco`s modified Eagle`s medium (DMEM) low (5.5mmol/l) or high (25mmol/l) in D(+)-glucose with sodium pyruvate and L-glutamine (Gibco), supplemented with 10% fetal calf serum (FCS; Gibco) and 1% penicillin/streptomycin. As osmotic control 19.5mmol/l L(-)-glucose (Invitrogen, Eugene, USA) was added to DMEM low in D(+)-glucose. Tissue samples were cultured in 12 well dishes (Iwaki, Tokyo, Japan) at 37°C, 5% CO_2 and 2.5%, 8% or 21% O_2 in an XVIVO incubation system Model G300C (BioSperix Ltd, Lacona, USA) for 2 days. After 24 hours explants were transferred to 12 well dishes containing fresh culture medium. Tissue samples were fixed in 4% formaldehyde (LaboNord, Vienna, Austria) and subsequently embedded in paraffin.

3.1.2 Cell culture

ACH-3P (Fig. 4) and HepG2 (Fig. 5) cells were cultured at 37°C, 5% CO_2 and 21% O_2 in 175cm^2 flasks (Nunc, Roskilde, Denmark) in DMEM containing low in D(+)-glucose, sodium pyruvate and L-glutamine (Gibco, Invitrogen Ltd, Paisley, UK). Medium was supplemented with 10% FCS and 1% penicillin/streptomycin. Cells were grown in 75cm^2 flasks (5 x 10^5 cells/flask; Nunc), 6 well dishes (5 x 10^4 cells/well; Iwaki, Tokyo, Japan) or 24 well dishes (1 x 10^4 cells/well; Corning, Lowell, USA). The day before any treatment, medium was replaced with fresh DMEM low in D(+)-glucose, without FCS, supplemented with 1% penicillin/streptomycin over night. On the

following day, the cells were treated with DMEM low (normoglycemia; 5.5mmol/l) or high (hyperglycemia; 25mmol/l) in D(+)-glucose, supplemented with 2% FCS and 1% penicillin/streptomycin, for up to three days at 37°C, 5% CO_2 and 2.5%, 8% or 21% oxygen in an XVIVO incubation system Model G300C. As osmotic control 19.5mmol/l L(-)-glucose was again added to DMEM low in D(+)-glucose. Media were replaced every 24h in the XVIVO incubation system.

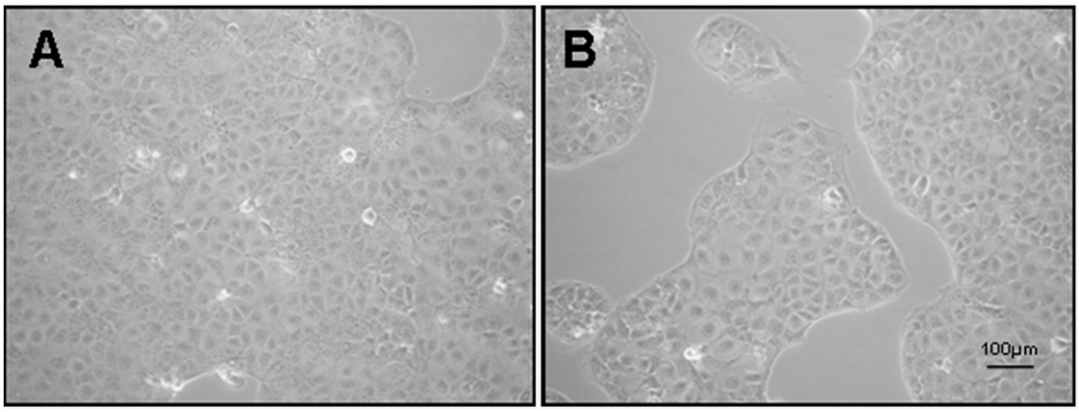

Figure 4 **ACH-3P cells in culture under normoglycemia at 21% oxygen.** (A) ACH-3P cells 90% confluent, (B) ACH-3P cells 40% confluent.

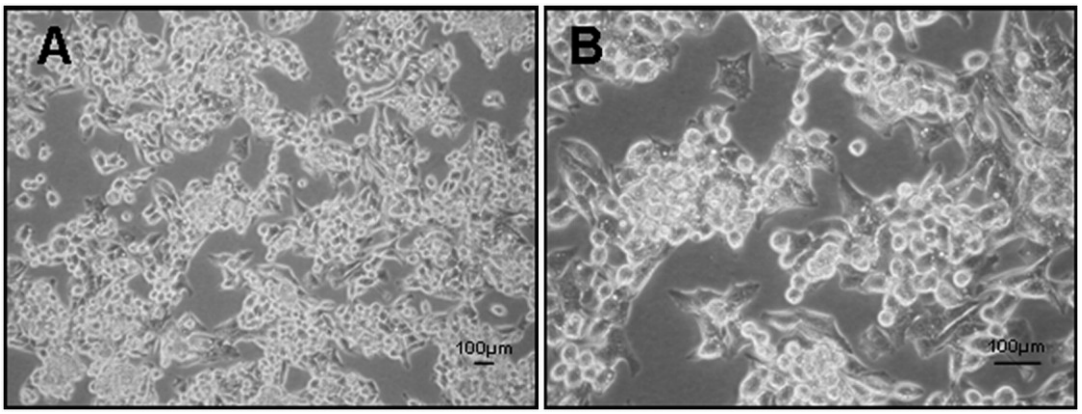

Figure 5 **HegG2 cells in culture under normoglycemia at 21% oxygen.** (A and B) HepG2 cells 80% confluent.

3.2 Proliferation assay

Cell proliferation was determined by automatic counting of viable and dead cells using CASY® Model TT (Schärfe System, Reutlingen, Germany). Proliferation of ACH-3P cells was determined after 1 to 3 days of treatment. For CASY® measurements, cells were enzymatically detached, and 50µl of cell suspension were diluted (1:200) in 10ml CASY®ton (Roche, Mannheim, Germany) and viable and dead cells were determined.

3.3 Cell cycle analysis

Cell cycle was analysed by flow cytometry at the Flow Cytometry Core Facility at the Center for Medical Research (ZMF) of the Medical University of Graz. After 3 days of treatment the cells were harvested, centrifuged, resuspended in 500µl phosphate buffered saline (PBS; Gibco) and fixed with 5ml ice-cold 70% ethanol (Merck, Darmstadt, Germany) at 4°C for 10min. After fixation, cells were centrifuged and washed twice with 5ml PBS. Pellets were resuspended in 250µl PI-staining buffer (Beckman Coulter, Brea, USA), incubated for 15min at 37°C and kept on ice until analysis. Cell cycle distribution was determined by FACSCalibur (BS Bioscience, Maryland, USA). The proportion of cells in each cell cycle phase (G_1, S and G_2/M) was determined by Moefit Software (Verity Software House, Topsham, USA).

3.4 Cell survival assays

Cell survival assays were performed by flow cytometry, at the Flow Cytometry Core Facility at the Center for Medical Research (ZMF) of the Medical University of Graz. After an incubation time of 3d cells were harvested, centrifuged, resuspended in 500µl PBS and fixed with 500µl 4% formaldehyde at 37°C for 10min. After fixation, cells were put on ice for at least 1min and stored at 4°C. Cell suspension was slowly mixed with ice-cold 100% methanol (Merck) by carefully vortexing and incubated at 4°C for further 30min. For staining, cells were centrifuged at room temperature and the pellet was dissolved in 2ml incubation buffer (100ml PBS + 500µl FCS) and centrifuged again. The new pellet was resuspended in 90µl incubation buffer and incubated 10min at room temperature. 2µl of cleaved caspase 3 (Asp175) Antibody-Alexa Fluor 488

Conjugate (Cell Signaling, Boston, USA) was added and subsequently incubated for 30 to 60min at room temperature in the dark. 2ml incubation buffer was added to the cells, which were centrifuged and resuspended in 300µl PBS. The stained cell suspension was analysed using FACSCalibur. The proportion in percent of cleaved caspase 3 positive was determined by Moefit Software.

3.5 Exposure of ACH-3P cells to 6-AN

6-aminonicotinamide (6-AN; Sigma-Adrich, Steinheim, Germany) blocks the $NADP^+$-dependent enzyme 6-phosphogluconate dehydrogenase (Lange and Proft, 1970, Rostand and Work, 1985) and therefore inhibits the pentose phosphate pathway. Culture medium was supplemented with 100µmol/l 6-AN. Stocks were prepared in DMSO, which was also used as vehicle control. Cells were treated for 3 days with medium supplemented with 6-AN.

3.6 ROS assays

3.6.1 Quantification of intracellular ROS

Intracellular ROS generation was measured using non-fluorescent 2,7-dichlorodihydrofluorescein diacetate, H_2DCFDA (Invitrogen), which becomes fluorescent through oxidation and remains in the cytosol after enzymatic intracellular hydrolysis. Relative increase in fluorescence intensity was used as indicator for oxidative stress. ACH-3P cells were cultured in 24 well dishes under normoglycemia, hyperglycemia and osmotic control conditions at 2.5%, 8% and 21% oxygen for up to 3 days. After treatment, cells were loaded with 10µmol/l H_2DCFDA for 15min and the dye was replaced by PBS (Gibco) subsequently. Fluorescence intensity was determined (485nm/520nm Ex/Em) using a FluoSTAR Optima 413 spectrofluorimeter (BMG Labtechnologies, Offenburg, Germany). For normalization to cell numbers after fluorescence measurements, cells were washed once with HBSS and loaded with 1µmol/l CellTrace™ calcein violet AM (Invitrogen) for 30min at 37°C to determine cell viability. Wells were measured in staining solution (355nm/460nm Ex/Em). Non-fluorescent calcein violet AM permeates cell membranes and is enzymatically

hydrolysed to a fluorescent charged form, retained in living cells. We used it as a proxy for the number of viable cells accounting for proliferation changes at various culture conditions. Subsequently, the signal obtained by intracellular ROS generation was normaized to that of calcein violet for each well.

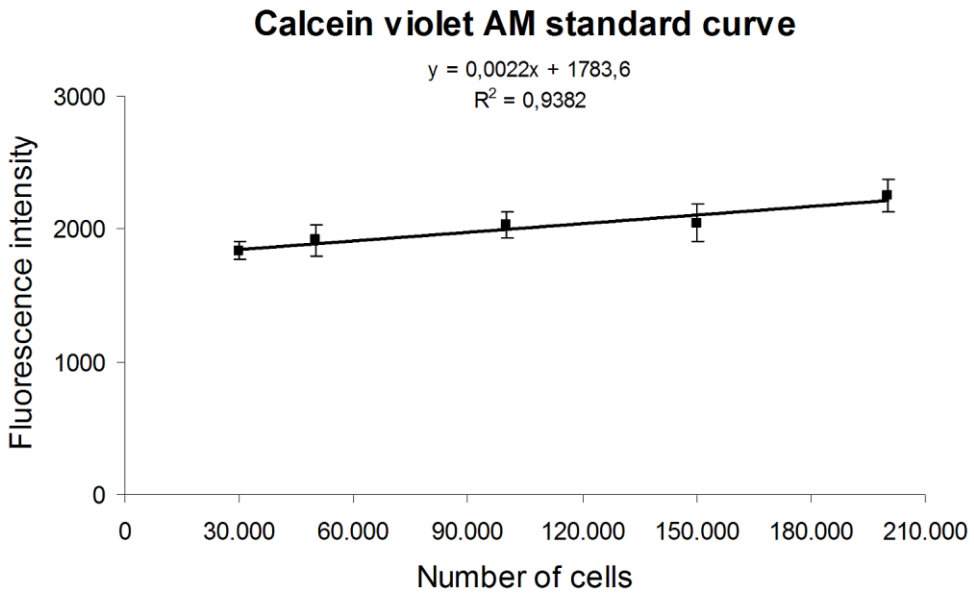

Figure 6 **Calcein violet AM standard curve at 355nm/460nm Ex/Em.** Varying cell numbers stained with calcein violet AM (1µmol/l); mean ± SD (n = 6).

3.6.2 Quantification of hydrogen peroxide (H_2O_2)

H_2O_2 released from ACH-3P cells after 3d under hyperglycemia at 21% oxygen was measured using Amplex Red (10-acetyl-3,7-dihydroxyphenoxazine) in combination with horseradish peroxidase (HRP). Cells were cultured in 24 well dishes under normo- and hyperglycemic conditions. After incubation, cells were washed once and incubated with HBSS containing 100µmol/l Amplex Red and 1U/ml HRP (Sigma Aldrich). The increase in resorufin fluorescence was immediately measured at 544nm/580nm (Ex/Em) for 20min using monochromatization and top excitation. In order to account for proliferation changes at various culture conditions resorufin fluorescence readings were normalized to cell numbers using DAPI staining as a proxy for the number of cells. To this end the cells were washed once and subsequently fixed with 4% formaldehyde for 15min at 37°C, washed again with HBSS and stained with 500µl DAPI (2.5µg/ml;

Invitrogen) for 10min at 37°C. Cell fluorescence was measured in PBS at 355nm/460nm (Ex/Em). Subsequently, the signal representing released H_2O_2 was normaized to that of DAPI staining for each well.

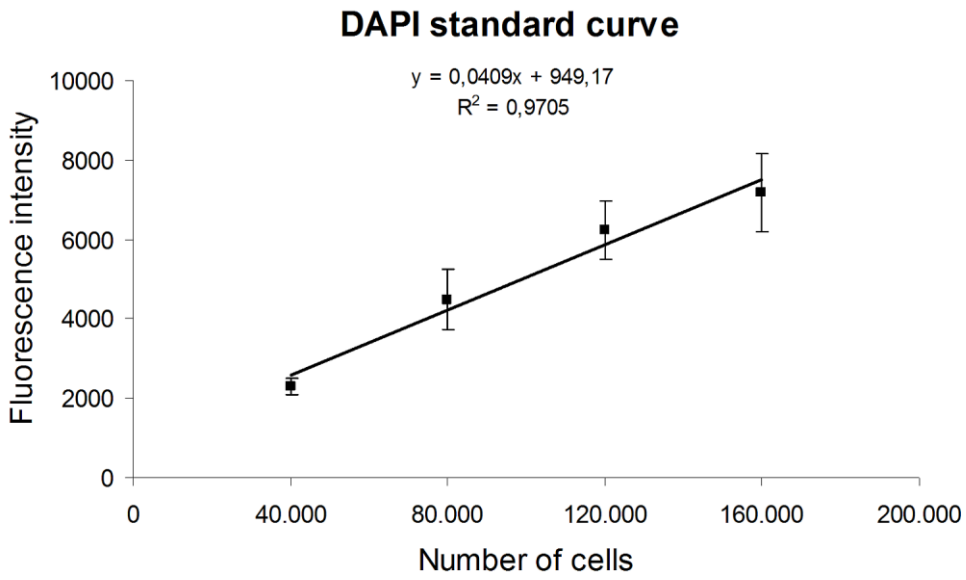

Figure 7 **DAPI standard curve at 355nm/460nm Ex/Em.** Varying cell numbers stained with DAPI (2.5µg/ml); mean ± SD (n = 6).

3.6.3 Visualisation of mitochondrial superoxide

Mitochondrial superoxide was assayed with MitoSOX™ Red (Invitrogen) that permeates living cells and targets mitochondria, where it is oxidised by superoxide yielding red fluorescence. After 3 days under normo- or hyperglycemia, cells were loaded with 5µmol/l MitSOX™ Red for 10min at 37°C. Microscopic fluorescence images were taken (Eclipse TE2000-U, Nikon, Vienna, Austria) at fixed exposure time. Subsequently, cells were incubated with 2.5µmol/l CellTracker™ Green CMFDA (Invitrogen) for 20min at 37°C to visualise living cells.

3.7 Mitochondrial activity

WST-1 reagent (Roche, Mannheim, Germany) was used to determine mitochondrial activity. This assay is based on a cleavage of tetrazolium salt WST-1(4-[3-(4-

Iodophenyl)-2-(4-nitophenyl)-2H-5-tetrazolio]-1,3-benzene disulfonate) to formazan by mitochondrial dehydrogenases. Cells were cultured for 1 to 3 days under normo-and hyperglycemic conditions. After each treatment period 100µl of WST-1 was added to each well containing 1ml culture medium and incubated for 1h at 37°C. Afterwards, 24 well dishes were shaken at 450rpm for 1min. The optical density was measured in a microplate spectrophotometer Tristar LB 941 (Berthold Technologies, Bad Wildbad, Germany) at 450nm with 620nm as wavelength reference. To determine background absorbance of the culture medium wells without cells after the addition of WST-1 were measured as well. These values were subtracted from the values of wells containing cells. After measurement of mitochondrial activity the cells were fixed with 4% formaldehyde for 15min at 37°C, washed once with HBSS and stained with 500µl DAPI (2.5µg/ml) diluted in PBS for 10min at 37°C. The DAPI solution was removed; cells were washed again and 1ml fresh PBS was added. Cell number was determined (355nm/460nm Ex/Em) using a microplate fluorescene spectrometer FluoSTAR Optima 413 (BMG Labtechnologies, Offenburg, Germany). For data analysis WST-1 values were normaized to number of cells.

3.8 ATP measurement

ACH-3P cells were cultured for 3 days under hyperglycemia at 21% oxygen. As positive control for decreased ATP production cells were treated under low and high glucose conditions in presence of antimycin A (10µmol/l). After the treatment period cells were lysed and ATP concentration was determined using a CellTiter-Glo® Luminescent Cell Viability Assay (Promega, Madison, USA) according to the manufacturer's instruction. In brief, the plate (6 well dish) was equilibrated at room temperature for approximately 30min. 2ml of the CellTiter-Glo® Reagent was added to each well. Subsequently, contents were mixed for 2min on an orbital shaker to induce cell lysis. To allow stabilisation of the luminescent signal the plate was incubated at room temperature for 10min. Control wells containing medium without cells were used to obtain a value for background luminescence. The data were normaized to total protein.

3.9 Exposure of ACH-3P cells to varying antioxidants

For antioxidant studies, culture medium was supplemented with 100µmol/l ascorbate, 100µmol/l Trolox® and 1mmol/l NAC (Sigma-Aldrich). Stock solutions of ascorbate and NAC were prepared in bidistilled water, Trolox® in ethanol. As vehicle control ethanol was added to medium and incubated under the same conditions for 3 days.

3.10 Exposure of ACH-3P cells to allopurinol, apocynin, VAS-2870 and BCNU

For inhibition of xanthine and NAPDH oxidase culture medium was supplemented with varying concentrations of inhibitors. 0.1-1mmol/l allopurinol, 100µmol/l and 250µmol/l apocynin (Sigma-Aldrich) and 1µmol/l VAS-2870 (Enzo Life Science, Plymouth Meeting, USA) were used. Stock solution of allopurinol was prepared in bidistilled water. Apocynin was diluted in ethanol and VAS-2870 stock was prepared in DMSO (Merck). 1, 3-bis-(2-chloroethyl)-1-nitrosourea, BCNU, (Sigma-Aldrich) inactivates glutathione reductase and interrupts recycling of glutathione disulfide to glutathione. It was dissolved in PBS and added at final concentrations of 5µmol/l, 10µmol/l and 15µmol/l. As vehicle, ethanol or DMSO was added to medium and incubated under the same conditions for 3 days.

3.11 Exposure of ACH-3P cells to antimycin A, oligomycin and FCCP

Antimycin A is an inhibitor of complex III of the mitochondrial electron transport chain. Oligomycin was used as ATPase (complex V) inhibitor and carbonyl cyanide 4-(trifluoromethoxy) phenylhydrazone, FCCP, (Sigma-Aldrich) as an uncoupler of oxidative phosphorylation, inhibiting mitochondrial O_2.- production. Antimycin A and oligomycin were added at a final concentration of 10µmol/l to the medium. FCCP was used at concentrations of 0.1µmol/l, 0.3µmol/l and 0.5µmol/l. Stocks were prepared in ethanol and DMSO, which were also used as vehicle controls. Cells were treated for 3 days.

3.12 Exposure of ACH-3P cells to U0126 and wortmannin

U0162 (Calbiochem, San Diego, USA) is a potent and specific inhibitor of MEK1 and MEK2, hence, it blocks the extracellular signal-regulated kinases 1 and 2 (ERK1/2) signaling pathway. Wortmannin (Calbiochem) was used as protein kinase B (Akt/PkB) inhibitor. U0126 and wortmannin were added to the medium at a final concentration of 10µmol/l and 100nmol/l, respectively. Stocks were prepared in DMSO, which was also used as vehicle control. Cells were treated for 3d.

3.13 RNA isolation

Total RNA was isolated using TRI Reagent (Applied Biosystems, Foster City, USA) according to the manufacturer's instruction. The RNA concentration was determined by a spectrophotometer NanoDrop ND-1000 (Peqlab Biotechnologies GmbH, Erlangen, Germany) and the RNA quality was assessed by gel red staining of denaturing agarose (Biozym, Vienna, Austria) gels.

3.14 Real-Time RT-PCR

RNA was reverse-transcribed using High-Capacity cDNA Reverse Transcription Kit (Applied Biosystems). Briefly, 2µg RNA from cells cultured under normo- or hyperglycemia were incubated with the kit components, in a total volume of 20µl, for 10min at 25°C, 120min at 37°C and 10sec at 85°C in a thermocycler Gene Amp® PCR System 9700 (Applied Biosystems).

Real-Time RT-PCR was performed using QuantiFast SYBR Green PCR Kit (Qiagen, Germantown, USA) for glutathione reductase 1 (Hs_GPX1_1_SG, QuantiTec Primer Assay; Qiagen), nuclear factor (erythroid-derived 2)-like 2 (Hs_ NFE2L2_a_SG, QuantiTec Primer Assay) and heme oxygenase (Hs_HMOX1_1_SG, QuantiTec Primer Assay). Ribosomal L30 (Hs_RPL30_1_SG, QuantiTec Primer Assay) served as internal control. Briefly, cDNA templates were 1:10 diluted and 13.2µl cDNA was mixed with 13.2µl SYBR Green (2x) and 3.3µl Primer (10x). A LightCycler 480 (Roche, Mannheim, Germany) was used to analyse gene expression levels in triplicates. The appropriate program involves initial denaturation of 5min at 95°C and a subsequent

two-step cycle at 95°C for 10sec and at 60°C for 30sec for 40 cycles. The Ct values were automatically calculated by the LightCycler 480 Software and relative gene expression was calculated by standard ΔΔCt method using expression level of RPL30 as reference.

3.15 RT^2 Profiler^{TM} PCR Array

Total RNA was treated with DNase for 10min at RT using RNase-Free DNase Set to digest remaining genomic DNA and subsequent cleaned up with an RNeasy Kit (Qiagen). Reverse transcription of DNase treated RNA was performed with RT^2 First Strand Kit (Qiagen). All subsequent treatment steps were carried out using the Human Oxidative Stress and Antioxidant Defense RT^2 Profiler^{TM} PCR Array (Qiagen) according to the manufacturer's instruction.

Briefly, 5µg total RNA was added to 5 x cDNA Elimination Buffer and RNase free H_2O, mixed gently and incubated for 5min at 42°C in a thermo cycler Gene Amp® PCR System 9700. Immediately, the mixture was chilled on ice for at least one minute. 4µl of 5 x RT Buffer 3, 1µl of Primer External Control Mix, 2µl RT Enzyme Mix 3 and 3µl of RNase free H_2O were mixed and added to the pre-treated RNA. Both, RT Cocktail and Genomic DNA Elimination Mixture were mixed gently with a pipettor and incubated at 42°C for exactly 15min and immediately the reaction was stopped by heating at 95°C for 5min in the thermo cycler und subsequent addition of 91µl H_2O to each 20µl of cDNA synthesis reaction. After synthesis of the first strand cDNA was mixed well and frozen at -20°C until use. On the following day the RT^2 SYBR® Green qPCR Master Mix was prepared and added to 102µl first strand cDNA. 25µl of the Experimental Cocktail was pipetted to each well of the PCR Array. The Array plates were carefully sealed with an optical adhesive film, centrifuged for 1min at room temperature at 1000 x g to remove bubbles and placed in a Real-Time LightCycler 480. The used appropriate program is listed in Tab. 1 and the ramp rate was adjusted to 1°C/sec. As heat activation 95°C for 10min with a ramp rate of 4.8°C/sec was chosen. The Ct values were automatically calculated by the LightCylcler 480 Software and relative gene expression was calculated by standard ΔΔCt method using expression level average of B2M, HPRT1 and RPL13A as reference.

Tabel 1

Two-step cycling program for Roche LightCycler 480

Cycles	Duration	Temperature
1	10min	95°C
45	15sec	95°C
	1min	60°C

3.16 Immunoseparation of ACH-3P cells using flow cytometry

Five x 10^6 cells were separated using flow cytometry at the Flow Cytometry Core Facility at the Center for Medical Research (ZMF) of the Medical University of Graz. For staining the membrane anchored HLA-G on living cells, ACH-3P cells were washed once with PBS, harvested, centrifuged, resuspended in PBS containing an HLA-G antibody (MEM-G/9, 1:200, 11-292-C100 Exbio, Vestec, Czech Republic) and incubated with agitation for 30min at room temperature (RT). Cells were washed once again and incubated with a secondary antibody (rabbit anti-mouse-FITC 488, 1:200, Invitrogen) for 30min at RT. After several washing steps, cells were centrifuged and resuspended in PBS; buffered formalin (1%) was added to cells. The stained living cells were separated using FACSCalibur, centrifuged and resuspended in DMEM low in D(+)-glucose and incubated over night in wells coated with 1% gelatine (Sigma-Aldrich).

3.17 Immunoseparation of ACH-3P cells using magnetic beads

For HLA-G separation cells were washed and harvested with accutase, centrifuged and resuspended in DMEM low in D(+)-glucose supplemented with 10% FCS and 1% penicillin/streptomycin. To obtain single cell suspension cells were filtered through a 70µM nylon cell strainer (BD Biosciences, Erembodegem, Belgium). Separation was performed with immunomagnetic dynabeads M-450 (Invitrogen), which were coated with 12µl of a monoclonal antibody for HLA-G (MEM-G/9) at 4°C using a mixer that

provides tilting and rotation of the reaction tube. After conjugation dynabeads were washed three times with PBS supplemented with 0.1% BSA (Sigma-Aldrich) and 2mmol/l EDTA (Invitrogen). Washed dynabeads and 1 x 10^6 cells were incubated for 30min at 4°C and mixed permanently. A Dynal magnet (Invitrogen) was used for 3min to separate HLA-G positive and negative cells. The supernatant containing HLA-G negative cells was centrifuged at 350 x *g* for 5min and resuspended in 2ml DMEM. The pellet comprising HLA-G positive cells was immediately dissolved in 2ml fresh DMEM. Both subpopulations were seeded out in 6 well dishes coated with 1% gelatine and cultured at 37°C (Hiden et al., 2007). The separation quality was determined by measuring mRNA expression of HLA-G using semi quantitative RT-PCR.

3.18 Semi quantitative RT-PCR

Semi quantitative RT-PCR was used to confirm immunoseparation of ACH-3P cells. Primer pairs for HLA-G (Forward: AGG AGA CAC GGA ACA CCA AG; Reverse: GGA GAG CCT ACC TGG AGG) were designed using the public web-page Primer3 (Ingenetix, Vienna, Austria). RPL30 (Forward: CCT AAG GCA GGA AGA TGG TG; Reverse: AG TCT GTT CTG GCA TGC TT; MWG Biotech AG, Ebersberg, Germany), a ribosomal protein, served as internal control. Total RNA (200ng) of HLA-G positive and negative cells was isolated immediately after immunoseparation as well as after a treatment period of 3 days. RNA was reverse transcribed and amplified using one step RT-PCR kit (Qiagen, Germantown, USA) according to the manufacturer's instruction. For HLA-G and RPL30 mRNA expression 29 and 24 cycles were utilized, respectively in a thermo cycler Gene Amp® PCR System 9700. The annealing temperature for both gene amplification was 60°C. After RT-PCR samples were loaded on a 2% agarose gel and band intensity was detected by Multimage III (Cell Bioscience, Santa Clara, USA). Gene expression was quantified with RPL30 using an AlphaView software (Cell Bioscience).

3.19 Immunofluorescent staining

Paraffin sections of 5µm were cut from each placenta and placed on Superfrost Plus slides (Menzel, Braunschweig, Germany), dried over night at 37°C and stored at room temperature. The sections were deparaffinised in xylene (Merck) and rehydrated through a series of graded alcohol. Antigen retrieval was performed in a 0.01mol/l citrate buffer at pH 6 using a microwave (3 x 7min). Sections were cooled down again for 20min at room temperature and subsequently rinsed three times in 1 x TBS containing 0.05% Tween (Merck) for 2min. For immunofluorescent double staining slides were incubated for 8min with a UV-Block (Dako, Glostrup, Denmark) to avoid unspecific background staining. Meanwhile, the primary antibodies for cytokeratin 7 (AP06204PU-N; Acris, San Diego, USA) and Ki-67 (Mib-1 M7240; Dako) were diluted 1:200 and 1:100 in antibody diluent (Dako), respectively. The sections were rinsed again three times in 1 x TBS containing 0.05% Tween and stained for 30min at room temperature for cytokeratin 7 and Ki-67. After washing in TBS, slides were incubated with fluorescent-labelled secondary antibodies (1:100, Alexa Fluor® 555 goat anti-mouse IgG and Alexa Fluor® 488 goat anti-rabbit IgG; Invitrogen) for 30min at room temperature. Nuclei were stained for 10min with DAPI (2.5µg/ml) diluted in 1 x TBS and rinsed several times in deionized water, dried for 15min at room temperature and mounted with ProLong® Gold anitfade reagent (Invitrogen). For analysis a Leica DM600B (Wetzlar, Germany) fluorescent microscope connected to an Olympus DP72 digital camera (Tokyo, Japan) was used. From each placenta 6 images were captured of randomly selected staining areas by Visiomorph software (Visiopharm, Hoersholm, Denmark). For proliferation studies all Ki-67 positive stained cytotrophoblast cells relative to all cytotrophoblast cells were manually counted using newCAST software (Visiopharm).

Tabel 2

Primary antibodies used for immonosepaeration and immunofluorescence

Antigen/Isotype	Clone	Dilution	Host	Company
HLA-G/mc	MEM-G/9	1:200	Mouse IgG	Exbio
Ki-67/mc	Ki-67	1:100	Mouse IgG	Dako
Cytokeratin 7/pc	/	1:200	Rabbit IgG	Acris

mc, monoclonal; pc, polyclonal

3.20 Analysis of MAPK, JNK, p38 and Akt/PkB phosphorylation

For phosphorylation studies, ACH-3P cells were cultured in 25cm^2 flaks (5 x 10^5 cells/flask) to 70% confluence. Cells were serum-starved over night and on the following day the serum free medium was replaced by DMEM low in D(+)-glucose containing 2% FCS for 2h. Subsequently, ACH-3P cells were treated for 15, 30 and 60min under normo-and hyperglycemic conditions in the presence of 2% FCS. As 0min control cells were harvested after 2h under 2% FCS and normoglycemia. ACH-3P cells treated for 30min in 15% FCS served as positive control for MAPK and Akt/PkB phosphorylation. UV-treated (30min) ACH-3P cells were used as positive control for JNK and p38 phosphorylation. Immediately after stimulation, the flasks were frozen at -20°C. On the following day the cells were lysed and immunoblotted.

3.21 Immunoblotting

ACH-3P cells were washed once with HBSS and lysed using RIPA lysis buffer (Sigma-Adrich). Total protein concentration was determined with Lowry protein assay according to the manufacturer's instructions. Total protein (40mg) was separated on a precast 10% Bis-Tris gel (NuPAGE, Invitrogen) and subsequently semi-dry blotted on a 0.45µm nitrocellulose membrane (Hybond; Amersham Biosciences, Piscataway, USA). Ponceau S solution (Sigma-Aldrich) was used to verify blotting efficiency. Immunolabeling was visualized by a chemiluminescent immunodetection kit (Western

Breeze, Invitrogen) according to the manufacturer's instructions. Beta-actin was used as loading control. The membrane was regenerated with a Restore™ Plus Western Blot Stripping Buffer (Pierce, Rockford, USA) according to the manufacturer's instruction. All antibodies, dilutions and manufacturers are shown in Tab. 3.

Tabel 3

Dilution and companies of the used antibodies for immunoblotting

Antigen	Dilution	Clone	Host	Company
phospho-ERK1/2 MAPK	1:1000	#9101	Rabbit	Cell Signaling
phopspho-p38	1:2000	#9216	Mouse	Cell Signaling
phospho-Akt/PkB	1:1000	#5106	Mouse	Cell Signaling
phospho-JNK	1:2000	#9255	Mouse	Cell Signaling
Cyclin B1	1:1000	#4138	Rabbit	Cell Signaling
beta -actin	1:20.000	ab6276	Mouse	Abcam

3.22 Antibody microarray

ACH-3P cells were treated in 25cm^2 flaks for 3 days under normo- and hyperglycemic conditions at 21% oxygen. To monitor the protein status of ACH-3P cells under hyperglycemia after the treatment period an Antibody Microarray (Full Moon BioSystems, Inc, Sunnyvale, USA) was performed. All preparation steps were carried out according to the manufacturer's instruction.

Briefly, cells were washed once with ice-cold 1 x PBS and around 2 x 10^6 cells were collected by scraping from the flaks. Cell suspension was washed again three times with ice-cold PBS and centrifuged at 4°C and 350 x *g* for 5min. Cell pellet was dissolved in 200µl Extraction Buffer, cell lysate was mixed rigorously by vortexing for 30sec and immediately incubated for 10min on ice and centrifuged at 4°C and 10.000 x

g for 15min. The clear supernatant was transferred to a new 1.5ml Eppendorf tube and kept on ice. Meanwhile, preparation of gel columns was performed. Therefore columns were reconstituted by adding 650µl of Labeling Buffer and vortexed vigorously for about 5sec. Air bubbles were removed by sharply tapping the bottom of the column. The columns were kept at RT for 30min to allow hydration. To remove excess fluid the columns were spun at 750 x *g* for 2min and subsequently the protein extracts (100µl) were carefully transferred to the centre the columns without disturbing the gel surface. Each column was placed in a collection tube and centrifuged at 750 x *g* for 2min. The purified protein was collected and used for further steps.

The protein concentration was determined using BCA protein assay according to the manufacturer's instruction. 2-10µg/µl protein was filled up to a volume of 75µl and 3µl of Biotin/DMF solution was added to each protein sample. The mixture was incubated at RT for 1h. 35µl of Stop Reagent was added and incubated for another 30min at RT with mixing. The samples were stored at -80°C until the following day.

On the next day the Antibody Microarray slides were warmed up to RT for 45min. In a 100 x 150mm Petri dish each slide was blocked with 30ml Blocking Solution on an orbital shaker rotating at 55rpm for 30min at RT. The slides were washed 6 x 10min with 1 x Washing Buffer at 55rpm and twice with Milli-Q grade H_2O.

The next step was to couple the protein sample. 50µg biotin labelled protein was mixed with 100µl Coupling Solution and vortexed briefly. In the meantime, antibody spots on the slides were marked with a PapPen (DakoPen; Dako). All 100µl Protein Coupling Mix was slowly pipetted on the slide and incubated in a Coupling Chamber for 1h at RT in the dark covered with aluminium foil. After coupling, the slides were again washed 6 x 10min with Washing Buffer and twice with Milli-Q grade H_2O.

For detection, 60µl of Cy3-Streptavidin (0.5mg/ml) was added to 60ml of Detection Buffer. Coupled slides were put in Petri dish and incubated with 30ml of Cy-3 Streptavidin Solution on an orbital shaker at 55rpm for 20min at RT in the dark and subsequently washed 6 x 10min with Washing Buffer and twice with Milli-Q grad H_2O. Excess water was shaken off and slides were dried with compressed nitrogen. The Microarray slides were scanned using DNA Microarray Scanner (Agilent Technologies, Santa Clara, USA) and relative protein expression was calculated using Gene pix pro 6.0 Software (Molecular Devises, Sunnyvale, USA). The protein expression was

normaized relative to total protein expression, which were expressed in every sample and condition.

3.23 Statistical analysis

Statistical analysis used Prism 5 (GraphPad Software, La Jolla, USA). Differences between two treatment conditions were tested with unpaired *t*-test. Differences between three or more groups were analysed with One Way ANOVA followed by Bonferroni test. Data were expressed as mean ± SD, mean ± SEM or median. *P* values of < 0.05 were considered statistically significant.

4 Results

4.1 Basal proliferation under normoglycemia is oxygen-independent

First the effect of varying oxygen concentrations on cell proliferation at varying oxygen concentrations was investigated. To this end ACH-3P cells were cultured for up to 3 days under normoglycemia at 2.5%, 8% and 21% oxygen. Subsequently, viable and dead cells were counted. Neither number of viable nor dead ACH-3P cells was significantly altered after 1 to 3 days under normoglycemic conditions at different oxygen concentrations (Fig. 8A and B).

The proportion of dead cells after 3 days of incubation amounted to 17%, 19% and 20% of total cells at 2.5%, 8% and 21% oxygen, respectively. These data suggest that basal proliferation of ACH-3P cells under normoglycemia is oxygen-independent.

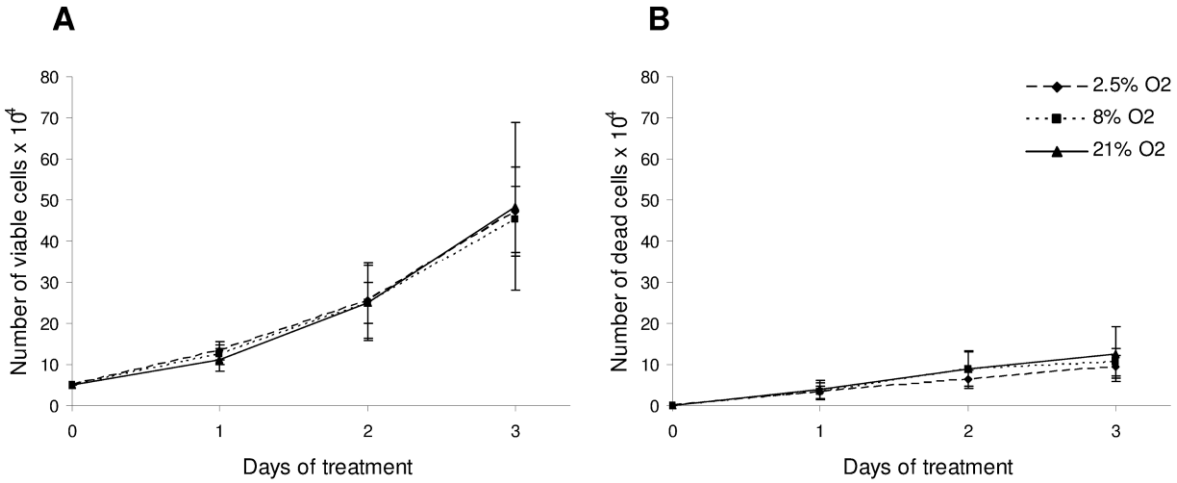

Figure 8 **Proliferation of ACH-3P cells up to 3 days under normoglycemia at 2.5%, 8% and 21% oxygen.** (A) Number of viable cells at 2.5%, 8% and 21% oxygen; (B) number of dead cells at 2.5% , 8% and 21% oxygen; mean ± SD (n = 6), data were obtained from three independent experiments.

4.2 Proliferation and cell cycle analysis of ACH-3P cells

Under hyperglycemic conditions, the number of viable cells did not differ after 1 to 3 days at 2.5% and 8% oxygen, compared to normoglycemic conditions. Likewise, also the number of dead cells was not affected by these conditions (Fig. 9A and C).

The absence of changes in cell number corresponded to cell cycle analysis, which did not show significant alterations in the G_1-, S- and G_2/M-phase (Fig. 9B and D). Hence, hyperglycemia did not affect cell growth and cell cycle at 2.5% and 8% oxygen.

However, at 21% oxygen, hyperglycemia led to decreased cell proliferation compared to normoglycemia and osmotic control. Two days under hyperglycemic conditions resulted in 40% fewer viable ACH-3P cells. Viable cells were even more decreased (up to 65%) after 3 days under hyperglycemia ($p<0.001$) compared to cells cultured under normoglycemic and osmotic control conditions. No alterations in dead cell count were observed (Fig. 9E).

Cell cycle analysis showed a significant increase in cells in S-phase and a tendency of decreased G_1-phase ($p=0.07$) under hyperglycemia at 21% oxygen. Compared to cells treated under normoglycemia, the G_2/M-phase was unchanged (Fig. 9F). These results indicate that reduced proliferation under hyperglycemia is caused by changes in G_1- and S- but not in the G_2/M-phase.

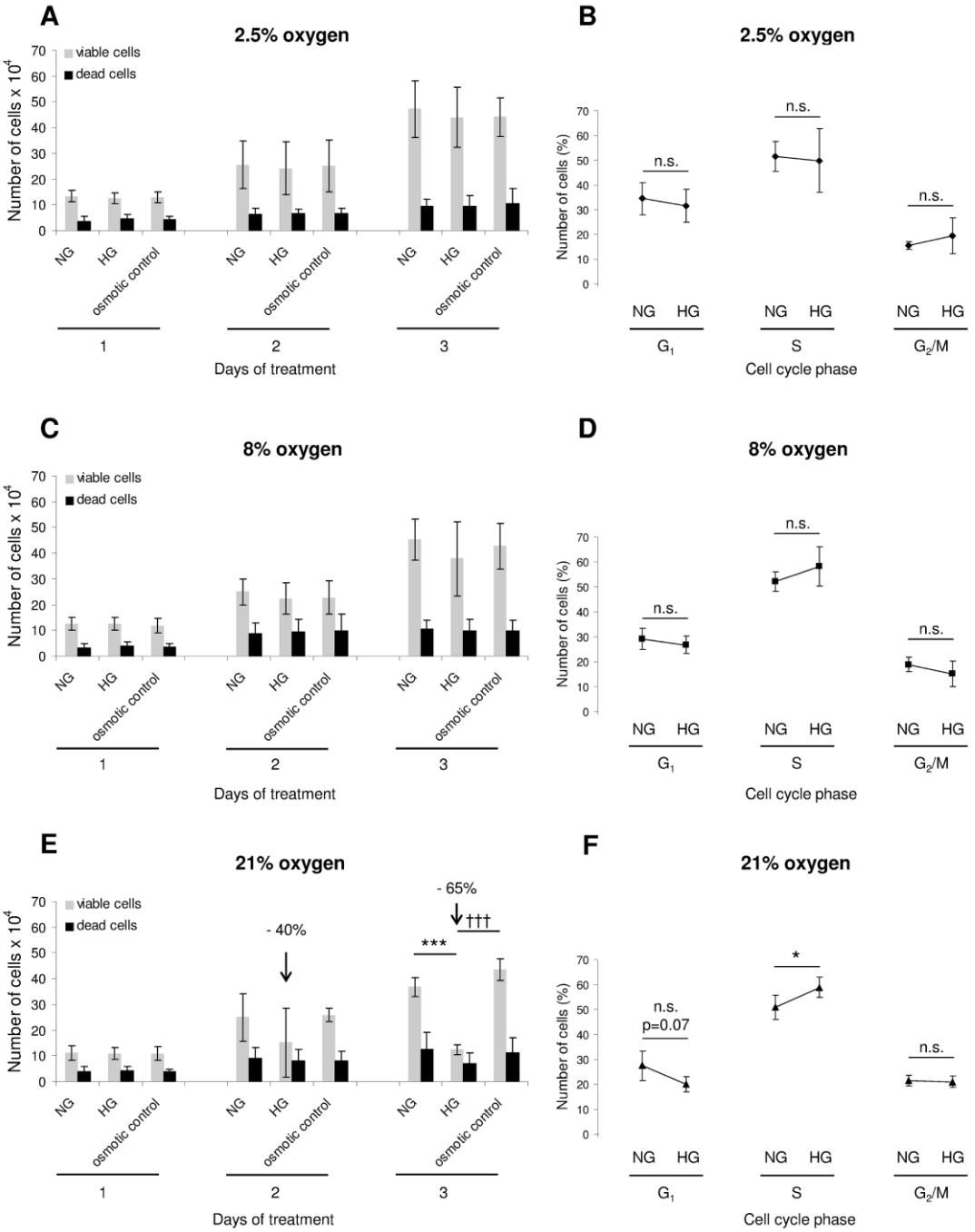

Figure 9 **Proliferation and cell cycle analysis of ACH-3P cells cultured for up to 3 days under normo- and hyperglycemia at 2.5%, 8% and 21% oxygen.** (A, C, E) Number of viable (grey bars) and dead (black bars) cells; mean ± SD (n = 6), data were obtained from three independent experiments; (B, D, F) cell cycle analysis (G_1-, S- and G_2/M-phase); mean ± SD (n = 4). $^{*}P < 0.05$, $^{***}P < 0.001$ vs. NG; $^{\#\#\#}P < 0.001$ vs. osmotic control. n.s. not significant. (A, C and E) Based on 18 replicates the coefficient of variation for 1, 2 and 3 days under NG was 17%, 35% and 23% at 2.5% oxygen, 19%, 20% and 18% at 8% oxygen and 25%, 37% and 10% at 21% oxygen, respectively. After 1, 2 and 3 days under HG the coefficient of variation was 16%, 43% and 27% at 2.5% oxygen, 20%, 27% and 38% at 8% oxygen and 21%, 88% and 14% at 21% oxygen, respectively.

4.3 Cell survival assay

To confirm the results of the proliferation assay under hyperglycemic conditions at 2.5%, 8% and 21% oxygen flow cytometry for cleaved caspase 3 was performed.

In Fig. 9A 17% of the total cell number were dead cells under normo- and hyperglycemia at 2.5% oxygen, likewise 2.5% and 3% cells are positive for cleaved caspase 3 (Fig 10). At 2.5% oxygen no significant alterations in dead and apoptotic cells were observed. A similar situation was monitored at 8% oxygen. 19% and 20% dead cells (Fig. 9C) were counted and 1.7% and 3.3% (Fig. 10) cells were cleaved caspase 3 positive under normo- and hyperglycemic conditions, respectively.

In Fig. 9E 26% and 36% cells of the total cell amount were determined as dead cells under normo- and hyperglycemic conditions, respectively. At 21% oxygen, significantly increased numbers of cleaved caspase 3 positive cells were detected. As shown in Fig. 10, 1.9% and 3.9% cleaved caspase 3 positive cells were measured under normo- and hyperglycemia, respectively. These data indicate that ACH-3P cells under high glucose and high oxygen conditions show higher apoptotic cells levels.

These results indicate that reduced cell proliferation under high glucose and high oxygen is certainly not only induced by cell death, however decreased proliferation may occur as a consequence of both, apoptosis and reduced cell growth.

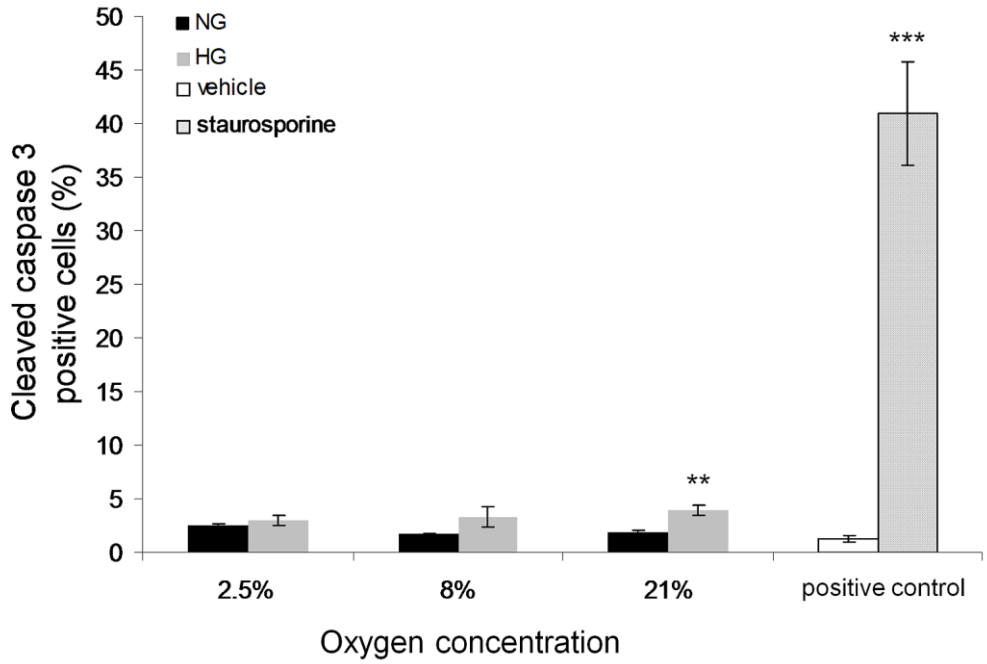

Figure 10 **Cleaved caspase 3 assay of ACH-3P cells after 3 days under hyperglycemia at 2.5%, 8% and 21% oxygen.** Percentage of cleaved caspase 3 positive cells under normo- and hyperglycemia at 2.5%, 8% and 21% oxygen. 2µmol/l staurosporine was added for 2h and served as positive control for apoptosis. Percentage of cells are presented as mean ± SD (n = 3). $^{**}P < 0.01$, $^{***}P < 0.001$ vs. NG and cells which were not treated with the apoptosis inducer staurosporine, respectively.

4.4 Proliferation under hyperglycemia in the presence of 6-AN

Here the effect of glucose by interfering glycolysis using 6-aminonicotinamide (6-AN) was investigated. This reagent inhibits the pentose phosphate pathway resulting in ATP depletion.

Fig. 11A shows that blocking 6-phosphogluconate dehydrogenase by 6-AN (Frolova et al., 2011) leads to decreased proliferation. However, incubation with 100µmol/l 6-AN increases the number of dead ACH-3P cells, suggesting that blocking the pentose phosphate pathway, and in further consequence glycolysis, results in enhanced cell death (Fig. 11B).

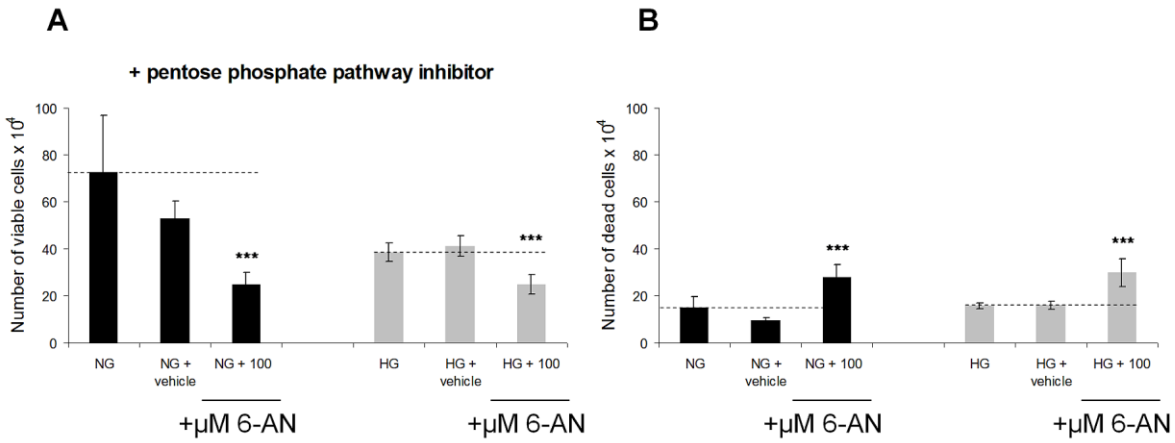

Figure 11 **Inhibition of the pentose phosphate pathway by 6-AN reduces number of viable cells under normo-and hyperglycemia at 21% oxygen due to increased numbers of dead ACH-3P cells.** (A) Number of viable cells under normo- and hyperglycemic conditions after the addition of 100µmol/l 6-AN, (B) number of dead cells under normo- and hyperglycemic conditions after the addition of 100µmol/l 6-AN. Number of viable and dead cells are presented in mean ± SD (n = 6). ***$P < 0.001$ vs. NG + vehicle and HG + vehicle, respectively.

4.5 Intracellular ROS generation of HepG2 cells under hyperglycemia

HepG2 cells served as positive control (Palmeira et al., 2007) for increased ROS production under hyperglycemia. Intracellular ROS generation using H_2DCFDA was significantly ($p<0.001$) enhanced (1.9-fold) after 2 days under high glucose concentrations compared to cells cultured under normoglycemia (Fig 12).

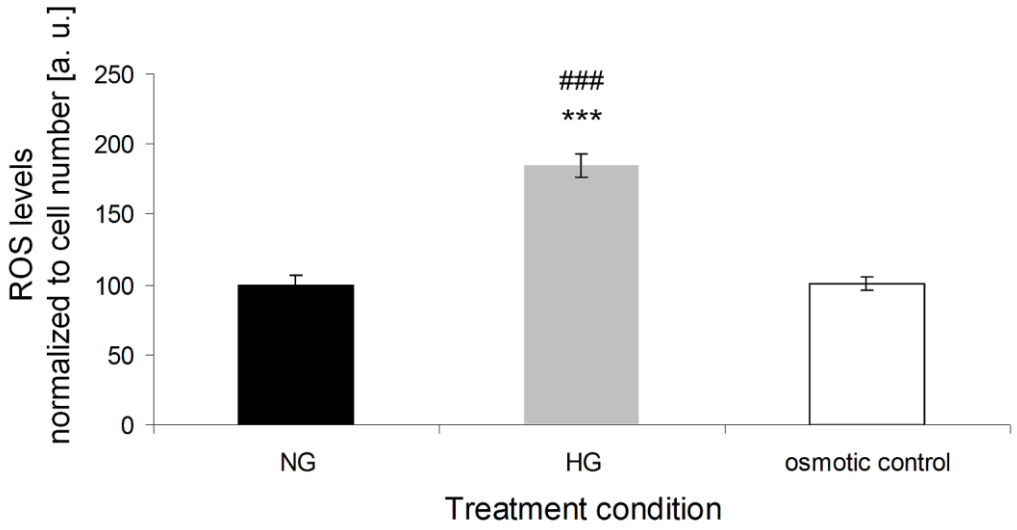

Figure 12 **HepG2 cells showed increased intracellular ROS production under hyperglycemia at 21% oxygen.** HepG2 cells were cultured for 2 days under normoglycemia (black bars), hyperglycemia (grey bars) and osmotic control conditions (white bars) at 21% oxygen; ROS levels were normalized to number of cells; mean ± SD (n = 9). ***$P < 0.001$ vs. NG; $^{###}P < 0.001$ vs. osmotic control.

After establishing the ROS assay using the specific fluorescent dye, H_2DCFDA, the next step was to adapt the assay for the specific tropoblast-derived cell model, ACH-3P.

4.6 ROS production of ACH-3P cells under hyperglycemia

Hyperglycemia can directly cause excessive production of ROS (Roberts and Sindhu, 2009). Thus, to determine whether hyperglycemia-induced proliferation changes at 21%, but not at 2.5% and 8% oxygen, are paralleled by changes in oxidative stress, intracellular and mitochondrial ROS levels were measured.

In Fig. 13A-F ROS levels were monitored after 3 days under normo- and hyperglycemic conditions at 2.5%, 8% and 21% oxygen. Fig. 13B shows increased ROS levels under hyperglycemia compared to cells cultured under normoglycemia (Fig. 13A) at 2.5% oxygen. A similar scenario is seen in Fig. 13D. At 8% oxygen enhanced ROS levels under hyperglycemia were observed compared to the control cells (Fig. 13C).

However, at 21% oxygen the situation was different ACH-3P cells exhibited decreased ROS levels under hyperglycemic conditions, which was clearly monitored in Fig. 13F. Normoglycemia (Fig. 13E) at 21% oxygen showed the highest ROS levels compared to cells treated at 2.5% and 8% oxygen.

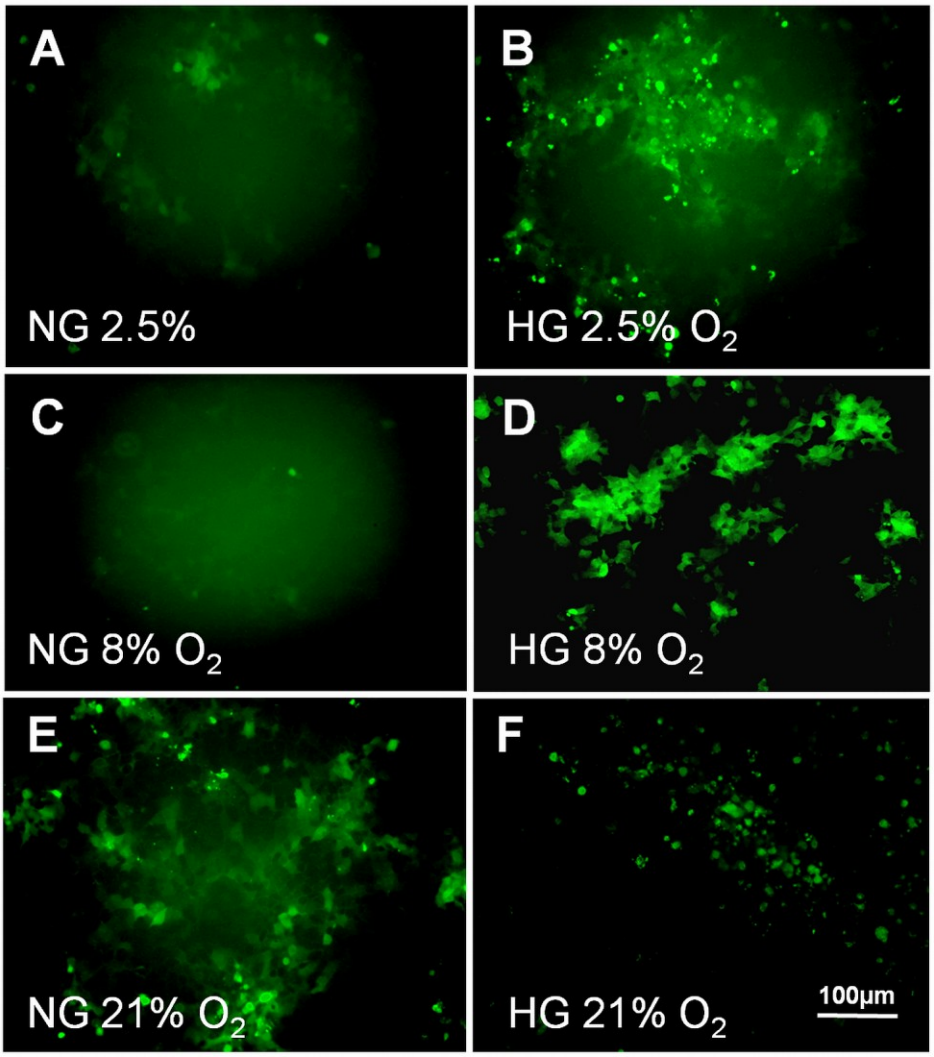

Figure 13 **Intracellular ROS production after 3 days under hyperglycemia at 2.5%, 8% and 21% oxygen.** For fluorescence microscopy images cells were loaded after the treatment period with H_2DCFDA (10µmol/l). (A, C, E) ACH-3P cells after 3 days under normoglycemia at 2.5%, 8% and 21% oxygen, respectively. (B, D, F) ACH-3P cells after 3 days under hyperglycemia at 2.5%, 8% and 21% oxygen, respectively.

Additionally, a time course experiment for up to 3 days was performed. Every day ROS levels were determined under normo- and hyperglycemia at 2.5%, 8% and 21% oxygen. ACH-3P cells were treated under the appropriate conditions and ROS levels were measured and normaized to number of cells.

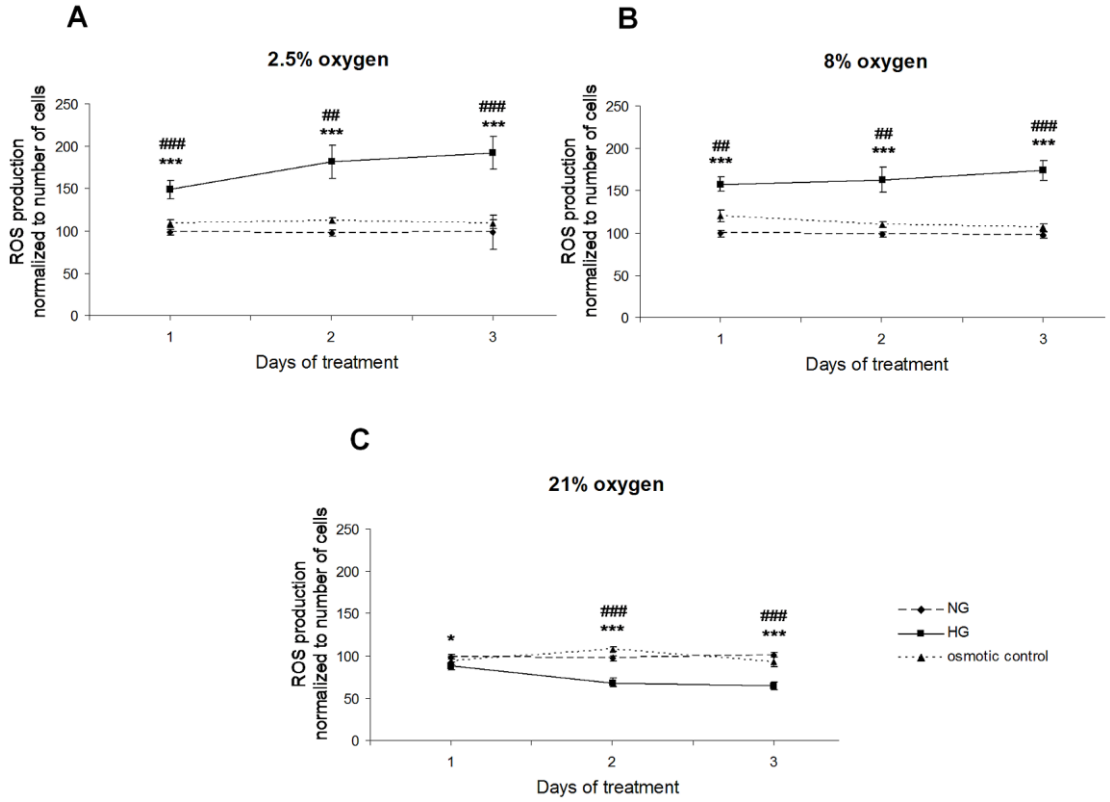

Figure 14 **Intracellular ROS production after 1 to 3 days under hyperglycemia at 2.5%, 8% and 21% oxygen.** ACH-3P cells were cultured under normoglycemia (NG), hyperglycemia (HG) and osmotic control conditions up to 3 days at (A) 2.5%, (B) 8% and (C) 21% oxygen. ROS levels were normaized to number of cells; mean ± SEM (n = 9), data were obtained from four independent experiments. $^{*}P < 0.05$, $^{**}P < 0.01$ and $^{***}P < 0.001$ vs. NG; $^{\#}P < 0.05$, $^{\#\#}P < 0.01$ and $^{\#\#\#}P < 0.001$ vs. osmotic control.

ROS levels were increased up to 3 days under hyperglycemic conditions at 2.5% oxygen. Already 1d after treatment ROS production was enhanced and the highest ROS levels at 2.5% oxygen were observed after 3 days under hyperglycemia (Fig. 14A). At 8% oxygen hyperglycemia also caused increased ROS production compared to control cells.

In contrast to the expectations, at 21% oxygen significantly lower ROS levels under hyperglycemia were observed compared to cells treated under normo- and osmotic control conditions (Fig. 14C).

Fig. 16A shows ROS levels after 3 days under high glucose concentration at 2.5%, 8% and 21% oxygen. Under hyperglycemia 2.1- and 2.2- fold more ROS were produced at 2.5% ($p<0.001$) and 8% oxygen ($p<0.01$ vs. NG; $p<0.05$ vs. osmotic control), respectively, compared to controls.

Interestingly, at 21% oxygen, ACH-3P cells generated 35% less ROS under hyperglycemia ($p<0.001$). Under normoglycemia the highest ROS generation was measured at 21% oxygen ($p<0.001$). ROS production under hyperglycemia at 21% oxygen was not significantly different from ROS levels under the same conditions at 2.5% and 8% oxygen. This suggests that ROS formation under long-term hyperglycemia is independent of oxygen, whereas under normoglycemia higher oxygen tension (21%) augments ROS formation (Fig. 14C and 15A). Already after 1d under hyperglycemia ROS levels were decreased ($p<0.05$) by up to 10% compared to normoglycemic conditions at 21% oxygen. They decreased even further by up to 30% (Fig 14C and 15B) after 2d under these conditions. The lowest ROS levels ($p<0.001$, decrease by 36%) were reached after 3d under hyperglycemia at 21% oxygen (Fig. 14C, 15A and B).

To corroborate the changes in intracellular ROS production found by H_2DCFDA, H_2O_2 release from ACH-3P cells was monitored using the Amplex Red assay. After 3d under hyperglycemia at 21% oxygen, H_2O_2 release was reduced by 28% ($p<0.001$) (Fig. 15C). Taken together, these results indicate decreased ROS levels in ACH-3P cells at high glucose and high oxygen concentrations.

Hyperglycemia up-regulates antioxidant genes

Expression levels of several antioxidant-response related genes were analysed with quantitative Real-Time RT-PCR. Hyperglycemia significantly increased mRNA levels of *HMOX1* (1.6-fold), *GPX1* (1.9-fold) and *NFE2L2* (2.3-fold) compared to normoglycemic conditions at 21% oxygen (Fig. 15D), indicating an up-regulation of these cellular antioxidant systems under hyperglycemia.

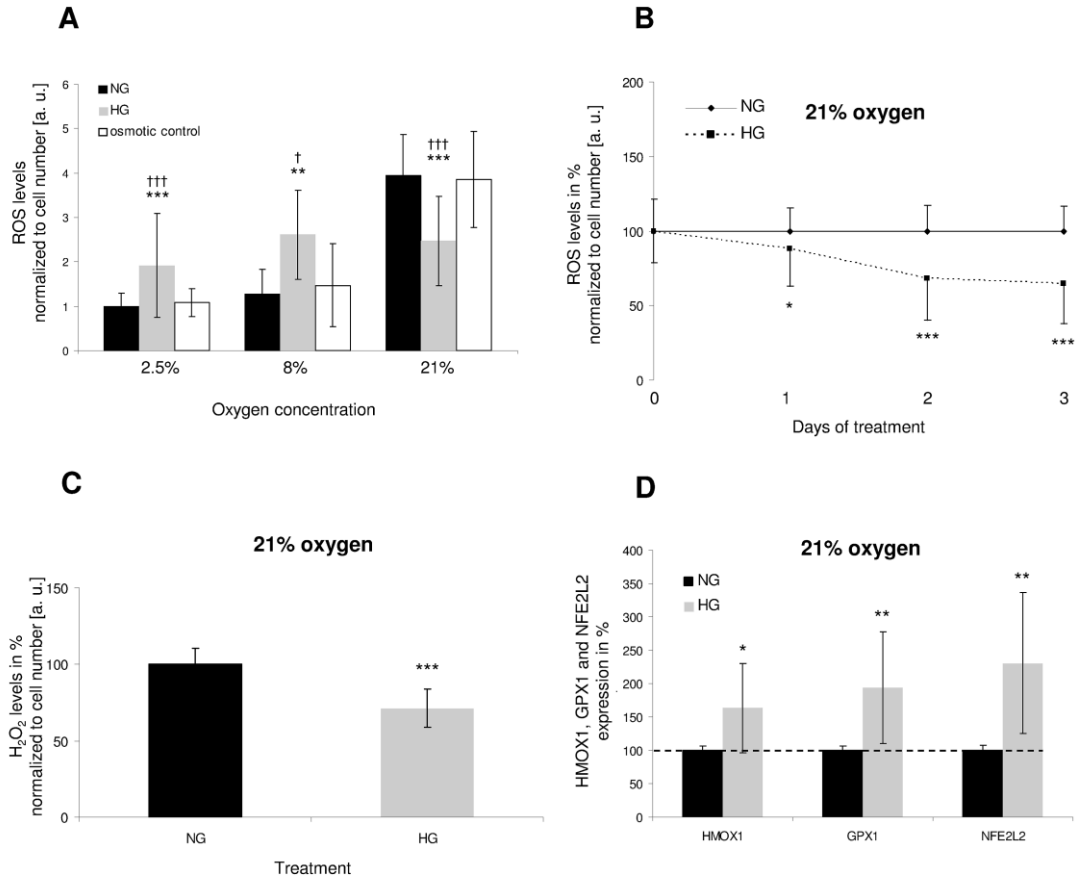

Figure 15 **Intracellular ROS levels of ACH-3P cells under hyperglycemia at 2.5%, 8% and 21% oxygen and expression levels of stress response genes at 21% oxygen.** (A) ACH-3P cells were cultured for 3d under normoglycemia (black bars), hyperglycemia (grey bars) and osmotic control conditions (white bars) at different oxygen concentrations; (B) ROS levels of ACH-3P cells after 0, 1, 2 and 3d under hyperglycemia at 21% oxygen. ROS levels were normalized to cell number and are presented as arbitrary units [a. u.], the ROS levels under normoglycemia (control) were set to 100%; (n = 9), (C) H_2O_2 release by ACH-3P cells after 3d under hyperglycemic conditions, H_2O_2 levels were normalized to cell number and are presented as arbitrary units [a. u.], (n = 12). (D) mRNA expression of *HMOX1, GPX1* and *NFE2L2* after 3d under hyperglycemia at 21% oxygen using quantitative Real-Time RT-PCR, expression levels were normalized to RPL30, (n = 3), data are presented as mean ± SD of four (A and B), two (C) and three (D) independent experiments, respectively. $^{*}P < 0.05$, $^{**}P < 0.01$, $^{***}P < 0.001$ vs. NG; $^{\dagger}P < 0.05$, $^{\dagger\dagger\dagger}P < 0.001$ vs. osmotic control.

4.7 Mitochondrial superoxide levels at 21% oxygen

In addition to cytosolic ROS sources, mitochondria produce ROS due to incomplete reduction of oxygen during electron transport in the mitochondrial electron transport chain (Murphy, 2009).

Mitochondrial superoxide levels were determined using MitoSOX^{TM} Red. Under hyperglycemic conditions (Fig. 16D) the cells showed elevated levels of superoxide compared to cells under normoglycemia (Fig. 16B).

Addition of two electron transport chain inhibitors, antimycin A and oligomycin, served as positive controls. Both inhibitors enhanced superoxide levels under normo- (Fig. 16B vs. F) and hyperglycemic (Fig. 16D vs. H) conditions at 21% oxygen. Different from total intracellular ROS levels, which were reduced under hyperglycemic conditions compared to control cells, mitochondrial superoxide levels were increased by hyperglycemia as compared to normoglycemia at 21% oxygen. This suggests that hyperglycemia differently alters ROS levels in mitochondria and the cytosol under the experimental conditions.

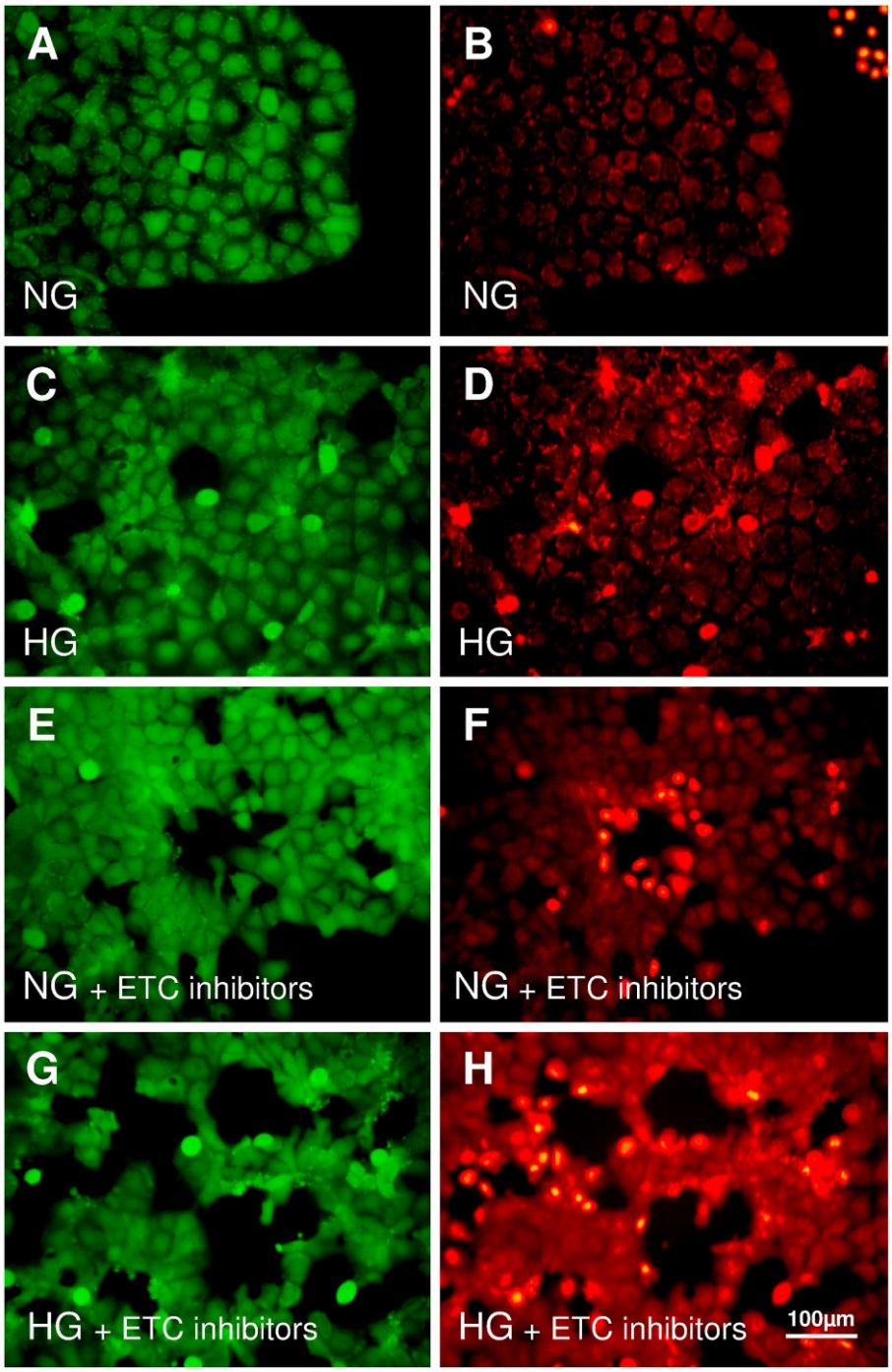

Figure 16 **Fluorescence microscopy of mitochondrial superoxide levels after 3 days under hyperglycemia at 21% oxygen.** After treatment, ACH-3P cells were loaded with CellTracker™ Green CMFDA (A, C, E, G) and MitoSOX™ Red (B, D, F, H). (A, B) Normoglycemia; (C, D) hyperglycemia; (E, F) normoglycemia in the presence of two mitochondrial electron transport chain (ETC) inhibitors (antimycin A and oligomycin); (G, H) hyperglycemia in the presence of antimycin A and oligomycin.

4.8 ATP production of ACH-3P cells under hyperglycemia at 21% oxygen

ATP production of ACH-3P cells treated 3 days under hyperglycemia at 21% oxygen was measured. Antimycin A was used as a positive control for reduced ATP production via the electron transport chain by inhibiting complex III. Therefore, antimycin A was added in a final concentration of 10µmol/l.

The relative light units were normalized to protein concentration per mg. Fig. 17 shows that ATP production is decreased under hyperglycemic conditions at 21% oxygen compared to ATP levels of cells treated under normoglycemia. Addition of antimycin A lead to the expected effect. Significantly reduced ATP production under normo- and hyperglycemic condition at 21% oxygen was monitored. These findings confirm the observation that ACH-3P cells produce more mitochondrial superoxide under hyperglycemia compared to control cells (Fig. 16D). Increased superoxide production caused by antimycin A (Fig. 16F and G) leads to significantly reduced ATP production under normo- and hyperglycemic conditions at 21% oxygen (Fig. 17).

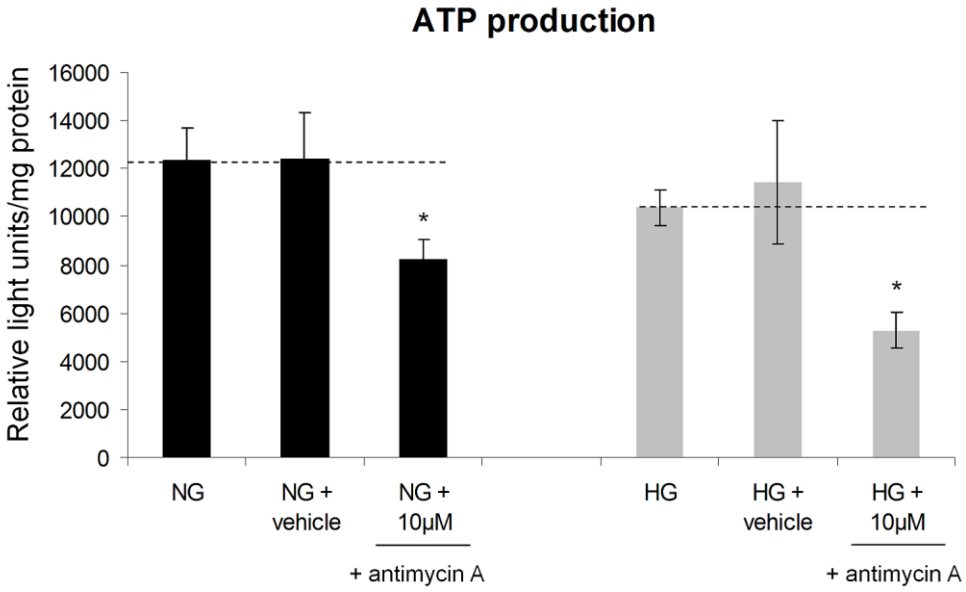

Figure 17 **ATP production in ACH-3P cells after 3 days under hyperglycemia at 21% oxygen.** ATP production of ACH-3P cell was measured after 3 days under normo- and hyperglycemic conditions at 21% oxygen. Addition of antimycin A (10µmol/l) was used as positive control to decrease ATP production under these conditions, mean ± SD (n = 3). **P* < 0.05 vs. NG + vehicle and HG + vehicle, respectably.

4.9 Mitochondrial activity under hyperglycemia

Mitochondrial activity was determined by measuring colour changes of WST-1 in culture medium mediated by dehydrogenases within the mitochondria. At 2.5% oxygen mitochondrial activity was significantly decreased after 2 and 3 days under hyperglycemia compared to cells cultured under normoglycemic and osmotic control conditions (Fig. 18A). Incubation under high glucose at 8% oxygen did not influence the activity of mitochondrial dehydrogenases in ACH-3P cells (Fig. 18B). Fig. 18C shows that at 21% oxygen hyperglycemia leads to significantly increased activity after 2 days of incubation, however after 3 days under hyperglycemic conditions and high oxygen concentration significantly reduced mitochondrial activity was observed. Moreover, the highest mitochondrial activity was detected at 2.5% oxygen independent of glucose concentrations.

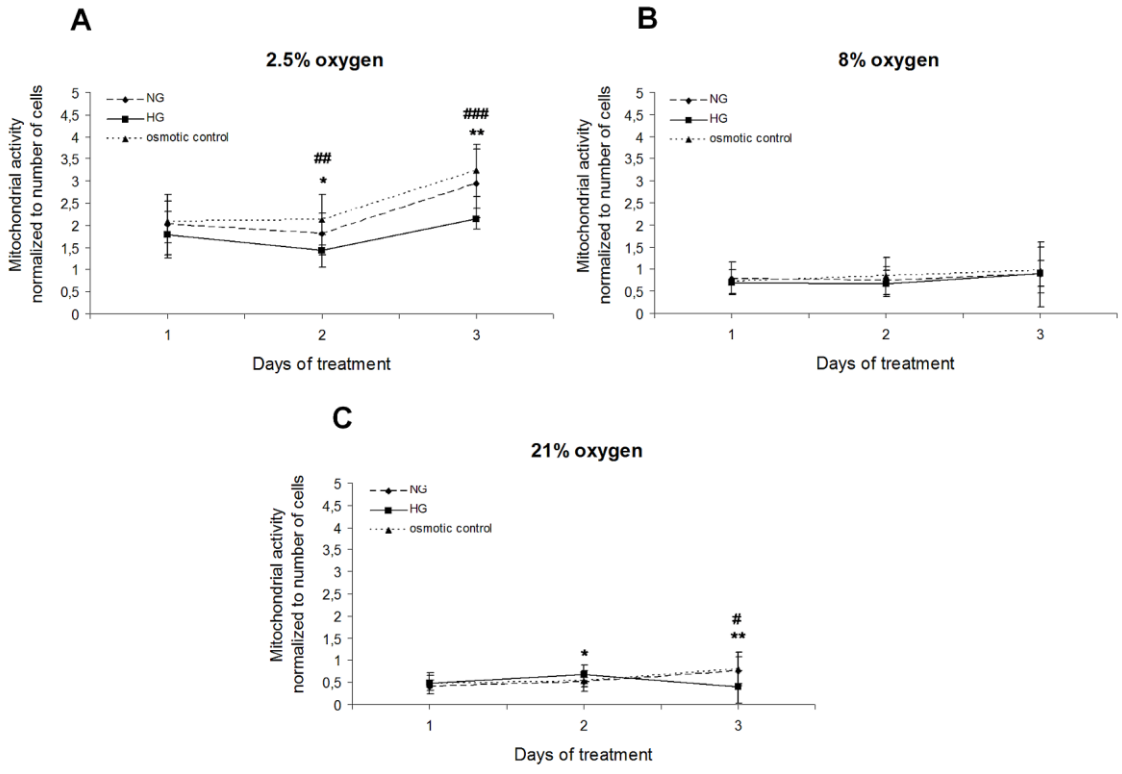

Figure 18 **Mitochondrial activity of ACH-3P cells after 1 to 3 days under hyperglycemia at 2.5%, 8% and 21% oxygen.** Mitochondrial activity of ACH-3P cells was determined in a time course experiment up to 3 days under normo- and hyperglycemic conditions. (A) Mitochondrial activity of ACH-3P cells at 2.5% oxygen, (B) mitochondrial activity of ACH-3P cells at 8% oxygen and (C) mitochondrial activity of ACH-3P at 21% oxygen, mean ± SD (n = 9); data were obtained from three independent experiments. $^{*}P < 0.05$, $^{**}P < 0.01$ vs. NG; $^{\#}P < 0.05$, $^{\#\#}P < 0.01$, $^{\#\#\#}P < 0.001$ vs. osmotic control.

4.10 Proliferation after addition of antioxidants at 21% oxygen

To investigate the mechanism behind decreased cell proliferation under hyperglycemia at 21% oxygen, the effects of antioxidants (ascorbate, Trolox® and NAC) on proliferation were determined. Whereas the glucose effect on cell number was confirmed again, addition of antioxidants to the culture medium had no effect on cell proliferation (Fig. 19A - C).

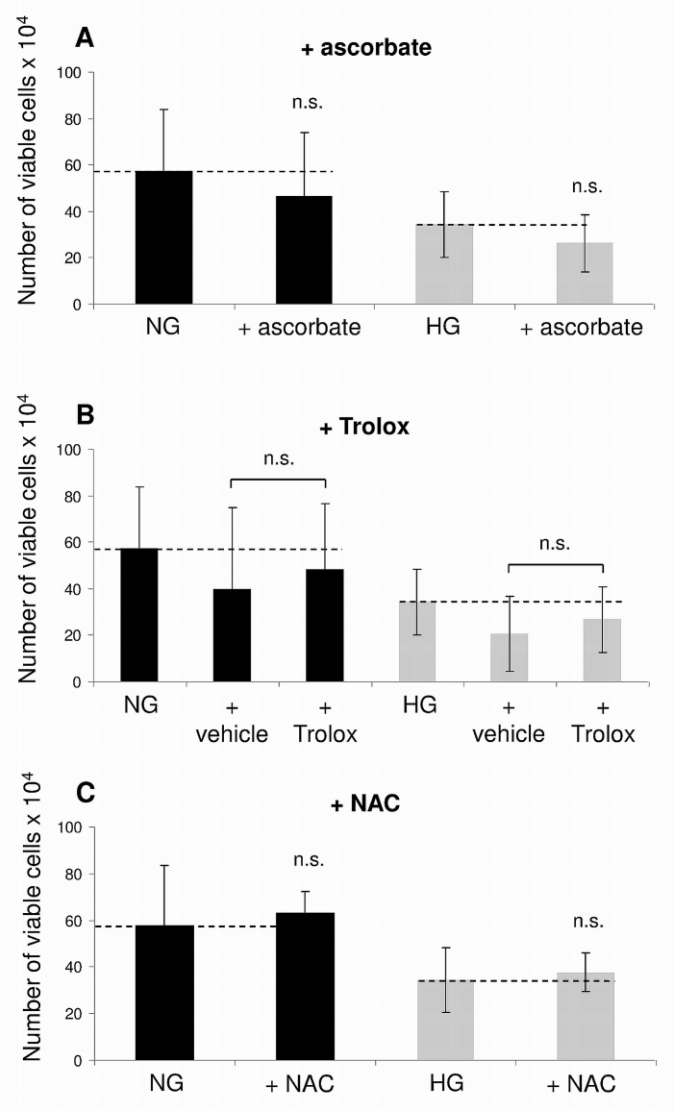

Figure 19 **Addition of antioxidants had no effect on cell proliferation under hyperglycemia at 21% oxygen.** ACH-3P cells were cultured for 3 days under normoglycemia (black bars) and hyperglycemia (grey bars) in the presence and absence of antioxidants at 21% oxygen. (A) Ascorbate (100µmol/l), (B) Trolox® (100µmol/l) and (C) NAC (1mmol/l); number of viable cells are presented as mean ± SD (n = 6); data were obtained from three independent experiments; n.s. not significant. Based on 18 replicates the coefficient of variation under NG and HG was 45% and 40%, respectively.

The number of dead cells was also not altered in any of the treatment conditions (Fig. 20). Thus, scavenging ROS by ascorbate, Trolox® and NAC did not restore proliferation of ACH-3P cells under hyperglycemia, suggesting no association between ROS and proliferation under these conditions.

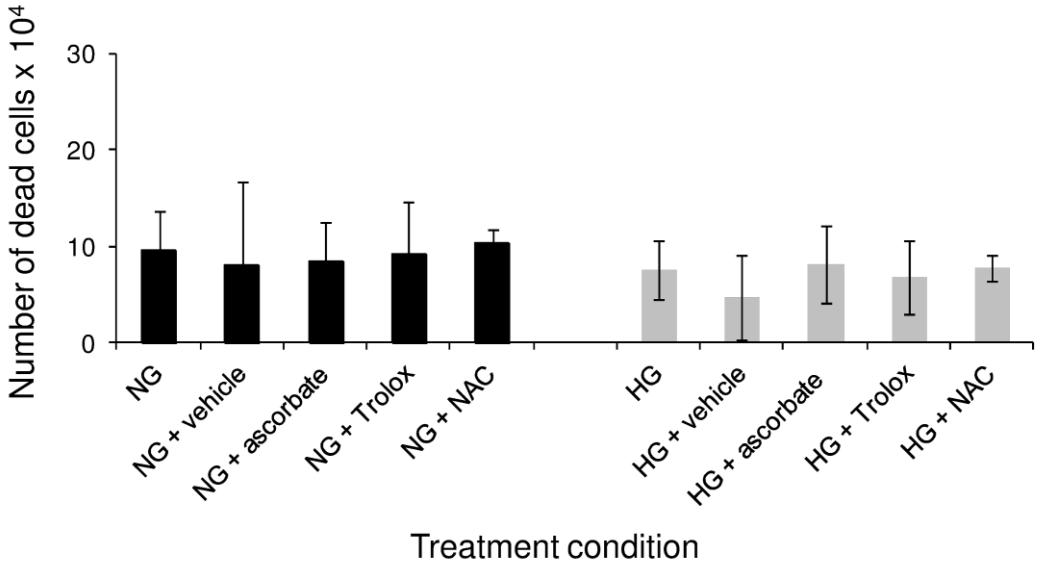

Figure 20 **Addition of antioxidants had no effect on the number of dead ACH-3P cells under hyperglycemia at 21% oxygen.** ACH-3P cells were cultured for 3 days under normoglycemia (black bars) and hyperglycemia (grey bars) in the presence and absence of antioxidants at 21% oxygen. (A) Ascorbate (100µmol/l), (B) Trolox® (100µmol/l) and (C) NAC (1mmol/l); number of dead cells are presented as mean ± SD (n = 6); data were obtained from three independent experiments.

To confirm the hypothesis that proliferation of ACH-3P is ROS-independent, the next step was to increase and decrease ROS levels by using specific inhibitors. The effects of the reagents used here on cytosolic and mitochondrial ROS formation are shown in Fig. 21.

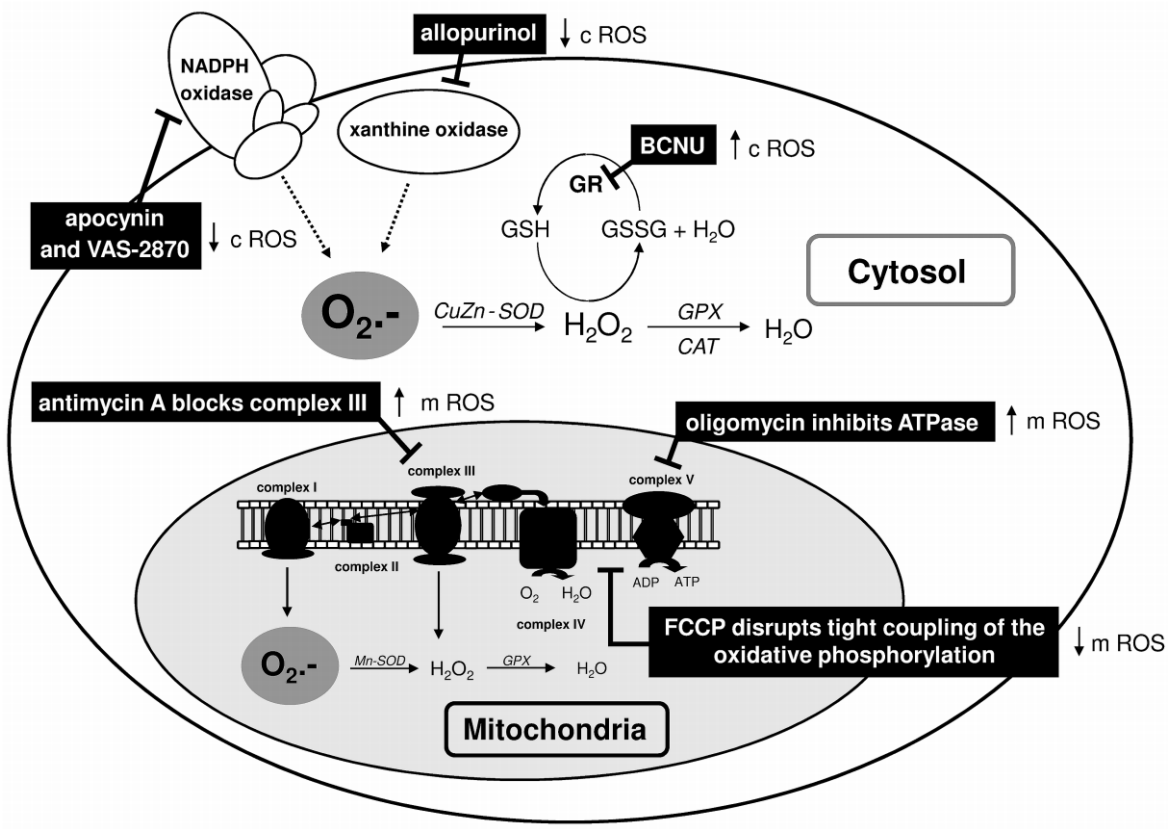

Figure 21 **Effect of inhibitors on increasing and decreasing cytosolic (c) and mitochondrial (m) ROS generation.** Allopurinol blocks xanthine oxidase and, therefore, reduces cytosolic ROS generation; apocynin and VAS-2870 are inhibitors for membrane-bound NADPH oxidase and lead to decreased ROS formation in the cytosol; BCNU inhibits glutathione reductase (GR) and thereby prevents recycling of the oxidized glutathione disulfide (GSSG) to the reduced form of glutathione (GSH), which may causes increased intracellular ROS production. FCCP disrupts the tight coupling of the oxidative phosphorylation and reduces mitochondrial superoxide anion (O_2.-) generation; antimycin A blocks complex III and oligomycin inhibits ATPase (complex V) in the mitochondrial electron transport chain leading to enhanced superoxide levels. GPX, glutathione peroxidase; CAT, catalase; CuZn-SOD, copper-zinc superoxide dismutase; Mn-SOD, manganese superoxide dismutase; H_2O_2, hydrogen peroxide.

4.11 Manipulated cytosolic ROS levels under hyperglycemia at 21% oxygen

Cytosolic ROS levels were manipulated using allopurinol, apocynin, VAS-2870 and BCNU, and measured how this affects cell proliferation. Xanthine and NADPH oxidases are known to generate cytosolic ROS (Gao and Gao, 2007, Rajesh et al., 2009). Inhibition of NADPH oxidase with apocynin (100µmol/l and 250µmol/l) or VAS-2870 (1µmol/l), a novel NADPH oxidase inhibitor, did not influence the number of viable cells under hyperglycemia (Fig. 22A and B). Also the inhibition of xanthine oxidase using allopurinol under hyperglycemic conditions did not increase cell proliferation to normoglycemic levels (Fig. 22C). The number of dead cells was not altered under the conditions used here (Fig. 23A-C). Hence, decreasing cytosolic ROS generation did not restore proliferation of ACH-3P cells, indicating that impaired proliferation under hyperglycemia does not depend on ROS formation.

Further experiments were carried out using an inhibitor of glutathione reductase (BCNU), which eventually leads to enhanced ROS generation. Addition of BCNU significantly reduced proliferation under normo- and hyperglycemic conditions in a dose-dependent manner (Fig. 22D). The number of dead cells was not altered under any of the conditions (Fig. 23A-D). In the absence and presence of 5µmol/l and 10µmol/l BCNU, proliferation was still significantly decreased under hyperglycemia compared to control cells. Thus, BCNU treatment did not restore the hyperglycemic levels to those of normoglycemia. Collectively, decreasing and increasing cytosolic ROS generation did not restore proliferation of ACH-3P cells under hyperglycemia at 21% oxygen.

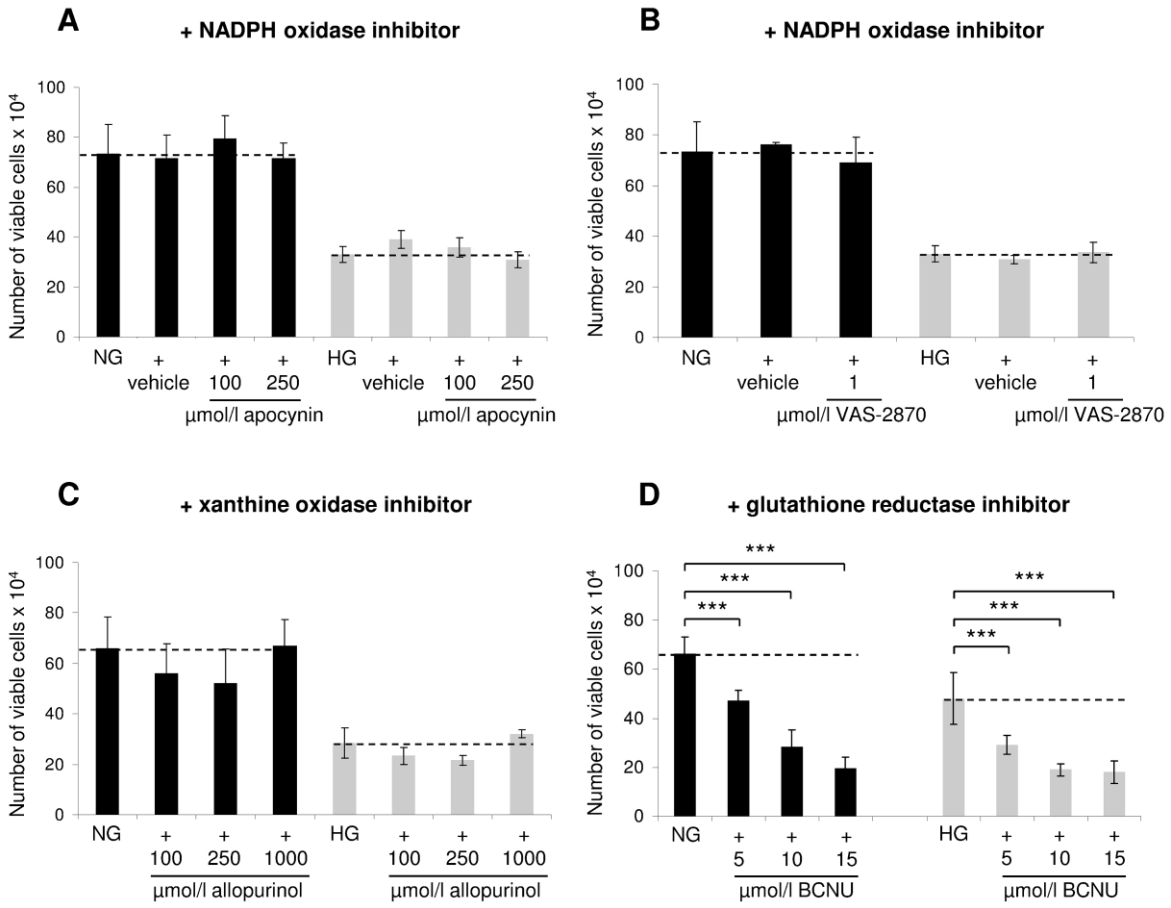

Figure 22 **Increased and decreased cytosolic ROS generation did not alter ACH-3P proliferation under hyperglycemia at 21% oxygen.** ACH-3P cells were treated for 3 days under normoglycemia (black bars) and hyperglycemia (grey bars) in the presence and absence of NADPH oxidase (apocynin and VAS-2870), xanthine oxidase (allopurinol) and glutathione reductase (BCNU) inhibitors at 21% oxygen. (A) Apocynin, (B) VAS-2870, (C) allopurinol, (D) BCNU. Number of viable cells are presented as mean ± SD (n = 6). ****P* < 0.001 vs. NG or HG and NG + vehicle or HG + vehicle. Based on 6 replicates the coefficient of variation under NG and HG was (A and B) 16% and 10%, (C) 19% and 21%, (D) 10% and 22%, respectively.

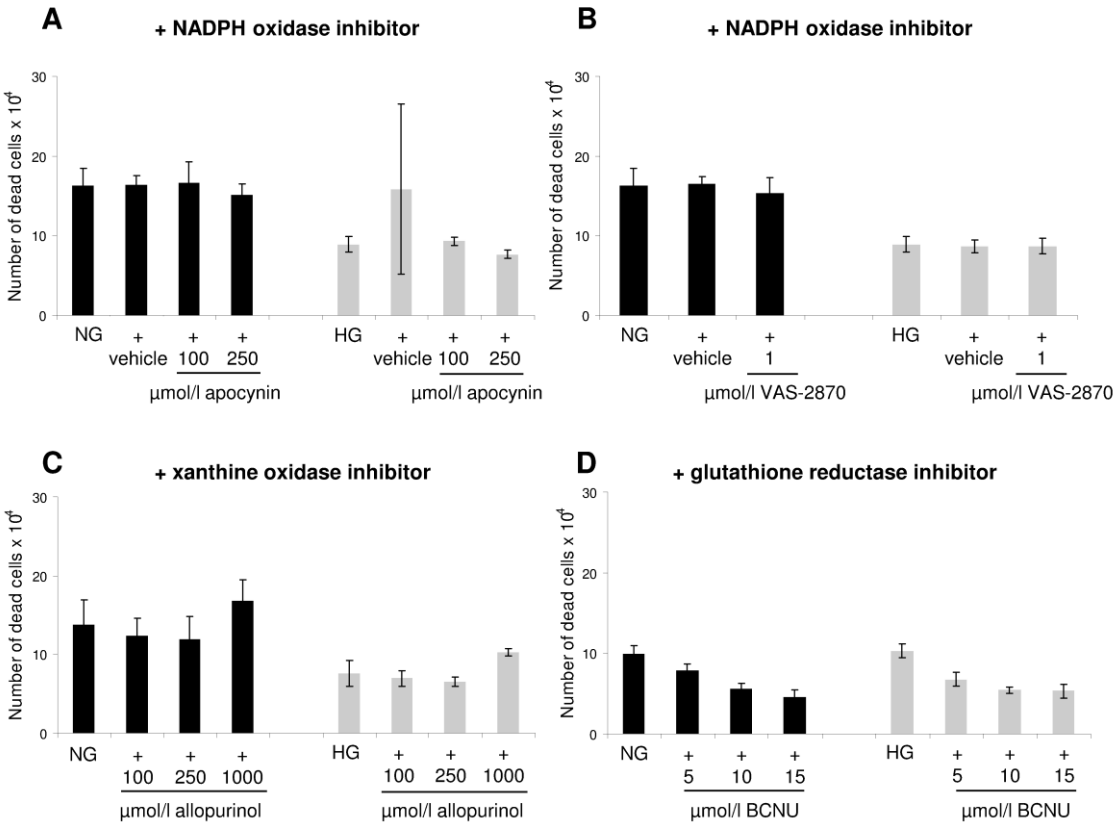

Figure 23 **Increased and decreased cytosolic ROS generation had no effect on the number of dead ACH-3P cells under hyperglycemia at 21% oxygen.** ACH-3P cells were treated for 3 days under normoglycemia (black bars) and hyperglycemia (grey bars) in the presence and absence of NADPH oxidase (apocynin and VAS-2870), xanthine oxidase (allopurinol) and glutathione reductase (BCNU) inhibitors at 21% oxygen. (A) Apocynin, (B) VAS-2870, (C) allopurinol, (D) BCNU. Number of dead cells are presented as mean ± SD (n = 6).

4.12 Enhanced and reduced mitochondrial superoxide levels at 21% oxygen

Hyperglycemia had a different effect on cellular and mitochondrial ROS levels. Therefore, the effect of mitochondrial ROS on cell proliferation by manipulating mitochondrial superoxide levels was investigated. Cells were treated with FCCP, antimycin A and oligomycin to reduce (FCCP) or elevate (antimycin A, oligomycin) superoxide levels under hyperglycemia at 21% oxygen. Varying concentrations of FCCP could not restore proliferation (Fig. 24A). After the addition of 0.5µmol/l FCCP, significantly fewer viable cells were observed under normo- and hyperglycemic conditions. Lower FCCP concentrations reduced the number of viable cells under hyperglycemia (Fig. 24A). The number of dead cells did not change under any of the conditions (Fig. 25A). Hence, decreased superoxide levels via mitochondria could not improve proliferation under hyperglycemia at 21% oxygen.

Forced elevation of superoxide levels with antimycin A (Henderson et al., 2009) (Fig. 24B) decreased the number of viable cells under normo- ($p<0.001$) and hyperglycemia compared to vehicle controls, while the number of dead cells was not changed (Fig. 25B and C). Oligomycin had a similar effect on proliferation (Fig. 24C).

Cell growth under hyperglycemia was still reduced after the addition of antimycin A and oligomycin compared to cells treated under normoglycemic conditions. These results suggest that mitochondrial ROS formation does not restore cell proliferation under hyperglycemia at 21% oxygen.

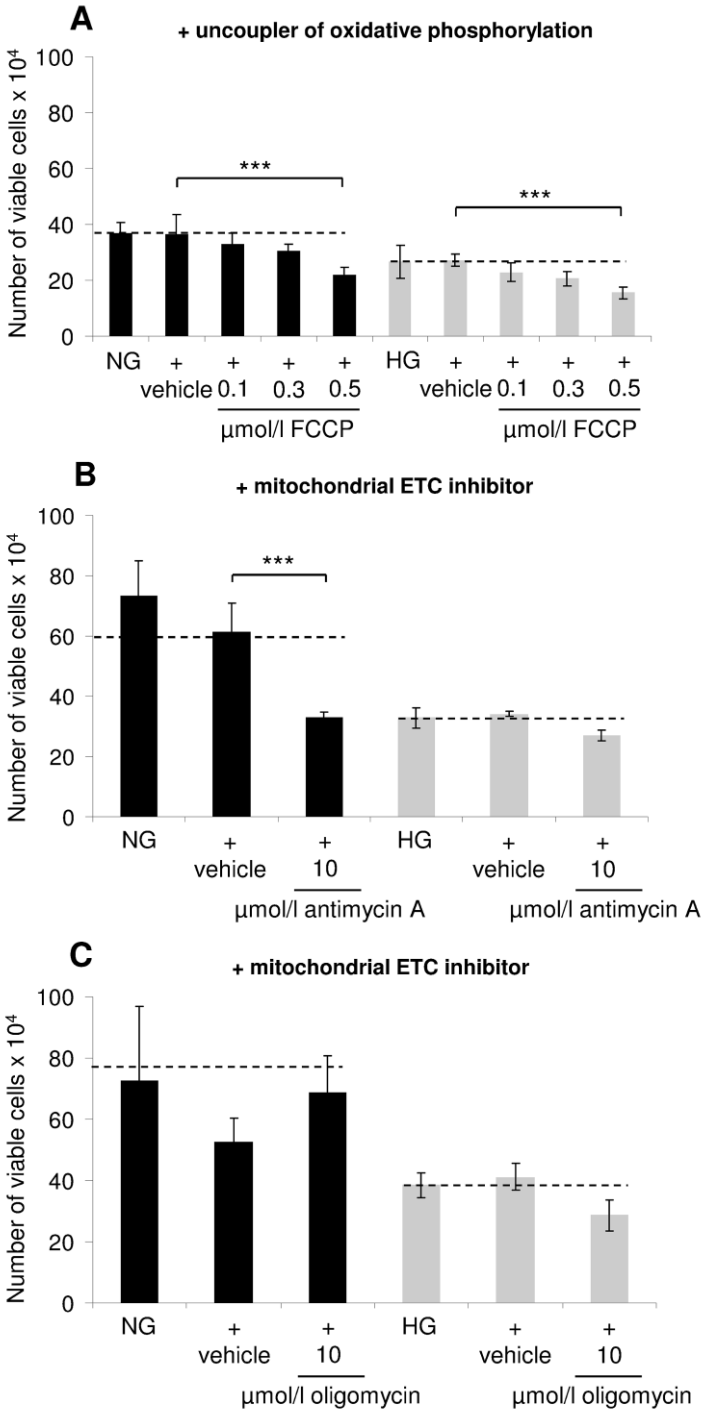

Figure 24 **Reduced or enhanced mitochondrial superoxide levels did not restore ACH-3P proliferation under hyperglycemia at 21% oxygen.** ACH-3P cells were treated for 3 days under normoglycemia (black bars) and hyperglycemia (grey bars) in the presence and absence of an uncoupler (FCCP) and two different mitochondrial electron transport chain (ETC) inhibitors (antimycin A and oligomycin) at 21% oxygen. Number of viable cells after addition of (A) FCCP, (B) antimycin A and (C) oligomycin. Number of viable cells are presented as mean ± SD (n = 6). ***$P < 0.001$ vs. NG + vehicle or HG + vehicle. Based on 6 replicates the coefficient of variation under NG and HG was (A) 10% and 22, (B) 16% and 10%, (C) 33% and 10%, respectively.

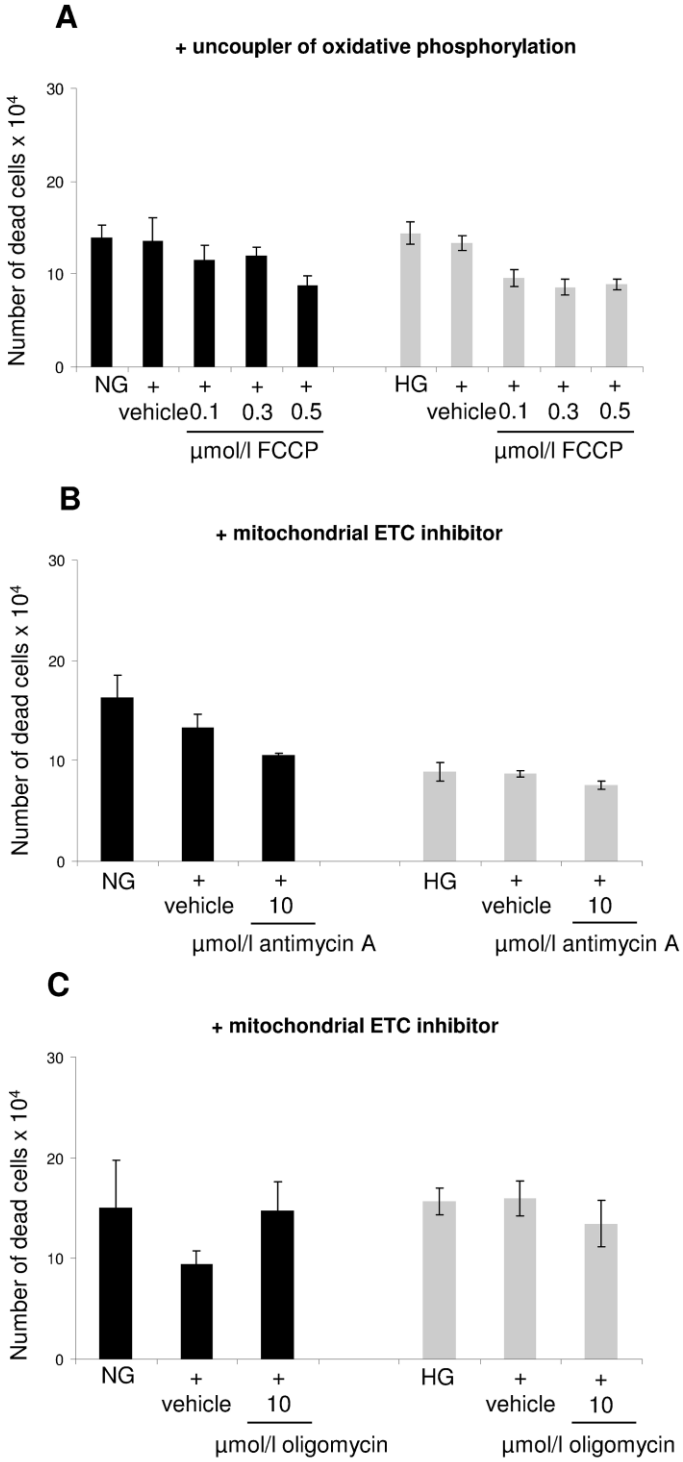

Figure 25 **Reduced and enhanced mitochondrial superoxide levels had no effect on the number of dead ACH-3P cells under hyperglycemia at 21% oxygen.** ACH-3P cells were treated for 3 days under normoglycemia (black bars) and hyperglycemia (grey bars) in the presence and absence of an uncoupler (FCCP) and two different mitochondrial electron transport chain (ETC) inhibitors (antimycin A and oligomycin) at 21% oxygen. Number of dead cells after addition of (A) FCCP, (B) antimycin A and (C) oligomycin. Number of dead cells are presented as mean ± SD (n = 6).

4.13 Antioxidant defense status under hyperglycemia

For the analysis of human oxidative stress and antioxidant defense status of ACH-3P cells a RT^2 Profiler™ PCR Array was used. This array provides an overview of gene expression under the used conditions.

In Fig. 26 the gene expression levels of several antioxidants are shown after 3 days under hyperglycemia at 8% and 21% oxygen. The following genes exhibited distinct differences in their expression patterns under hyperglycemia at 8% as well as at 21% oxygen: glutathione peroxidase 1 (*GPX1*), glutathione transferase zeta 1 (*GSTZ1*), superoxide dismutase 1-3 (*SOD*), peroxiredoxin 1 and 2 (*PRDX*), catalase (*CAT*), cold shock domain containing E1 (*CSDE1*), cytoglobin (*CYGB*) and dual oxidase 1 (DUOX1).
In general, at 8% oxygen (Fig. 26A, C, E and F) after 3 days under hyperglycemia increased antioxidant levels were detected compared to cells treated under normoglycemic conditions. However, the highest expression levels of the above mentioned genes were observed under high glucose and high oxygen levels. Conspicuously, at 21% oxygen increased *GPX1*, *GSTZ1*, *SOD2* and *3*, *PRDX1* and *2*, *CAT*, *CSDE1*, *CYGB* and *DUOX1* were observed. Furthermore, *GPX1* expression had been confirmed by Real-Time RT-PCR as shown in Fig. 15D. Significantly ($p<0.001$) increased *GPX1* levels were monitored under hyperglycemia 21% oxygen.

These results from the RT^2 Profiler™ PCR Array and from the Real-Time PCR support the hypothesis that ACH-3P cells produce more ROS under hyperglycemic conditions at 8% oxygen, which cannot be scavenged by cellular antioxidants. Assumedly, cells cultured under hyperglycemia at 21% oxygen adapted to high glucose concentration by up-regulating several antioxidants. This may lead to decreased intracellular ROS levels within ACH-3P cells.

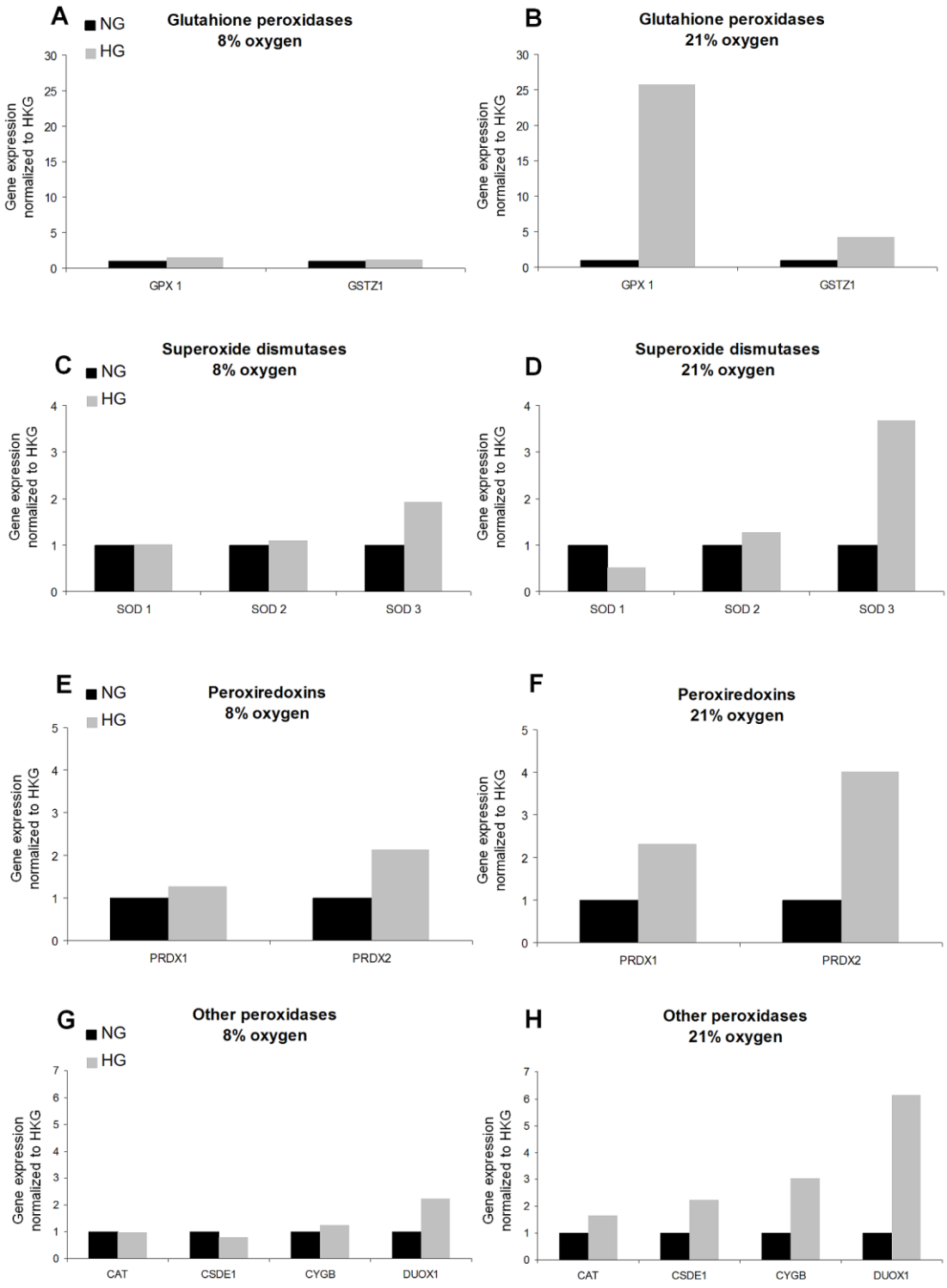

Figure 26 **Antioxidant status of ACH-3P cells after 3 days under hyperglycemia at 21% oxygen.** Expression of several antioxidants and oxidative stress related genes. (A and B) Glutathione peroxidase 1 (*GPX1*) and glutathione transferase zeta 1 (*GSTZ1*), (C and D) superoxide dismutase 1-3 (*SOD*), (E and F) peroxiredoxin 1 and 2 (*PRDX*), (G and H) catalase (*CAT*), cold shock domain containing E1 (*CSDE1*), cytoglobin (*CYGB*) and dual oxidase 1 (*DUOX1*) expression under hyperglycemia at 8% and 21% oxygen, respectively. Gene expression was normalized to house keeping genes (HKG).

4.14 Protein expression under hyperglycemia

Using a protein array, differently expressed proteins under normoglycemic vs. hyperglycemic conditions at 21% oxygen were determined. In Fig. 27 all significantly expressed proteins are shown.

The following proteins were significantly down-regulated under hyperglycemia compared to cells treated under control conditions: Cullin-1 ($p<0.001$), cyclin-dependent kinase 3 (Cdk3; $p<0.001$), p27Kip1 ($p<0.001$), CDC47 ($p<0.001$), CDC34 ($p<0.01$), cyclin B1 ($p<0.05$) and cyclin C ($p<0.001$).

Whereas Cullin-2 ($p<0.05$), p73 ($p<0.05$), p73a ($p<0.01$), E2F-3 ($p<0.05$), RAD51 ($p<0.001$) and cyclin D1 were up-regulated under high glucose concentrations.

These results indicate that long-term hyperglycemia has a high impact on protein expression at 21% oxygen.

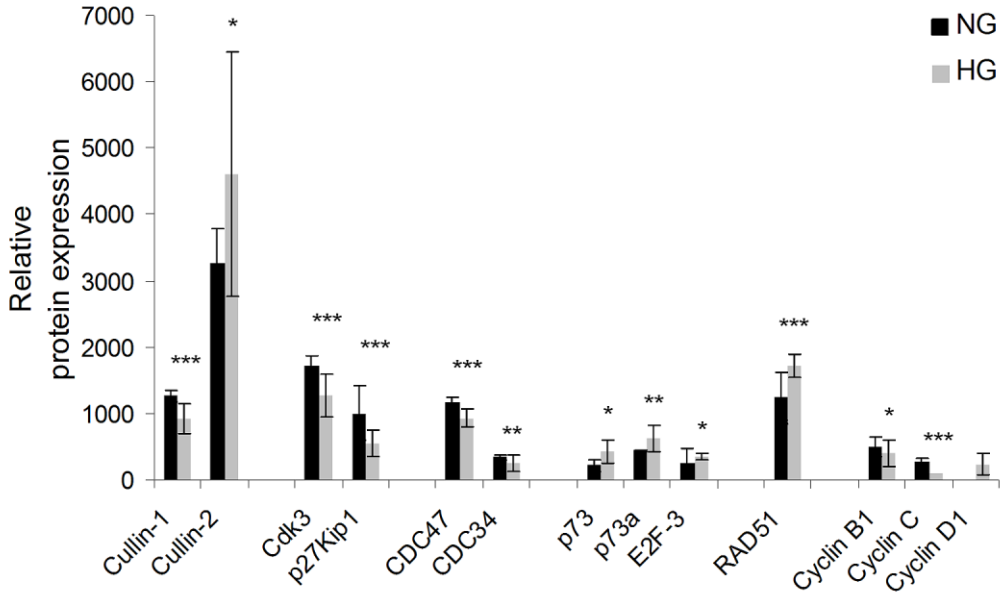

Figure 27 **Protein expression after 3 days under hyperglycemia at 21% oxygen.** Significant differently expressed proteins under normoglycemic vs. hyperglycemic conditions; mean ± SD (n = 3). *$P < 0.05$, **$P < 0.01$ and ***$P < 0.001$ vs. NG

4.15 Cyclin B1 protein expression

Western blot analysis was performed to confirm the protein array data from cyclin B1 (Fig. 27). ACH-3P cells were cultured for 3 days under hyperglycemia at 21% oxygen. Band intensity of cyclin B1 was normaized to beta-actin, which was used as loading control. In Fig. 29A it becomes obvious that less cyclin B1 protein expression under hyperglycemia was observed compared to cells treated under normoglycemic conditions. After normalization a decrease of 50% in cyclin B1 expression was monitored (Fig. 28B). These data reflect the observation that ACH-3P cells may be arrested at a point past S-phase of the cell cycle (Fig. 9F) and do no enter mitosis.

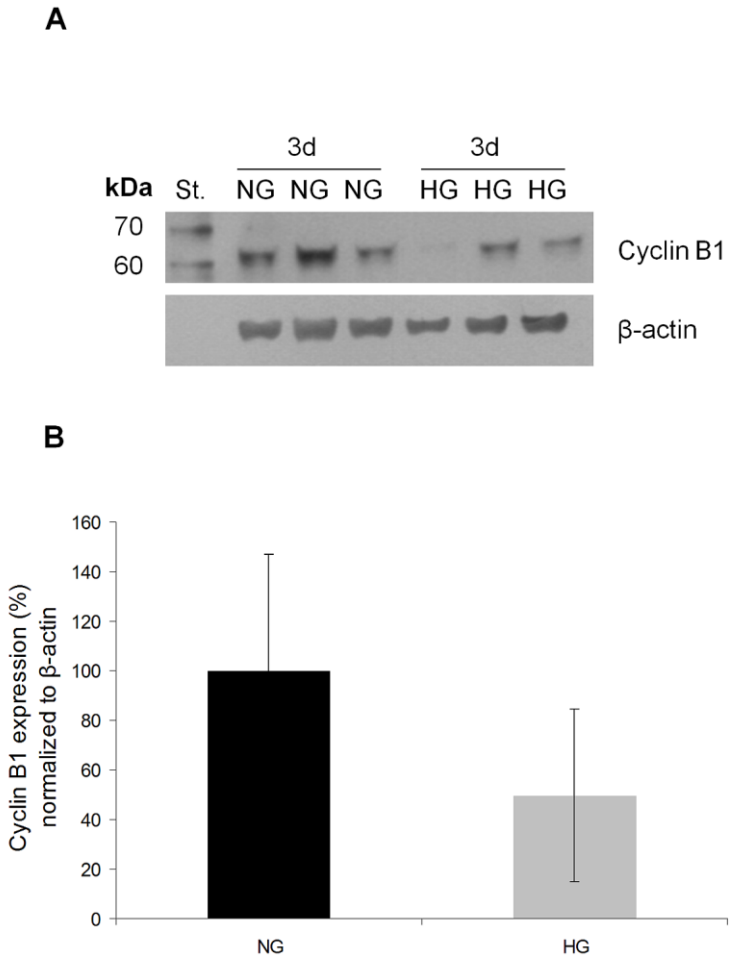

Figure 28 **Cyclin B1 expression after 3 days under hyperglycemia at 21% oxygen.** (A) Cyclin B1 protein expression of ACH-3P cells after 3 days under normo- (NG) and hyperglycemic (HG) conditions at 21% oxygen. Lane 1: standard (Magic Marker, Invitrogen); Lane 2-4: 3 days under normoglycemia, Lane 5-7: 3 days under hyperglycemia. (B) Protein expression was normaized to beta-actin, which was used as loading control; mean ± SD (n = 3).

4.16 Analysis of protein phosphorylation

To delineated which signaling pathway is involved and affected by hyperglycemia leading to reduced proliferation at 21% oxygen, phosphorylation of ERK1/2, JNK, p38 and Akt/PkB was measured. ACH-3P cells were treated for 15, 30 and 60min with 5.5mmol/l and 25mmol/l D(+)-glucose at 21% oxygen. Afterwards immunoblotting was performed. As loading control beta-actin was used and band signal intensity of phospho-ERK1/2 was normalized to loading control.

Western blot analysis showed no phosphorylation of Akt/PkB, JNK and p38 under normo- and hyperglycemic conditions at 21% oxygen (data not shown).

Phosphorylation of ERK1/2 was increased after 15, 30 and 60min under hyperglycemia compared to cells treated under normoglycemic conditions (Fig. 29). However, as shown in Fig. 29 lane 8, phosphorylation decreases after 60min under high glucose concentrations compared to 15 and 30min treatment periods.

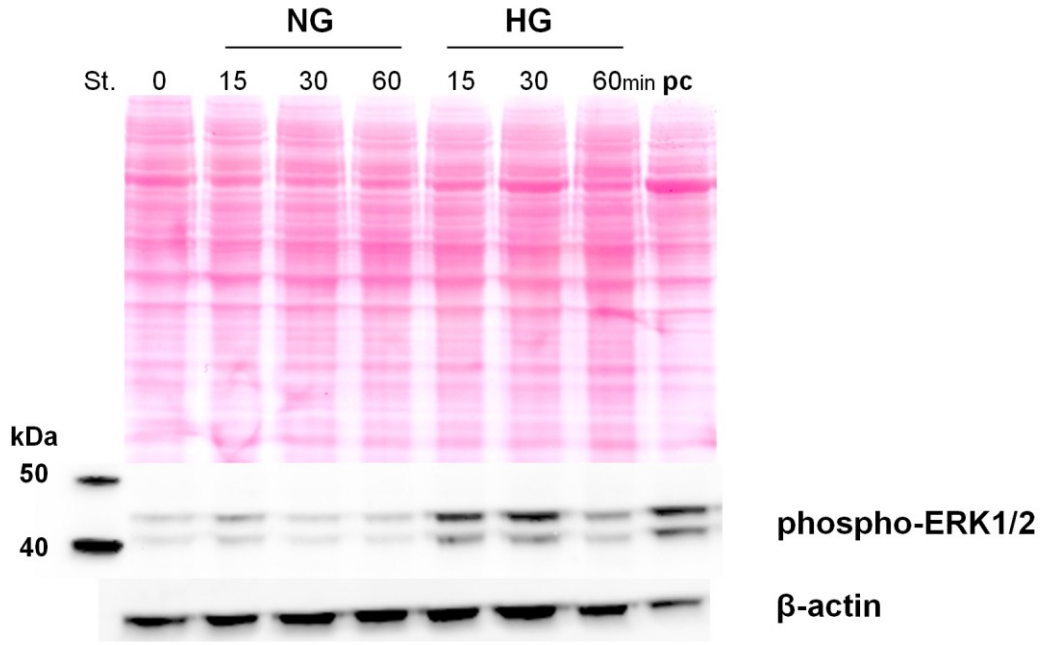

Figure 29 **ERK1/2 phosphorylation of ACH-3P cells under hyperglycemia at 21% oxygen.** Lane 1: standard (Magic marker, Invitrogen); Lane 2: 0min control; Lane 3: 15min under normoglycemia; Lane 4: 30min under normoglycemia; Lane 5: 60min under normoglycemia; Lane 6: 15min under hyperglycemia; Lane 7: 30min under hyperglycemia; Lane 8: 60min under hyperglycemia; Lane 9: positive control (pc), ACH-3P cells treated 30min with 15% FCS under normoglycemia.

4.17 Inhibition of ERK1/2 and Akt/PkB signaling pathway

The number of viable cells was significantly increased ($p<0.001$) in the presence of the ERK1/2 inhibitor U0126 under hyperglycemia at 21% oxygen compared to cell cultured with vehicle under the same conditions, suggesting that inhibition of ERK1/2 partially abolished the high glucose effect (Fig. 30).

Blocking Akt/PkB signaling pathway by addition of wortmannin (100nmol/l) did not restore proliferation of ACH-3P under hyperglycemia and high oxygen levels compared to control cells (Fig. 30).
However, the combination of both inhibitors resulted in the same effect as U0126 alone.

Indeed, the effect of hyperglycemia was not completely abolished by inhibition of ERK1/2, proliferation under hyperglycemia was still significantly decreased ($p<0.01$) under hyperglycemia compared to cells treated under normoglycemic conditions. This indicates that ERK1/2 but not Akt/PkB is involved in the hyperglycemia-mediated effect. The partial effect of the ERK1/2 inhibitor suggests that also other mitogen-activated protein kinases like ERK5, JNK and p38 might be involved.

Certainly, the number of dead cells under hyperglycemic conditions was also affected by ERK1/2 and Akt/PkB inhibition. Significantly more dead cells were found using U0126 and wortmannin either singly or in combination compared to cells treated with vehicle control (Fig. 31).

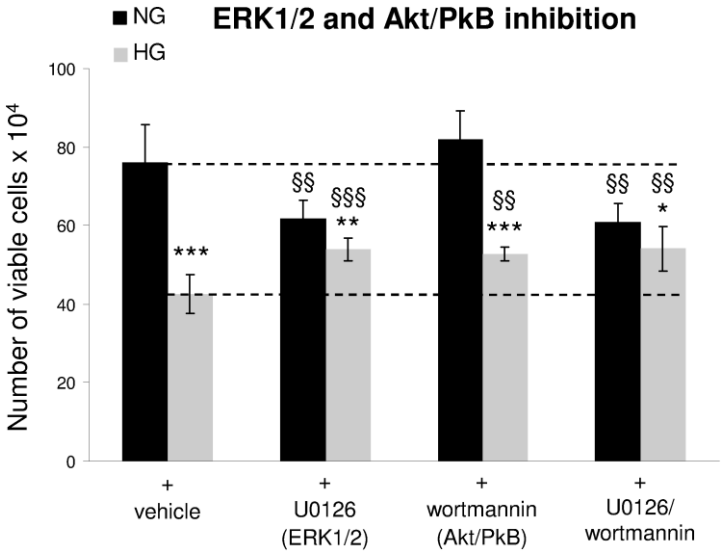

Figure 30 **Inhibition of ERK1/2 signaling pathway leads to increased ACH-3P cell proliferation under hyperglycemia at 21% oxygen.** ACH-3P cells were treated for 3d under normoglycemia (black bars) and hyperglycemia (grey bars) in the presence and absence (DMSO vehicle) of 10µmol/l U0126 (ERK1/2 inhibitor) or 10nmol/l wortmannin (Akt/PkB inhibitor) at 21% oxygen. Number of viable cells are presented as mean ± SD (n = 6). **P* < 0.05, ***P* < 0.01 and ****P* < 0.001 vs. NG + vehicle, NG + U0126, NG + wortmannin or NG + U0126/wortmannin, respectively; $^{§§}P < 0.01$ and $^{§§§}P < 0.001$ vs. NG + vehicle or HG + vehicle, respectively. Based on 6 replicates the coefficient of variation under NG + vehicle and HG + vehicle was 13% and 12%, respectively.

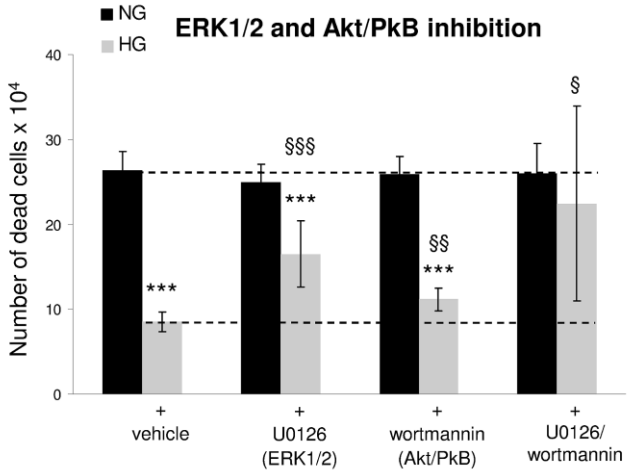

Figure 31 **Inhibition of ERK1/2 and Akt/PkB signaling pathway affected number of dead ACH-3P cells under hyperglycemia at 21% oxygen.** ACH-3P cells were treated for 3 days under normoglycemia (black bars) and hyperglycemia (grey bars) in the presence and absence of 10µmol/l U0126 (ERK1/2 inhibitor) and 10nmol/l wortmannin (Akt/PkB inhibitor) at 21% oxygen. Number of dead cells are presented as mean ± SD (n = 6). ****P* < 0.001 vs. NG + vehicle, NG + U0126, NG + wortmannin or NG + U0126/wortmannin, respectively; $^{§§}P < 0.01$ and $^{§§§}P < 0.001$ vs. HG + vehicle.

4.18 HLA-G expression of first-trimester trophoblasts

ACH-3P cells were separated into both subpopulations, HLA-G positive and negative cells. Villous cytotrophoblast cells at the tip of the anchoring villus represent the HLA-G negative cells, whereas invading extravillous cytotrophoblasts are characterized by HLA-G expression (Fig. 32).

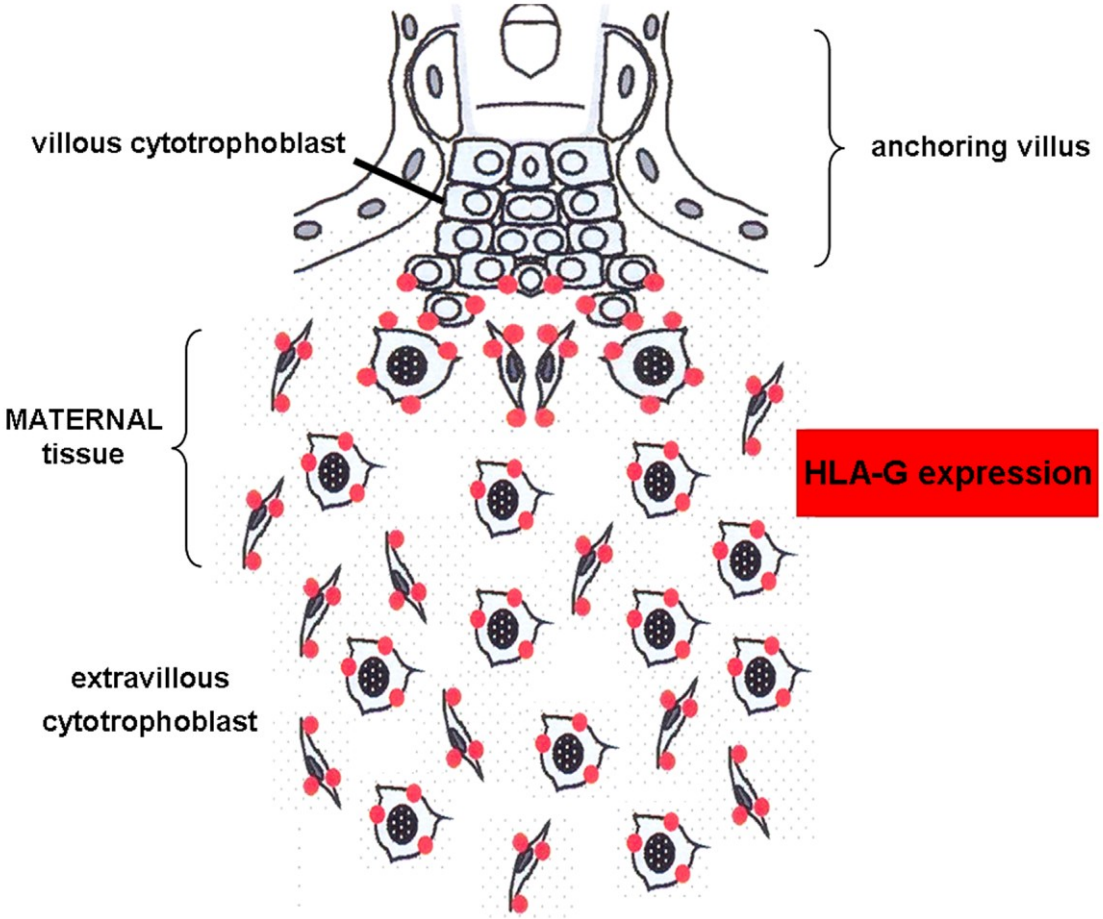

Figure 32 **Trophoblast invasion and HLA-G expression of extravillous cytotrophoblasts.** From the tip of the anchoring villus mononuclear extravillous cytotrophoblasts invade the uterine tissue. Towards the invasion process trophoblast cells differentiate and as a consequence human leukocyte antigen-G (HLA-G) becomes expressed; adapted from (Benirschke et al., 2006).

4.18.1 Stable separation in HLA-G positive and negative ACH-3P cells

With a specific antibody against HLA-G ACH-3P cells were separated into HLA-G positive and negative cells. ACH-3P cells were cultured under normoglycemia at 21% oxygen, separated, passaged once and immunoseparation was confirmed using semi quantitative RT-PCR. RNA from HLA-G positive and negative cells was isolated and semi quantitative RT-PCR after normalization with an internal control RPL30 revealed that immunoseparation of ACH-3P cells using magnetic beads resulted in distinct subpopulations of HLA-G positive and negative cells (Fig. 33A, B).

The use of flow cytometry resulted in a similar efficiency of HLA-G separation. However, in the current study separation with magnetic beads was performed, due to the high cell numbers with would be necessary for flow cytometry. Additionally, flow cytometry of 5 x 10^6 cells takes too long, resulting in damage of cell viability and in a low number of viable cells. Particularly, HLA-G negative cells were hardly harvested after flow cytometry. These data indicate that the use of magnetic beads is a more suitable method for the immunoseparation into HLA-G positive and negative cells.

HLA-G positive and negative cells were cultured for 3 days under normo- and hyperglycemia at 2.5% and 21% oxygen. RT-PCR and further normalization with RPL30 showed a stable separation of both subpopulations under normo- and hyperglycemic conditions over a time period of 3 days at 2.5% oxygen (Fig. 33C and D).

At 21% oxygen no viable cells could be harvested under any glucose concentration, thus analysis of RT-PCR data under these conditions could not be performed.

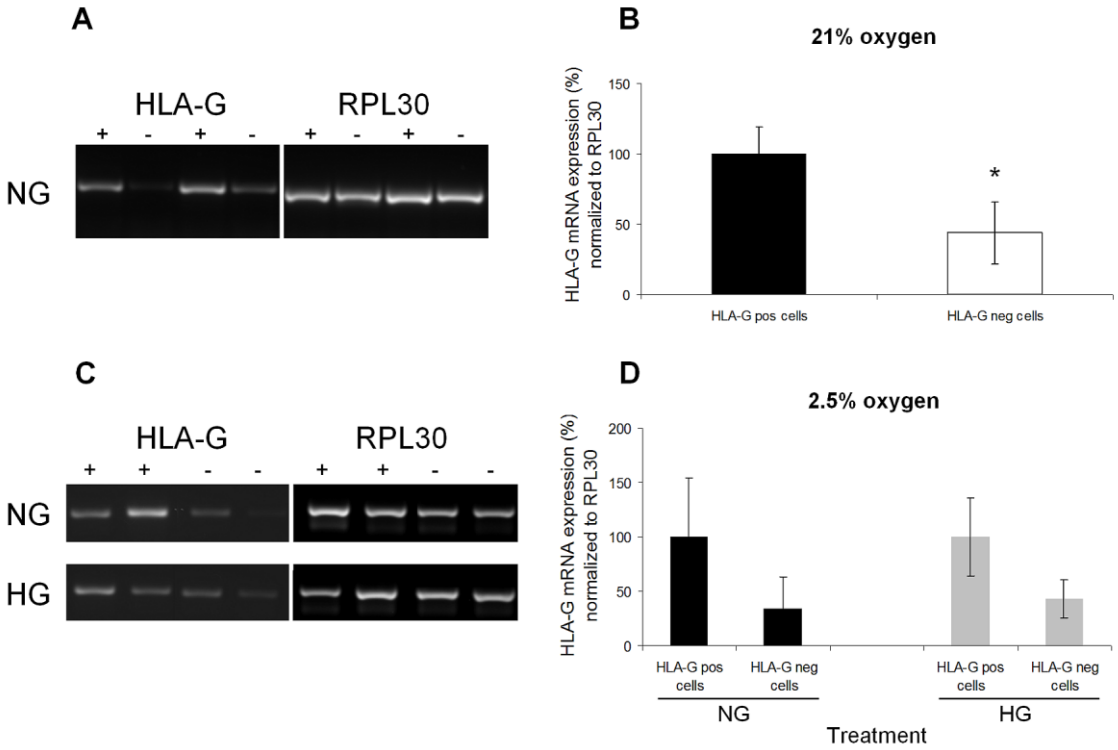

Figure 33 **Expression of HLA-G mRNA in ACH-3P cells after immunoseparation.** Short-term culture at 21% oxygen (over night; A and B) and long-term culture at 2.5% oxygen (3d; C and D) of ACH-3P cells separated into HLA-G positive and negative cells. (A) Semi quantitative RT-PCR for HLA-G mRNA expression of HLA-G positive and negative cells after immunoseparation and culture over night under normoglycemia (NG) at 21% oxygen. (B) mRNA expression of HLA-G as shown in (A) after normalization to the ribosomal protein L30 (RPL30), which served as internal control; mean ± SD (n = 2), data were obtained from three independent experiments. (C) Semi quantitative RT-PCR for HLA-G mRNA expression of HLA-G positive and negative cells after 3d under normo- (NG) and hyperglycemic (HG) conditions at 2.5% oxygen. (D) mRNA expression of HLA-G as shown in (C) after normalization to RPL30; mean ± SD (n = 2). *$P < 0.05$ HLA-G positive cells vs. HLA-G negative cells.

4.18.2 Proliferation of HLA-G positive and negative cells

HLA-G positive and negative ACH-3P cells were cultured under normo- and hyperglycemia at 2.5%, 8% and 21% oxygen for 3 days. Hyperglycemia significantly decreased the number of viable cells in both subpopulations at 2.5% (Fig. 34A). At 8% oxygen the number of viable was reduced under hyperglycemic conditions, however not significant (Fig. 34B). The number of dead cells was not affected under the conditions used here. This indicates that elevated glucose levels as typically present in maternal diabetes affect trophoblast development in early pregnancy and may contribute to pregnancy pathologies (Hiden and Desoye, 2010).

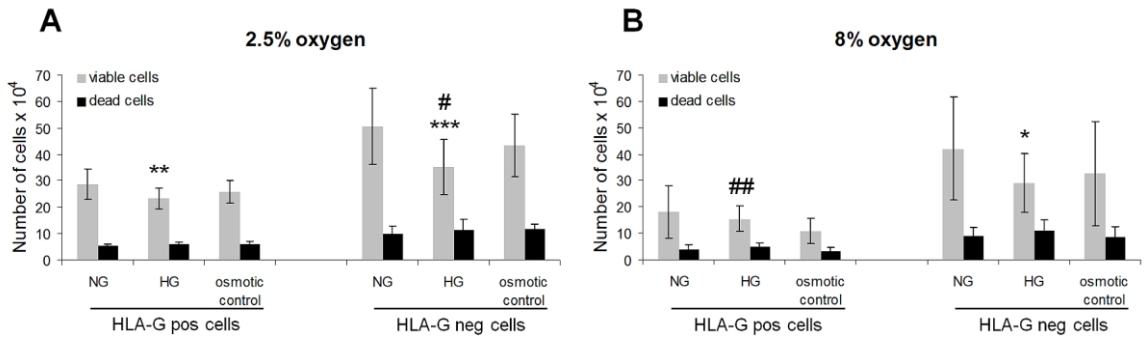

Figure 34 **Proliferation of HLA-G positive and negative ACH-3P cells cultured for 3d under normo- (NG) and hyperglycemia (HG) at 2.5% and 8% oxygen.** (A) Number of viable (grey bars) and dead (black bars) cells cultured for 3 days under normo- (NG) and hyperglycemia (HG) at 2.5% oxygen, (B) and 8% oxygen; mean ± SD (n = 6), data were obtained from three independent experiments. $^{*}P < 0.05$, $^{**}P < 0.01$ and $^{***}P < 0.001$ vs. NG; $^{\#}P < 0.05$ and $^{\#\#}P < 0.01$ vs. osmotic control.

As expected (Benirschke K et al., 2006), we showed that HLA-G negative cells proliferate stronger at 2.5% and 8% oxygen than HLA-G positive cells resulting in 1.7- and 2.1- fold more viable cells, respectively. In this scenario it is tempting to speculate that the difference in cell numbers represents different proliferation rates of HLA-G negative cytotrophoblasts at the tips of the cell columns and HLA-G positive non-proliferating and invasive extravillous trophoblasts.

At 21% oxygen no viable cells could be detected. HLA-G positive and negative cells detached during the incubation period, indicating cell death; hence, cell numbers

after 3 days were too low to be reliably determined. The proliferation reducing effect of 21% oxygen was also found in another first trimester human cytotrophoblast cell line (Kilburn et al., 2000). After 1 to 2d changes in the cell morphology at 21% oxygen, compared to cells cultured at 2.5% and 8% oxygen were monitored (data not shown).

4.19 First-trimester placental villous explants under hyperglycemia

4.19.1 Proliferation of villous explants under hyperglycemia

Placental villous explants from first trimester pregnancies (week 7, 8 and 10 of gestation) were used as a more complex tissue model. Proliferation of villous explants under normo- and hyperglycemic conditions at 2.5%, 8% and 21% oxygen was determined using a proliferation marker (Ki-67). Immunofluorescent staining was performed for cytokeratin 7 (green) and Ki-67 (red). DAPI was used as nuclear staining. Afterwards six random pictures per section were taken. All cytotrophoblast (CT) and Ki-67 positive CTs were counted.

Fig. 35 shows the immunofluorescent staining of placental villous explants. Each picture was counted and a median of each placenta was determined in every condition.

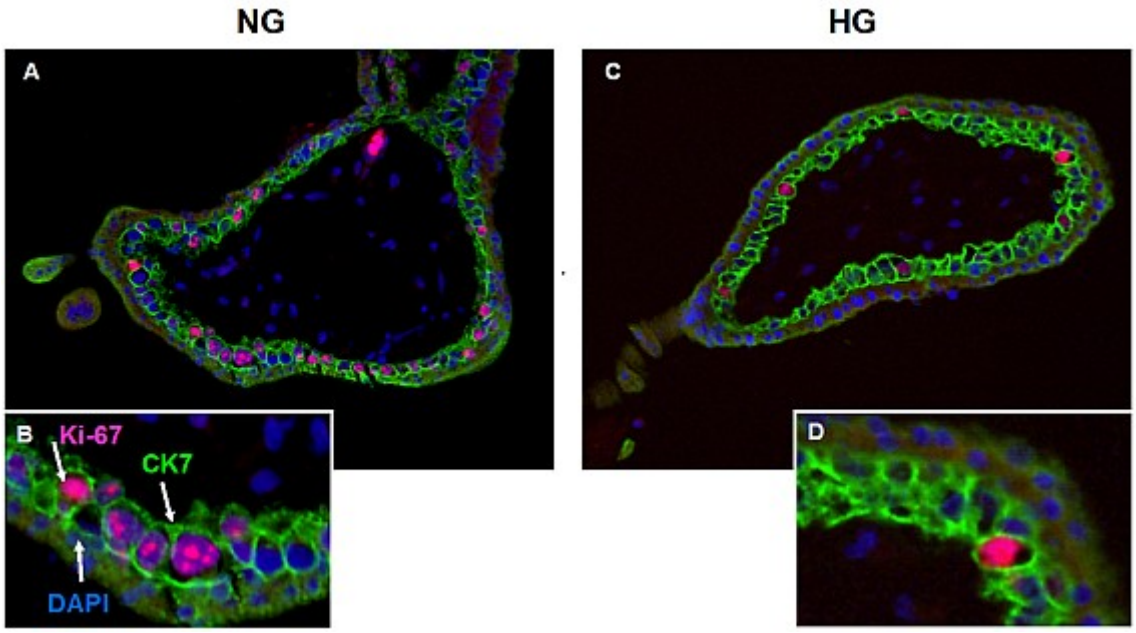

Figure 35 **Proliferation of placental villous explants under hyperglycemia at 21% oxygen.** Staining for proliferation marker (Ki-67), cytokeratin 7 (CK7) and nuclei (DAPI). (A) Explants under NG at 21% oxygen (magnification x 200); (B) explants under NG at 21% oxygen (magnification x 600); (C) explants under HG at 21% oxygen (magnification x 200) and (D) explants under HG at 21% oxygen (magnification x 600).

At 2.5% oxygen proliferation of placental explants was not significantly altered after 2 days under hyperglycemia compared to tissue cultured under normoglycmic conditions. After separation of early (7) and late (8 and 10) weeks of gestation during the first trimester no changes in Ki-67 positive cytotrophoblasts under hyperglycemia at 2.5% oxygen were observed (Fig. 36A).

Hyperglycemia increased the proliferation of placental explants in the beginning of the first trimester (week 7 of gestation) significantly at 8% oxygen. However, in week 8 and 10 of gestation no proliferation changes were monitored under hyperglycemia at 8% oxygen compared to control conditions (Fig. 36B).

In Fig. 36C placental explants in week 7, 8 and 10 of gestation showed reduced proliferation under hyperglycemia at 21% oxygen. The effect was more prominent in week 7, however proliferation was still reduced in week 8 and 10 of gestation, suggesting that proliferation is influenced by the gestational weeks.

Taken together, these data indicate that placental explants showed similar results compared with the trophoblast-derived cell line ACH-3P, which only showed reduced proliferation under hyperglycemia at 21% oxygen (Fig. 9E). Likewise, placental explants exhibited impaired proliferation under hyperglycemic conditions at 21% oxygen, whereas 2.5% oxygen had no effect and 8% oxygen significantly increased proliferation under hyperglycemic conditions.

However, at 21% oxygen the proliferation changes are not significant, but there is a tendency of reduced proliferation under high glucose concentrations. Indeed human tissue can display biological variance, leading to the knowledge that such studies need more replicates to get more precise data.

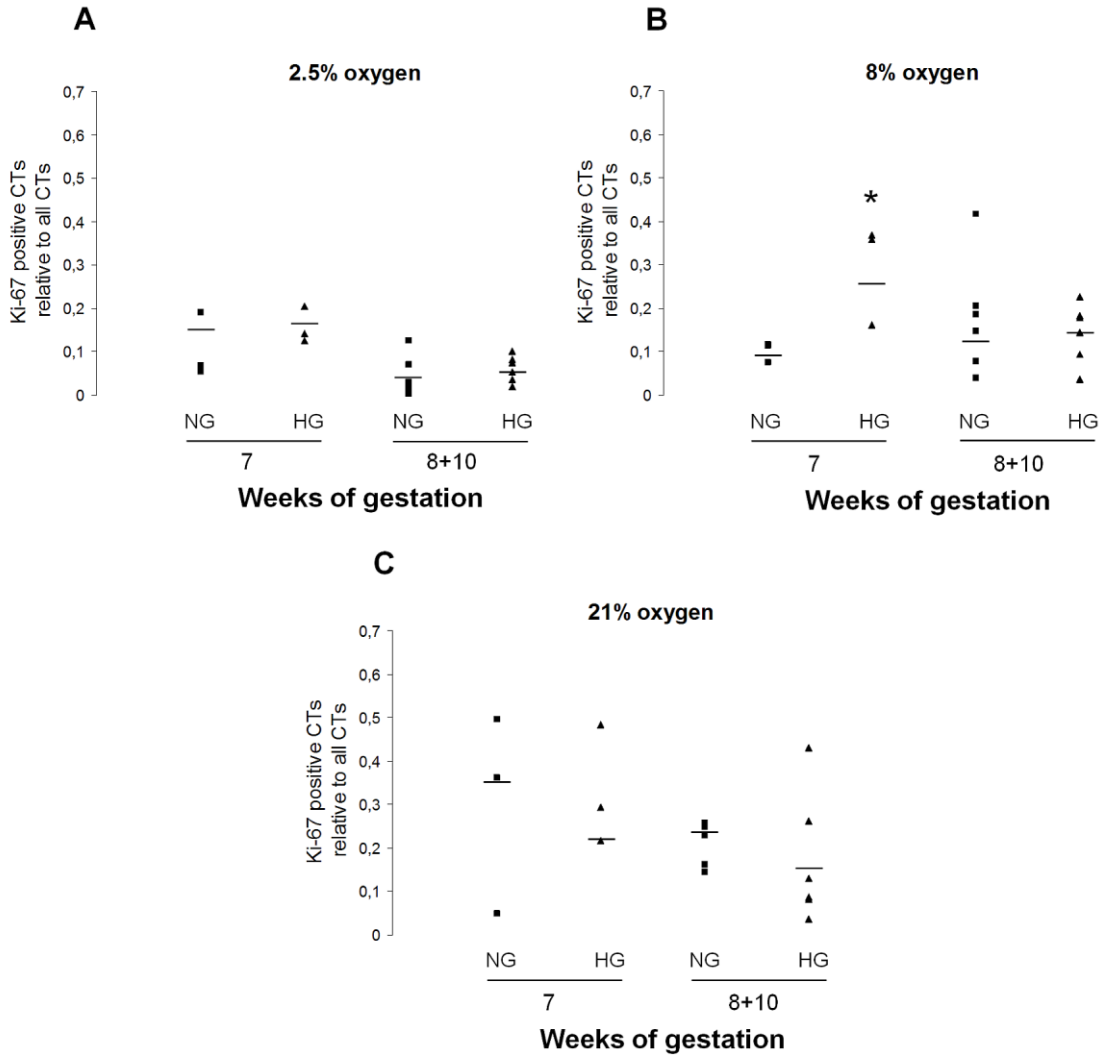

Figure 36 **Proliferation of first-trimester placental villous explants (week 7, 8 and 10 of gestation) under hyperglycemia at 2.5%, 8% and 21% oxygen.** (A, B, C) Number of Ki-67 positive cytotrophoblasts (CT) relative to all cytotrophoblast cells at 2.5%, 8% and 21% oxygen, respectively; Ki-67 positive cytotrophoblasts are presented as median; data were obtained from three individual placentas. **P* < 0.05 vs. NG.

5 Discussion

The effects of maternal diabetes on the placenta at the end of gestation have received much attention (Hiden and Desoye, 2010). However, only little information is available on placental development in the first trimester of a diabetic pregnancy. The present *in vitro* study focused on the trophoblast, the key placental cell type in early pregnancy, and investigated its growth in response to the diabetic environment. Long-term hyperglycemic conditions *in vitro* were used to represent one component of the diabetic environment *in vivo*. The experiments were carried out under varying oxygen conditions (2.5%, 8% and 21%) to mimic the increasing oxygen concentrations *in vivo* at the end of the first trimester of pregnancy. Heterogeneous ACH-3P cells closely resemble many characteristics of different aspects of primary first-trimester trophoblasts and combine these with the potential to proliferate, which the primary trophoblasts do not do *in vitro* (Hiden et al., 2007).

This is the first study in which oxygen was used as a modulator of the hyperglycemic response. The key findings of the present study were: (1) Long-term hyperglycemia reduced ACH-3P cell proliferation at 21% oxygen, high-glucose conditions did not affect cell growth under lower oxygen concentrations, (2) hyperglycemia increased trophoblast ROS levels independently of oxygen, (3) the hyperglycemic effect on proliferation was independent of ROS levels, (4) reduced proliferation was mediated by MAPK signaling, among others, (5) decreased cell growth of trophoblasts were confirmed by *placental explants* studies, and (6) both subpopulations, HLA-G positive and negative cells, were sensitive to both oxygen and glucose independent from each other.

In none of the experiments the number of dead cells was altered, however cell survival assays showed significantly increased apoptotic cells under hyperglycemia at 21% oxygen. Thus, in conclusion, hyperglycemia may affect trophoblasts as a consequence of both, apoptosis and reduced cell growth. Certainly, the main effect of high glucose and high oxygen presented in the current study is reduced cell proliferation.

5.1 Oxygen-dependent proliferation under hyperglycemia

At about week 12 of gestation maternal blood flow towards the placenta is fully established leading to enhanced oxygen tension within the organ (Huppertz et al., 2009). The rapid increase of placental oxygen concentrations is associated with increased oxidative stress. ROS production occurs in normal pregnancies, but is even more pronounced in pregnancies complicated by diabetes (King and Loeken, 2004).

It is tempting to speculate that this could be an explanation for the findings that hyperglycemia-reduced proliferation is oxygen-dependent, while basal proliferation is not modified by oxygen concentrations. Previous proliferation studies under hyperglycemic conditions in different cell types and tissues showed inconsistent findings. Decreased proliferation (Weiss et al., 2001, Favaro et al., 2008) as well as enhanced cell growth (Kobayashi et al., 2005, Di Paolo et al., 1996) were observed, indicating that the hyperglycemia effect on proliferation is cell-specific.

Additionally, a cell survival assay showed that ACH-3P cells exhibit more cleaved caspase 3 positive cells under hyperglycemia at 21% oxygen compared to cells treated under control conditions, indicating that also increased apoptosis occurs in ACH-3P cells under these conditions. However, the percentage of cleaved caspase 3 positive cells is still low, suggesting apoptosis alone does not cause decreased cell numbers. That implies and confirms the hypothesis that hyperglycemia and high oxygen reduce cell proliferation.

Cell cycle analysis showed modifications in specific cell cycle phases at 21% oxygen. Long-term hyperglycemia resulted in reduced G_1-phase and significantly increased S-phase cell populations, whereas G_2/M-phase was not affected under these conditions. This may reflect an arrest at some point past S-phase of the cell cycle. Hyperglycemia may affect cyclins and cyclin-dependent kinase inhibitors (Huang et al., 2007). Therefore, cyclin B1 expression was measured in ACH-3P cells after 3 days under hyperglycemia at 21% oxygen. Decreased levels of cyclin B1 protein were determined under these conditions compared to control cells. These data also suggest that ACH-3P cells are arrested at some point past S-phase of the cell cycle (Fig. 28A and B). This

would confirm the observation of cell cycle analysis (Fig. 9F). However, the specific mechanisms underlying cell cycle changes in the used setting are still unknown.

5.2 Oxygen-independent ROS formation under hyperglycemia

In placental explants, an increase of oxidative stress markers after hypoxia-reoxygenation has been reported (Cindrova-Davies et al., 2007), suggesting that ROS formation is oxygen-dependent. Furthermore, a large body of evidence shows increased ROS levels caused by hyperglycemia in different cell types (Ihnat et al., 2007, Forbes et al., 2008). Thus, previous observations indicate that both oxygen and high-glucose concentrations can lead to oxidative stress in cells and tissues.

To examine the underlying mechanisms leading to decreased trophoblast proliferation at 21% oxygen, ROS levels and H_2O_2 release in these cells were determined. Intracellular ROS production was enhanced under hyperglycemia at 2.5% and 8% oxygen compared to cells cultured under normoglycemic conditions. This set of data indicates that at 2.5% and 8% oxygen under hyperglycemia ACH-3P cells produced significantly more ROS, which did not affect proliferation. At 21% oxygen the situation was different: ACH-3P cells showed higher ROS generation and H_2O_2 release under normoglycemia. Indeed, ROS levels under hyperglycemia were not significantly altered at 21% oxygen compared to cells after 3d under high-glucose concentrations at 2.5% and 8% oxygen. These findings, independently obtained by two different methods, indicate that ROS production under normoglycemia is oxygen-dependent, but oxygen-independent under hyperglycemia.

Additionally, the time course of ROS production was measured. At 2.5% and 8% oxygen the ROS levels were already significantly enhanced after 1 day under hyperglycemia compared to cells treated under normoglycemic conditions. ROS production was even increased up to 3 days under these conditions (Fig.14A and B). At 21% oxygen the ROS levels are already significantly decreased after 1 day under hyperglycemia compared to normoglycemic conditions with further decrease up to 3 days (Fig. 15C and 16B). Thus, ROS levels were reduced by hyperglycemia at 21% oxygen already before an effect on cell proliferation was observed. This further substantiates the conclusion that ROS and proliferation changes are independent.

In a likely scenario, reduced ROS levels under hyperglycemia at 21% oxygen can be the consequence of cell adaption to high-glucose concentrations by up-regulating cellular antioxidant systems, which may have an impact on proliferation and cell cycle. Such effects of hyperglycemia on antioxidant systems have been reported previously (Weidig et al., 2004, Matsunami et al., 2009) and were confirmed here. In general, antioxidants showed higher expression levels under hyperglycemia at 21% oxygen compared to cell treated under control conditions (Fig. 26B, D, F and H). Furthermore, at 8% oxygen the expression of several antioxidants was decreased under normo- and hyperglycemia compared to cells cultured at high oxygen levels of 21% (Fig. 26A, C, E, and G). These data have been confirmed for three specific antioxidants by Real-Time RT-PCR. Hyperglycemia up-regulated heme oxygenase, glutathione peroxidase 1 and nuclear factor (erythroid-derived 2)-like 2 compared to normoglycemic conditions. All three genes encode proteins with a special function as antioxidants, strongly supporting the notion that ACH-3P cells had adjusted to the diabetic environment (Fig. 15D). In conclusion, ACH-3P cells may exhibit increased antioxidants levels to scavenge excessive ROS production under high glucose and high oxygen conditions.

In addition, mitochondrial mass in the human placenta increases with gestational age suggesting an increase in superoxide production by mitochondria throughout the course of pregnancy (Myatt and Cui, 2004). It has been shown that first-trimester trophoblast mitochondria are resistant against hyperglycemia-induced high amplitude swelling (Jones et al., 2001). Recent work highlighted the influence of mitochondrial superoxide on cell proliferation (Sun et al., 2010). As shown in Fig. 16D superoxide levels were increased in cells treated under hyperglycemia and 21% oxygen. Likewise, ATP production (Fig. 17) and mitochondrial activity (Fig. 18C) were also reduced under hyperglycemia at 21% oxygen, suggesting that ACH-3P cells produce more superoxide via mitochondria. Decreased ATP production and diminished mitochondrial activity confirm the observation of increased superoxide levels (Fig. 16D) under high glucose and high oxygen conditions. Therefore, the next hypothesises was that elevated mitochondrial ROS formation contributes to decreased proliferation.

5.3 Cytosolic versus mitochondrial ROS and their influence on proliferation

To investigate whether cytosolic and mitochondrial ROS influence proliferation at 21% oxygen ROS generation in both cell compartments was modulated (Fig. 21). Addition of antioxidants, such as ascorbate (Peng et al., 2005), Trolox® (Leloup et al., 2009) and NAC (Poncin et al., 2010), which are known to decrease intracellular ROS levels, had no beneficial impact on proliferation under hyperglycemic conditions (Fig. 19A-C).

Proliferation could not be restored by supplementation of any antioxidant. These findings were in line with previous observations in endothelial progenitor cells where addition of antioxidants (SOD, catalase, ascorbate, NAC) did not alter proliferation under hyperglycemic conditions (Chen et al., 2007). This may represent a cell-specific effect since catalase completely reversed the proliferation effect of high-glucose treatment in aortic smooth muscle cells (Peiro et al., 2001). Interestingly, decreasing and increasing cytosolic and mitochondrial ROS levels did not modify ACH-3P proliferation under hyperglycemia, suggesting ROS and cell proliferation are not associated in ACH-3P cells under the conditions used here, which further corroborates the lack of effect of the antioxidants applied.

In mammalian cells, the mitogen-activated protein kinase (MAPK) signal transduction pathway plays a crucial role in regulation of proliferation. Hyperglycemia was shown to increase p38 MAPK activity resulting in CREB activation (Xu et al., 2003), thus is unlikely to account for the proliferation reduction. However, glucose has been reported to diminish PI3K and Akt/PkB phosphorylation as well as Akt/PkB activity in endothelial cells. Therefore, this may lead to the speculation that hyperglycemia-impaired PI3K-AKT signaling may promote decreased proliferation in diabetes (Varma et al., 2005).

Analysis of phosphorylation showed increased phospho-ERK1/2 expression after 15, 30 and 60min under hyperglycemia at 21% oxygen, whereas Akt/PkB was not phosphorylated under normo- and hyperglycemic conditions. Though, phosphorylation of proteins is a dynamic intracellular process.

Lin et al. showed that enhanced ERK1/2 phosphorylation leads to increased cell proliferation (Li et al., 2004). These previous findings are not consistent with the results that ERK1/2 phosphorylation is increased and cell proliferation is reduced in ACH-3P cells under hyperglycemia at 21% oxygen, assuming that phosphorylation proceeds during the entire treatment period due to the glucose stimulus caused by medium exchanges every day. Hence, these results suggest that phosphorylation analyses are not the appropriate method to delineate the signaling pathway involved in the present study.

The current results indicate that high-glucose levels do not control proliferation by using intracellular ROS as signaling molecules (Fig 37). To gain insight into potential pathways involved, the present study focused on two key kinases Akt/PkB and ERK1/2.

Therefore, ACH-3P cells were cultured for 3 days under hyperglacmia at 21% oxygen with or without specific inhibitors. Akt/PkB inhibition did not restore proliferation under hyperglycemia at 21% oxygen, indicating that Akt/PkB is not involved. However, inhibition of ERK1/2 partially abolished reduced proliferation under hyperglycemia at 21% oxygen. Thus, signaling through the MAPkinase pathway contributes to the effect of hyperglycemia but the involvement of other mechanisms cannot be excluded (Fig. 30).

These data indicate that inhibiting ERK1/2 and Akt/PkB by U0126 and wortmannin, respectively, and subsequent determination of viable and dead cells is the most appropriate method to identify putative mechanisms underlying diminished proliferation under the used experimental setting.

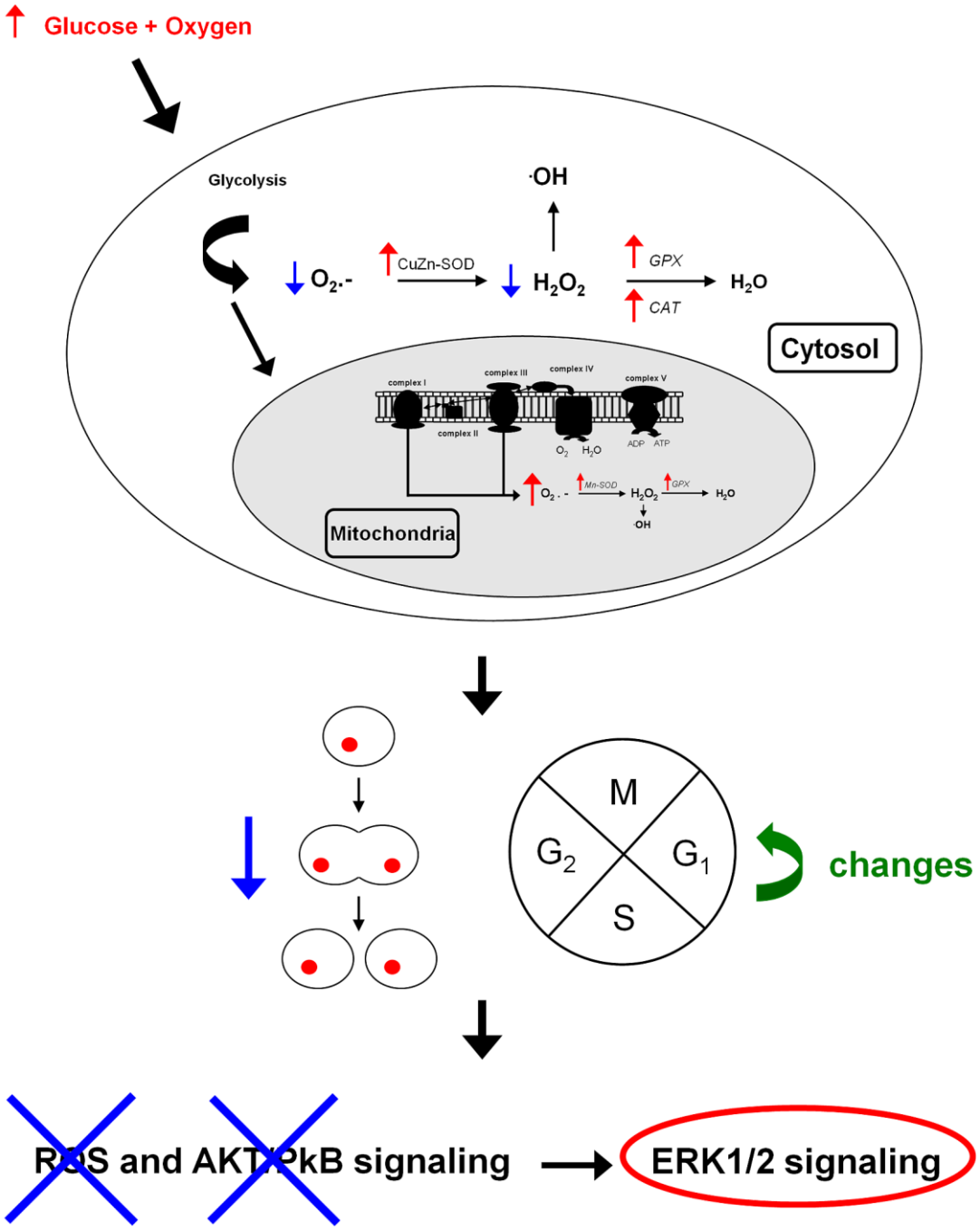

Figure 37 **Proliferation and cell cycle changes caused by high glucose and high oxygen levels are ROS-independent.** A combination of hyperglycemia and high oxygen (21%) leads to reduced ACH-3P cell proliferation, because of changes in the cell cycle (G_1- and S-phase). However, ROS and Akt/PkB signaling are not involved in these processes. Certainly, ERK1/2 may play a crucial role in decreased cell growth under hyperglycemia at 21% oxygen in human trophoblasts. GPX, glutathione peroxidase; CAT, catalase; CuZn-SOD, copper-zinc superoxide dismutase; Mn-SOD, manganese superoxide dismutase; H_2O_2, hydrogen peroxide; ·OH, hydroxyl radical; O_2.-, superoxide anion; Akt/PkB, protein kinase B; ERK1/2, extracellular signal-regulated kinases 1/2.

5.4 HLA-G expression

After separation of HLA-G positive and negative ACP-3P cells, at 21% oxygen no viable cells could be detected after 3 days. HLA-G positive and negative cells detached during the incubation period, indicating cell death; hence, cell numbers after 3 days were too low to be reliably determined. This data suggests that both subpopulations, HLA-G positive and negative trophoblast cells, are sensitive towards increased oxygen concentrations. This data suggests that also *in vivo* both subpopulations, HLA-G positive and negative trophoblast cells, are sensitive towards increased oxygen concentrations. This may explain why a premature onset of maternal placental circulation results in oxidative damage of the trophoblast and early pregnancy loss (Jauniaux et al., 2003).

Current evidence supports the concept that embryo and placenta develop in a low oxygen environment in the first trimester. Thus, the early gestation placenta is acutely sensitive to oxygen caused stress, due to poorly expressed protection systems, such as antioxidants (James et al., 2006). Increased oxygen concentrations may lead to enhanced oxygen-mediated damage resulting in decreased proliferation and increased cell death. Interestingly, unseparated ACH-3P cells do not show the deleterious response to high oxygen concentrations, suggesting the need for a soluble factor or a direct cell-cell contact of HLA-G positive and negative cells to stabilize the cells.

5.5 Proliferation of placental explants under hyperglycemia

Proliferation of placental villous explants showed different response to hyperglycemia at varying oxygen concentrations. At 2.5% oxygen proliferation was not influenced by glucose, whereas at 8% oxygen increased cell growth was observed in week 7 of gestation under hyperglycemia. The result of reduced proliferation of ACH-3P cells under hyperglycemia at 21% oxygen was confirmed with placental explants. The more complex tissue model also showed decreased cytotrophoblast proliferation under hyperglycemia at 21% oxygen. Thus, a combination of high glucose and high oxygen resulted in diminished proliferation in human first trimester placentas.

In the present study a combination of high glucose and high oxygen in first trimester placental villous explants has been investigated for the fist time. However, the main challenge is that the response of explants critically depends on the week of gestation at which pregnancy has been terminated. Nevertheless, in conclusion, the results of proliferation studies, using ACH-3P cells as an *in vitro* model, correlate with cell growth studies in the more complex tissue model.

5.6 Pathophysiological implications

Early in pregnancy the oxygen tension in the intervillous space and within the placenta is low. At this stage hyperglycemia may not affect the development and proliferation of the trophoblast, and hence placental growth. Later in the first trimester, when the oxygen tension rises, the trophoblast becomes sensitive to the hyperglycemic environment and reduces its proliferation. This may result in diminished nutrient delivery to the fetus, ultimately resulting in reduced growth of the fetus proper (Pedersen et al., 1984). In this scenario the trophoblast would be the primary target of the diabetic environment and the fetus would respond with some delay. Some support for this speculation comes from the observation that fetal growth was delayed only at week 12 pm, but not at week 8 pm, although the oxygen tension rises the most between week 8 and 10 pm (Brown et al., 1992).

In the current study it was demonstrated for the first time that a ROS-independent decrease of proliferation under hyperglycemia can be caused by elevated oxygen concentrations. These findings suggest that in diabetes reduced trophoblast proliferation may have an impact on embryonic growth at the time of oxygen increase at the end of the first trimester of pregnancy. Thus, we propose that maternal diabetes alters placental development during the first trimester of pregnancy. Whether the increased risk for preeclampsia, miscarriage and intrauterine growth restriction in diabetic pregnancies (Biggers and Summers, 2008, Sibai, 2000, Mammon et al., 2005) is related to the impaired trophoblast growth remains an open question.

6 References

BENIRSCHKE K, KAUFMANN P & BAERGEN R (2006) *Pathology of the human placenta.,* New York, Springer Science & Business Media.

BIGGERS, J. D. & SUMMERS, M. C. (2008) Impact of hyperglycemia on early embryo development and embryopathy: in vitro experiments using a mouse model. *Hum Reprod,* 23**,** 2874-5.

BISCHOF, P. & IRMINGER-FINGER, I. (2005) The human cytotrophoblastic cell, a mononuclear chameleon. *Int J Biochem Cell Biol,* 37**,** 1-16.

BROWN, Z. A., MILLS, J. L., METZGER, B. E., KNOPP, R. H., SIMPSON, J. L., JOVANOVIC-PETERSON, L., SCHEER, K., VAN ALLEN, M. I., AARONS, J. H. & REED, G. F. (1992) Early sonographic evaluation for fetal growth delay and congenital malformations in pregnancies complicated by insulin-requiring diabetes. National Institute of Child Health and Human Development Diabetes in Early Pregnancy Study. *Diabetes Care,* 15**,** 613-9.

BURTON, G. J. (2009) Oxygen, the Janus gas; its effects on human placental development and function. *J Anat,* 215**,** 27-35.

BURTON, G. J., JAUNIAUX, E. & CHARNOCK-JONES, D. S. (2010) The influence of the intrauterine environment on human placental development. *Int J Dev Biol,* 54**,** 303-12.

CHEN, Y. H., LIN, S. J., LIN, F. Y., WU, T. C., TSAO, C. R., HUANG, P. H., LIU, P. L., CHEN, Y. L. & CHEN, J. W. (2007) High glucose impairs early and late endothelial progenitor cells by modifying nitric oxide-related but not oxidative stress-mediated mechanisms. *Diabetes,* 56**,** 1559-68.

CHOI, S. W., BENZIE, I. F., MA, S. W., STRAIN, J. J. & HANNIGAN, B. M. (2008) Acute hyperglycemia and oxidative stress: direct cause and effect? *Free Radic Biol Med,* 44**,** 1217-31.

CINDROVA-DAVIES, T., SPASIC-BOSKOVIC, O., JAUNIAUX, E., CHARNOCK-JONES, D. S. & BURTON, G. J. (2007) Nuclear factor-kappa B, p38, and stress-activated protein kinase mitogen-activated protein kinase signaling pathways regulate proinflammatory cytokines and apoptosis in human placental explants in response to oxidative stress: effects of antioxidant vitamins. *Am J Pathol,* 170**,** 1511-20.

CUI, X. L., BROCKMAN, D., CAMPOS, B. & MYATT, L. (2006) Expression of NADPH oxidase isoform 1 (Nox1) in human placenta: involvement in preeclampsia. *Placenta,* 27**,** 422-31.

DENNERY, P. A. (2007) Effects of oxidative stress on embryonic development. *Birth Defects Res C Embryo Today,* 81**,** 155-62.

DI PAOLO, S., GESUALDO, L., RANIERI, E., GRANDALIANO, G. & SCHENA, F. P. (1996) High glucose concentration induces the overexpression of transforming growth factor-beta through the activation of a platelet-derived growth factor loop in human mesangial cells. *Am J Pathol,* 149**,** 2095-106.

DWORAKOWSKI, R., ALOM-RUIZ, S. P. & SHAH, A. M. (2008) NADPH oxidase-derived reactive oxygen species in the regulation of endothelial phenotype. *Pharmacol Rep,* 60**,** 21-8.

FAVARO, E., MICELI, I., BUSSOLATI, B., SCHMITT-NEY, M., CAVALLO PERIN, P., CAMUSSI, G. & ZANONE, M. M. (2008) Hyperglycemia induces apoptosis of human pancreatic islet endothelial cells: effects of pravastatin on the Akt survival pathway. *Am J Pathol,* 173**,** 442-50.

FORBES, J. M., COUGHLAN, M. T. & COOPER, M. E. (2008) Oxidative stress as a major culprit in kidney disease in diabetes. *Diabetes,* 57**,** 1446-54.

FREINKEL, N. (1980) Banting Lecture 1980. Of pregnancy and progeny. *Diabetes,* 29**,** 1023-35.

FROLOVA, A. I., O'NEILL, K. & MOLEY, K. H. (2011) Dehydroepiandrosterone Inhibits Glucose Flux Through the Pentose Phosphate Pathway in Human and Mouse Endometrial Stromal Cells, Preventing Decidualization and Implantation. *Mol Endocrinol*.

GAO, L. & MANN, G. E. (2009) Vascular NAD(P)H oxidase activation in diabetes: a double-edged sword in redox signalling. *Cardiovasc Res,* 82**,** 9-20.

GAO, Q. & GAO, Y. M. (2007) Hyperglycemic condition disturbs the proliferation and cell death of neural progenitors in mouse embryonic spinal cord. *Int J Dev Neurosci,* 25**,** 349-57.

GEORGE, J. & STRUTHERS, A. D. (2009) Role of urate, xanthine oxidase and the effects of allopurinol in vascular oxidative stress. *Vasc Health Risk Manag,* 5**,** 265-72.

GILL, P. S. & WILCOX, C. S. (2006) NADPH oxidases in the kidney. *Antioxid Redox Signal,* 8**,** 1597-607.

GNUDI, L., THOMAS, S. M. & VIBERTI, G. (2007) Mechanical forces in diabetic kidney disease: a trigger for impaired glucose metabolism. *J Am Soc Nephrol,* 18**,** 2226-32.

GUPTE, S., LABINSKYY, N., GUPTE, R., CSISZAR, A., UNGVARI, Z. & EDWARDS, J. G. Role of NAD(P)H oxidase in superoxide generation and endothelial dysfunction in Goto-Kakizaki (GK) rats as a model of nonobese NIDDM. *PLoS One,* 5**,** e11800.

HARRIS, L. K. (2010) Review: Trophoblast-vascular cell interactions in early pregnancy: how to remodel a vessel. *Placenta,* 31 Suppl**,** 93-8.

HENDERSON, J. R., SWALWELL, H., BOULTON, S., MANNING, P., MCNEIL, C. J. & BIRCH-MACHIN, M. A. (2009) Direct, real-time monitoring of superoxide generation in isolated mitochondria. *Free Radic Res,* 43**,** 796-802.

HIDEN U & DESOYE G (2010) The human placenta in diabetes. IN MCCANCE DR, S. D., MARESH JG (Ed.) *A practical manual of diabetes in pregnancy.* Oxford:Wiley-Blackwell.

HIDEN U, FROEHLICH J & DESOYE G (2011) Diabetes and the Placenta. IN HELEN H, KAY D & NELSON M AND WANG Y (Eds.) *The Placenta: From Development to Disease.* Blackwell Publishing Ltd.

HIDEN, U., WADSACK, C., PRUTSCH, N., GAUSTER, M., WEISS, U., FRANK, H. G., SCHMITZ, U., FAST-HIRSCH, C., HENGSTSCHLAGER, M., POTGENS, A., RUBEN, A., KNOFLER, M., HASLINGER, P., HUPPERTZ, B., BILBAN, M., KAUFMANN, P. & DESOYE, G. (2007) The first trimester human trophoblast cell line ACH-3P: a novel tool to study autocrine/paracrine regulatory loops of human trophoblast subpopulations-TNF-alpha stimulates MMP15 expression. *BMC Dev Biol,* 7**,** 137.

HUANG, J. S., CHUANG, L. Y., GUH, J. Y., HUANG, Y. J. & HSU, M. S. (2007) Antioxidants attenuate high glucose-induced hypertrophic growth in renal tubular epithelial cells. *Am J Physiol Renal Physiol,* 293**,** F1072-82.

HUPPERTZ, B. (2008) Placental origins of preeclampsia: challenging the current hypothesis. *Hypertension,* 51**,** 970-5.

HUPPERTZ, B., GAUSTER, M., ORENDI, K., KONIG, J. & MOSER, G. (2009) Oxygen as modulator of trophoblast invasion. *J Anat,* 215**,** 14-20.

IHNAT, M. A., THORPE, J. E., KAMAT, C. D., SZABO, C., GREEN, D. E., WARNKE, L. A., LACZA, Z., CSELENYAK, A., ROSS, K., SHAKIR, S., PICONI, L., KALTREIDER, R. C. & CERIELLO, A. (2007) Reactive oxygen species mediate a cellular 'memory' of high glucose stress signalling. *Diabetologia,* 50**,** 1523-31.

JAMES, J. L., STONE, P. R. & CHAMLEY, L. W. (2006) The regulation of trophoblast differentiation by oxygen in the first trimester of pregnancy. *Hum Reprod Update,* 12**,** 137-44.

JAUNIAUX, E. & BURTON, G. J. (2005) Pathophysiology of histological changes in early pregnancy loss. *Placenta,* 26**,** 114-23.

JAUNIAUX, E., HEMPSTOCK, J., GREENWOLD, N. & BURTON, G. J. (2003) Trophoblastic oxidative stress in relation to temporal and regional differences in maternal placental blood flow in normal and abnormal early pregnancies. *Am J Pathol,* 162**,** 115-25.

JAUNIAUX, E., WATSON, A. L., HEMPSTOCK, J., BAO, Y. P., SKEPPER, J. N. & BURTON, G. J. (2000) Onset of maternal arterial blood flow and placental oxidative stress. A possible factor in human early pregnancy failure. *Am J Pathol,* 157**,** 2111-22.

JONES, C. J., WEISS, U., SIMAN, C. M. & DESOYE, G. (2001) Mitochondria from human trophoblast and embryonic liver cells are resistant to hyperglycaemia-associated high-amplitude swelling. *Diabetologia,* 44**,** 389-91.

KANETO, H., KATAKAMI, N., MATSUHISA, M. & MATSUOKA, T. A. (2010) Role of reactive oxygen species in the progression of type 2 diabetes and atherosclerosis. *Mediators Inflamm,* 2010**,** 453892.

KILBURN, B. A., WANG, J., DUNIEC-DMUCHOWSKI, Z. M., LEACH, R. E., ROMERO, R. & ARMANT, D. R. (2000) Extracellular matrix composition and hypoxia regulate the expression of HLA-G and integrins in a human trophoblast cell line. *Biol Reprod,* 62**,** 739-47.

KING, G. L. & LOEKEN, M. R. (2004) Hyperglycemia-induced oxidative stress in diabetic complications. *Histochem Cell Biol,* 122**,** 333-8.

KOBAYASHI, Y., NARUSE, K., HAMADA, Y., NAKASHIMA, E., KATO, K., AKIYAMA, N., KAMIYA, H., WATARAI, A., NAKAE, M., OISO, Y. & NAKAMURA, J. (2005) Human proinsulin C-peptide prevents proliferation of rat aortic smooth muscle cells cultured in high-glucose conditions. *Diabetologia,* 48**,** 2396-401.

KORGUN, E. T., CELIK-OZENCI, C., ACAR, N., CAYLI, S., DESOYE, G. & DEMIR, R. (2006) Location of cell cycle regulators cyclin B1, cyclin A, PCNA, Ki67 and cell cycle inhibitors p21, p27 and p57 in human first trimester placenta and deciduas. *Histochem Cell Biol,* 125**,** 615-24.

LANGE, K. & PROFT, E. R. (1970) Inhibition of the 6-phosphogluconate dehydrogenase in the rat kidney by 6-aminonicotinamide. *Naunyn Schmiedebergs Arch Pharmakol,* 267**,** 177-80.

LAPPAS, M., HIDEN, U., FROEHLICH, J., DESOYE, G., HAUGEL-DE MOUZON, S. & JAWERBAUM, A. The Role of Oxidative Stress in the Pathophysiology of Gestational Diabetes Mellitus. *Antioxid Redox Signal*.

LELOUP, C., TOURREL-CUZIN, C., MAGNAN, C., KARACA, M., CASTEL, J., CARNEIRO, L., COLOMBANI, A. L., KTORZA, A., CASTEILLA, L. & PENICAUD, L. (2009) Mitochondrial reactive oxygen species are obligatory signals for glucose-induced insulin secretion. *Diabetes,* 58**,** 673-81.

LI, S., GERRARD, E. R., JR. & BALKOVETZ, D. F. (2004) Evidence for ERK1/2 phosphorylation controlling contact inhibition of proliferation in Madin-Darby canine kidney epithelial cells. *Am J Physiol Cell Physiol,* 287**,** C432-9.

LOREGGER, T., POLLHEIMER, J. & KNOFLER, M. (2003) Regulatory transcription factors controlling function and differentiation of human trophoblast--a review. *Placenta,* 24 Suppl A**,** S104-10.

MAKINO, A., SCOTT, B. T. & DILLMANN, W. H. (2010) Mitochondrial fragmentation and superoxide anion production in coronary endothelial cells from a mouse model of type 1 diabetes. *Diabetologia,* 53**,** 1783-94.

MAMMON, K., KESHET, R., SAVION, S., PEKAR, O., ZASLAVSKY, Z., FEIN, A., TODER, V. & TORCHINSKY, A. (2005) Diabetes-induced fetal growth retardation is associated with suppression of NF-kappaB activity in embryos. *Rev Diabet Stud,* 2**,** 27-34.

MANN, G. E., ROWLANDS, D. J., LI, F. Y., DE WINTER, P. & SIOW, R. C. (2007) Activation of endothelial nitric oxide synthase by dietary isoflavones: role of NO in Nrf2-mediated antioxidant gene expression. *Cardiovasc Res,* 75**,** 261-74.

MATSUNAMI, T., SATO, Y., SATO, T., ARIGA, S., SHIMOMURA, T. & YUKAWA, M. (2009) Oxidative stress and gene expression of antioxidant enzymes in the streptozotocin-induced diabetic rats under hyperbaric oxygen exposure. *Int J Clin Exp Pathol,* 3**,** 177-88.

MOSER, G., ORENDI, K., GAUSTER, M., SIWETZ, M., HELIGE, C. & HUPPERTZ, B. (2010) The art of identification of extravillous trophoblast. *Placenta,* 32**,** 197-9.

MURPHY, M. P. (2009) How mitochondria produce reactive oxygen species. *Biochem J,* 417**,** 1-13.

MYATT, L. (2010) Review: Reactive oxygen and nitrogen species and functional adaptation of the placenta. *Placenta,* 31 Suppl**,** S66-9.

MYATT, L. & CUI, X. (2004) Oxidative stress in the placenta. *Histochem Cell Biol,* 122**,** 369-82.

NISHIKAWA, T., EDELSTEIN, D., DU, X. L., YAMAGISHI, S., MATSUMURA, T., KANEDA, Y., YOREK, M. A., BEEBE, D., OATES, P. J., HAMMES, H. P., GIARDINO, I. & BROWNLEE, M. (2000) Normalizing mitochondrial superoxide production blocks three pathways of hyperglycaemic damage. *Nature,* 404**,** 787-90.

PALMEIRA, C. M., ROLO, A. P., BERTHIAUME, J., BJORK, J. A. & WALLACE, K. B. (2007) Hyperglycemia decreases mitochondrial function: the regulatory role of mitochondrial biogenesis. *Toxicol Appl Pharmacol,* 225**,** 214-20.

PEDERSEN, J. F., MOLSTED-PEDERSEN, L. & MORTENSEN, H. B. (1984) Fetal growth delay and maternal hemoglobin A1c in early diabetic pregnancy. *Obstet Gynecol,* 64**,** 351-2.

PEDERSEN, J. F., SORENSEN, S. & MOLSTED-PEDERSEN, L. (1998) Serum levels of human placental lactogen, pregnancy-associated plasma protein A and endometrial secretory protein PP14 in first trimester of diabetic pregnancy. *Acta Obstet Gynecol Scand,* 77**,** 155-8.

PEIRO, C., LAFUENTE, N., MATESANZ, N., CERCAS, E., LLERGO, J. L., VALLEJO, S., RODRIGUEZ-MANAS, L. & SANCHEZ-FERRER, C. F. (2001) High glucose induces cell death of cultured human aortic smooth muscle cells through the formation of hydrogen peroxide. *Br J Pharmacol,* 133**,** 967-74.

PENG, Y., KWOK, K. H., YANG, P. H., NG, S. S., LIU, J., WONG, O. G., HE, M. L., KUNG, H. F. & LIN, M. C. (2005) Ascorbic acid inhibits ROS production, NF-kappa B activation and prevents ethanol-induced growth retardation and microencephaly. *Neuropharmacology,* 48**,** 426-34.

PEUCHANT, E., BRUN, J. L., RIGALLEAU, V., DUBOURG, L., THOMAS, M. J., DANIEL, J. Y., LENG, J. J. & GIN, H. (2004) Oxidative and antioxidative status in pregnant women with either gestational or type 1 diabetes. *Clin Biochem,* 37**,** 293-8.

PONCIN, S., COLIN, I. M., DECALLONNE, B., CLINCKSPOOOR, I., MANY, M. C., DENEF, J. F. & GERARD, A. C. (2010) N-acetylcysteine and 15 deoxy-{delta}12,14-prostaglandin J2 exert a protective effect against autoimmune thyroid destruction in vivo but not against interleukin-1{alpha}/interferon {gamma}-induced inhibitory effects in thyrocytes in vitro. *Am J Pathol,* 177**,** 219-28.

POSTON, L. & RAIJMAKERS, M. T. (2004) Trophoblast oxidative stress, antioxidants and pregnancy outcome--a review. *Placenta,* 25 Suppl A**,** S72-8.

QI, W., CHEN, X., GILBERT, R. E., ZHANG, Y., WALTHAM, M., SCHACHE, M., KELLY, D. J. & POLLOCK, C. A. (2007) High glucose-induced thioredoxin-interacting protein in renal proximal tubule cells is independent of transforming growth factor-beta1. *Am J Pathol,* 171**,** 744-54.

RAJESH, M., MUKHOPADHYAY, P., BATKAI, S., MUKHOPADHYAY, B., PATEL, V., HASKO, G., SZABO, C., MABLEY, J. G., LIAUDET, L. & PACHER, P. (2009) Xanthine oxidase inhibitor allopurinol attenuates the development of diabetic cardiomyopathy. *J Cell Mol Med,* 13**,** 2330-41.

RAMALHO-SANTOS, J., VARUM, S., AMARAL, S., MOTA, P. C., SOUSA, A. P. & AMARAL, A. (2009) Mitochondrial functionality in reproduction: from gonads and gametes to embryos and embryonic stem cells. *Hum Reprod Update,* 15**,** 553-72.

ROBERTS, C. K. & SINDHU, K. K. (2009) Oxidative stress and metabolic syndrome. *Life Sci,* 84**,** 705-12.

ROLO, A. P. & PALMEIRA, C. M. (2006) Diabetes and mitochondrial function: role of hyperglycemia and oxidative stress. *Toxicol Appl Pharmacol,* 212**,** 167-78.

ROSTAND, S. G. & WORK, J. (1985) Effect of 6-aminonicotinamide on renin release in isolated rat kidney: possible role for the pentose pathway. *Am J Physiol,* 249**,** F213-9.

SIBAI, B. M. (2000) Risk factors, pregnancy complications, and prevention of hypertensive disorders in women with pregravid diabetes mellitus. *J Matern Fetal Med,* 9**,** 62-5.

STAUN-RAM, E. & SHALEV, E. (2005) Human trophoblast function during the implantation process. *Reprod Biol Endocrinol,* 3**,** 56.

STOWE, D. F. & CAMARA, A. K. (2009) Mitochondrial reactive oxygen species production in excitable cells: modulators of mitochondrial and cell function. *Antioxid Redox Signal,* 11**,** 1373-414.

SUN, J., XU, Y., SUN, S., SUN, Y. & WANG, X. (2010) Intermittent high glucose enhances cell proliferation and VEGF expression in retinal endothelial cells: the role of mitochondrial reactive oxygen species. *Mol Cell Biochem,* 343**,** 27-35.

THAME, M., OSMOND, C., BENNETT, F., WILKS, R. & FORRESTER, T. (2004) Fetal growth is directly related to maternal anthropometry and placental volume. *Eur J Clin Nutr,* 58**,** 894-900.

VARMA, S., LAL, B. K., ZHENG, R., BRESLIN, J. W., SAITO, S., PAPPAS, P. J., HOBSON, R. W., 2ND & DURAN, W. N. (2005) Hyperglycemia alters PI3k and Akt signaling and leads to endothelial cell proliferative dysfunction. *Am J Physiol Heart Circ Physiol,* 289**,** H1744-51.

WEIDIG, P., MCMASTER, D. & BAYRAKTUTAN, U. (2004) High glucose mediates pro-oxidant and antioxidant enzyme activities in coronary endothelial cells. *Diabetes Obes Metab,* 6**,** 432-41.

WEISS, U., CERVAR, M., PUERSTNER, P., SCHMUT, O., HAAS, J., MAUSCHITZ, R., ARIKAN, G. & DESOYE, G. (2001) Hyperglycaemia in vitro alters the proliferation and mitochondrial activity of the choriocarcinoma cell lines BeWo, JAR and JEG-3 as models for human first-trimester trophoblast. *Diabetologia,* 44**,** 209-19.

WENTZEL, P., EJDESJO, A. & ERIKSSON, U. J. (2003) Maternal diabetes in vivo and high glucose in vitro diminish GAPDH activity in rat embryos. *Diabetes,* 52**,** 1222-8.

WENTZEL, P. & ERIKSSON, U. J. (1998) Antioxidants diminish developmental damage induced by high glucose and cyclooxygenase inhibitors in rat embryos in vitro. *Diabetes,* 47**,** 677-84.

WHITLEY, G. S. & CARTWRIGHT, J. E. (2010) Cellular and molecular regulation of spiral artery remodelling: lessons from the cardiovascular field. *Placenta,* 31**,** 465-74.

XIA, L., WANG, H., MUNK, S., KWAN, J., GOLDBERG, H. J., FANTUS, I. G. & WHITESIDE, C. I. (2008) High glucose activates PKC-zeta and NADPH oxidase through autocrine TGF-beta1 signaling in mesangial cells. *Am J Physiol Renal Physiol,* 295**,** F1705-14.

XU, Z. G., KIM, K. S., PARK, H. C., CHOI, K. H., LEE, H. Y., HAN, D. S. & KANG, S. W. (2003) High glucose activates the p38 MAPK pathway in cultured human peritoneal mesothelial cells. *Kidney Int,* 63**,** 958-68.

XUE, M., QIAN, Q., ADAIKALAKOTESWARI, A., RABBANI, N., BABAEI-JADIDI, R. & THORNALLEY, P. J. (2008) Activation of NF-E2-related factor-2 reverses biochemical dysfunction of endothelial cells induced by hyperglycemia linked to vascular disease. *Diabetes,* 57**,** 2809-17.

YU, T., ROBOTHAM, J. L. & YOON, Y. (2006) Increased production of reactive oxygen species in hyperglycemic conditions requires dynamic change of mitochondrial morphology. *Proc Natl Acad Sci U S A,* 103**,** 2653-8.

ZHANG, D. X. & GUTTERMAN, D. D. (2007) Mitochondrial reactive oxygen species-mediated signaling in endothelial cells. *Am J Physiol Heart Circ Physiol,* 292**,** H2023-31.

7 Publications

Fröhlich JD, Huppertz B, Abuja PM, König J, Desoye G. *Oxygen modulates the response of first-trimester trophoblasts to hyperglycemia.* Am J Pathol, accepted.

König J, Huppertz B, Desoye G, Parolini O, Fröhlich JD, Weiß G, Dohr G, Sedlmayr P, Lang I. *Amnion-derived mesenchymal stromal cells show angiogenic properties but resist differentiation into mature endothelial cells.* Stem Cells Dev, accepted.

Hiden U, Froehlich J, Desoye G. Diabetes and the Placenta. In: Helen H, Kay D, Nelson M and Wang Y, editors. The Placenta: From Development to Disease. Blackwell Publishing Ltd.; 2011. p. 228-236.

Lappas M, Hiden U, Froehlich J, Desoye G, Haugel-de Mouzon S, Jawerbaum A. The Role of Oxidative stress in the Pathophysiology of Gestational Diabetes Mellitus. Antioxidant Redox Signal, 2011.